*Acta Numerica* (2013), pp. 289–396
doi:10.1017/S0962492913000056
© Cambridge University Press, 2013
Printed in the United Kingdom

# Finite element methods for surface PDEs*

Gerhard Dziuk
*Abteilung für Angewandte Mathematik,*
*Albert-Ludwigs-Universität Freiburg im Breisgau,*
*Hermann-Herder-Straße 10,*
*D–79104 Freiburg im Breisgau, Germany*
*E-mail:* gerd@mathematik.uni-freiburg.de

Charles M. Elliott
*Mathematics Institute,*
*University of Warwick,*
*Coventry CV4 7AL, UK*
*E-mail:* c.m.elliott@warwick.ac.uk

In this article we consider finite element methods for approximating the solution of partial differential equations on surfaces. We focus on surface finite elements on triangulated surfaces, implicit surface methods using level set descriptions of the surface, unfitted finite element methods and diffuse interface methods. In order to formulate the methods we present the necessary geometric analysis and, in the context of evolving surfaces, the necessary transport formulae. A wide variety of equations and applications are covered. Some ideas of the numerical analysis are presented along with illustrative numerical examples.

## CONTENTS

1 Introduction 290
2 Parametrized surfaces and hypersurfaces 291
3 Partial differential equations on surfaces 301
4 Triangulated surfaces 305
5 Partial differential equations on moving surfaces 323
6 More surface PDEs 343
7 PDEs on implicit surfaces 351
8 Implicit surface finite element method 363
9 Unfitted bulk finite element method 368
10 Applications 382
References 391

* Colour online for monochrome figures available at journals.cambridge.org/anu.

https://doi.org/10.1017/S0962492913000056 Published online by Cambridge University Press

## 1. Introduction

Surface partial differential equations arise in a wide variety of applications. Further, they are examples of partial differential equations on manifolds. As such they provide a remaining challenge within the general subject of the numerical analysis of partial differential equations. The framework is essentially geometric because the domain in which the equation holds is curved. They are linked naturally to the geometric equations for surfaces such as the minimal surface equation, motion by mean curvature and Willmore flow. In an earlier *Acta Numerica* article (Deckelnick, Dziuk and Elliott 2005) we surveyed numerical methods for geometric partial differential equations and mean curvature flow.

The purpose of this article is to give an account of numerical methods for surface partial differential equations. Our interest and research in this field was stimulated in 2003 during the Isaac Newton Institute programme 'Computational challenges in partial differential equations'. Since this time there has been burgeoning interest in both the numerical analysis of such problems and the application to complex physical models.

The starting point was the use of surface finite elements to compute solutions to the Poisson problem for the Laplace–Beltrami operator on a curved surface proposed and analysed in Dziuk (1988). Here an important concept is the use of triangulated surfaces on which finite element spaces are constructed and then used in variational formulations of surface PDEs using surface gradients. This approach was extended by Dziuk and Elliott (2007*b*) to parabolic (including nonlinear and higher-order) equations on stationary surfaces. The evolving surface finite element method (ESFEM) was introduced by Dziuk and Elliott (2007*a*) in order to treat conservation laws on moving surfaces. The key idea is to use the Leibniz (or transport) formula for the time derivative of integrals over moving surfaces in order to derive weak and variational formulations. An interesting upshot is that the velocity and mean curvature of the surface which appear in certain formulations of the partial differential equation do not appear explicitly in variational formulations. This gives a tremendous advantage to numerical methods that exploit this, such as those of Dziuk and Elliott (2007*a*, 2010). Further numerical analysis of surface finite element methods may be found in Dziuk and Elliott (2012, 2013) and Dziuk, Lubich and Mansour (2012). Applications to complex physical and biological models may be found in Eilks and Elliott (2008), Elliott and Stinner (2010), Barreira, Elliott and Madzvamuse (2011) and Elliott, Stinner and Venkataraman (2012).

Another approach is to use implicit surface methods. The starting point for these methods is the level set method for evolving surfaces (Sethian 1999, Osher and Fedkiw 2003). Here the idea is to use a level set function $\phi$ to define a degenerate partial differential equation whose solution solves

https://doi.org/10.1017/S0962492913000056 Published online by Cambridge University Press

the surface equation on all level sets of $\phi$. Such methods are formulated in Bertalmío, Cheng, Osher and Sapiro (2001), Greer, Bertozzi and Sapiro (2006), Burger (2009) and Dziuk and Elliott (2008, 2010).

Further, we describe in some detail numerical schemes based on the use of diffuse interfaces. These arise in phase field approximations of interface problems (Caginalp 1989, Deckelnick *et al.* 2005), and it is natural to exploit the methodology to generate methods for solving partial differential equations on the interfaces (Rätz and Voigt 2006, Elliott, Stinner, Styles and Welford 2011).

An important feature of the methods described in this article is the avoidance of *charts* both in the problem formulation and the numerical methods. The surface finite element method is based simply on triangulated surfaces and requires the geometry solely through knowledge of the vertices of the triangulation. On the other hand, the methods based on implicit surfaces require only the level set function $\phi$. All the geometry is then encoded in $\phi$.

The layout of the article is as follows. In Section 2 we set basic notation and concepts concerning geometric quantities, surface gradients and integration by parts for parametrized surfaces, using maps $X$, and hypersurfaces, using level set functions $\phi$. Elliptic partial differential equations on surfaces are formulated in Section 3. Surface finite elements on triangulated surfaces are formulated and analysed for elliptic equations in Section 4.

Complex applications involving surfaces and interfaces frequently require the formulation and approximation of parabolic equations on moving surfaces. In Section 5 we formulate a scalar conservation law with a diffusive flux on a moving surface and formulate the evolving surface finite element method. Of particular note is the transport theorem for moving surfaces, which is valid triangle by triangle on an evolving surface. This is exploited together with transport property of the finite element basis functions to obtain a method which does not require explicit knowledge of the curvature or velocity, merely knowledge of the triangle vertices. Some more time-dependent equations are discussed in Section 6.

Implicit surface formulations and their numerical approximations are discussed in Sections 7 and 8. Methods which use finite elements in the higher-dimensional ambient space but with variational forms on surfaces or localized narrow bands are considered in Section 9. Finally, we briefly discuss some applications in Section 10.

## 2. Parametrized surfaces and hypersurfaces

In this section we introduce the elementary geometric analysis which is necessary to treat partial differential equations on surfaces. It is our opinion that numerical methods have to be intimately related to the analysis of the problems.

https://doi.org/10.1017/S0962492913000056 Published online by Cambridge University Press

We begin in Section 2.1 by recalling some facts from elementary differential geometry concerning parametrized surfaces. We continue in Section 2.2 with hypersurfaces in $\mathbb{R}^{n+1}$ and the basic analysis concepts for such hypersurfaces. We introduce the necessary geometric concepts, for example the notion of curvature. The formula for integration by parts is proved, and we formulate the co-area formula. In Section 2.3 we introduce global coordinates in a neighbourhood of a hypersurface, the Fermi coordinates. These will be quite useful for the numerical analysis of PDEs on surfaces. For theoretical reasons we will introduce the oriented distance function. For the treatment of surface PDEs the Poincaré inequality on surfaces is central; its proof is in Section 2.4.

### *2.1. Parametrized surfaces*

Let $n \in \mathbb{N}$. We call $\Gamma \subset \mathbb{R}^{n+1}$ an *n-dimensional parametrized $C^k$-surface* ($k \in \mathbb{N} \cup \{\infty\}$) if, for every point $x_0 \in \Gamma$, there exists an open set $U \subset \mathbb{R}^{n+1}$ with $x_0 \in U$, an open connected set $V \subset \mathbb{R}^n$ and a map $X : V \to U \cap \Gamma$ with the properties $X \in C^k(V, \mathbb{R}^{n+1})$, $X$ is bijective and rank $\nabla X = n$ on $V$.

The map $X$ is called a local *parametrization* of $\Gamma$ while $X^{-1}$ is called a local *chart*. A collection $(X_i)_{i\in I}, X_i \in C^k(V_i, \mathbb{R}^{n+1})$ of local parametrizations such that $\cup_{i\in I} X_i(V_i) = \Gamma$ is called a *$C^k$-atlas*. If $X_i(V_i) \cap X_j(V_j) \neq \emptyset$, then the map $X_i^{-1} \circ X_j$ by assumption is a $C^k$-diffeomorphism.

A function $f : \Gamma \to \mathbb{R}$ is *k-times differentiable* if all the functions $f \circ X_i : V_i \to \mathbb{R}$ are $k$-times differentiable.

Let $X \in C^2(V, \mathbb{R}^{n+1})$ be a local parametrization of $\Gamma$, $\theta \in V$. We define the *first fundamental form* $G(\theta) = (g_{ij}(\theta))_{i,j=1,\dots,n}$, $\theta \in V$ by

$$g_{ij}(\theta) = \frac{\partial X}{\partial \theta_i}(\theta) \cdot \frac{\partial X}{\partial \theta_j}(\theta), \quad i, j = 1, \dots, n.$$

Superscript indices denote the inversion of the matrix $G$ so that

$$(g^{ij})_{i,j=1,\dots,n} = G^{-1},$$

and by $g = \det(G)$ we denote the determinant of the matrix $G$.

The *Laplace–Beltrami operator* on $\Gamma$ is defined for a twice differentiable function $f : \Gamma \to \mathbb{R}$ as follows. Let $F(\theta) = f(X(\theta))$, $\theta \in V$. Then

$$(\Delta_\Gamma f)(X(\theta)) = \frac{1}{\sqrt{g(\theta)}} \sum_{i,j=1}^{n} \frac{\partial}{\partial \theta_j} \left( g^{ij}(\theta) \sqrt{g(\theta)} \frac{\partial F}{\partial \theta_i}(\theta) \right). \tag{2.1}$$

The *tangential gradient* is given by

$$(\nabla_\Gamma f)(X(\theta)) = \sum_{i,j=1}^{n} g^{ij}(\theta) \frac{\partial F}{\partial \theta_j}(\theta) \frac{\partial X}{\partial \theta_i}(\theta). \tag{2.2}$$

https://doi.org/10.1017/S0962492913000056 Published online by Cambridge University Press

*2.2. Hypersurfaces*

**Definition 2.1.** Let $k \in \mathbb{N} \cup \{\infty\}$. $\Gamma \subset \mathbb{R}^{n+1}$ is called a $C^k$-hypersurface if, for each point $x_0 \in \Gamma$, there exists an open set $U \subset \mathbb{R}^{n+1}$ containing $x_0$ and a function $\phi \in C^k(U)$ with the property that $\nabla\phi \neq 0$ on $\Gamma \cap U$ and such that

$$U \cap \Gamma = \{x \in U \mid \phi(x) = 0\}. \tag{2.3}$$

The linear space

$$T_x\Gamma = \big\{\tau \in \mathbb{R}^{n+1} \mid \exists\, \gamma : (-\epsilon, \epsilon) \to \mathbb{R}^{n+1} \text{ differentiable,} \\ \gamma((-\epsilon,\epsilon)) \subset \Gamma, \gamma(0) = x \text{ and } \gamma'(0) = \tau\big\}$$

is called the *tangent space* to $\Gamma$ at $x \in \Gamma$. It is easy to show that $T_x\Gamma = [\nabla\phi(x)]^\perp$, the set of all vectors that are orthogonal to $\nabla\phi(x)$, where $\phi$ is as in (2.3). In particular, $T_x\Gamma$ is an $n$-dimensional subspace of $\mathbb{R}^{n+1}$.

A vector $\nu(x) \in \mathbb{R}^{n+1}$ is called a *unit normal vector* at $x \in \Gamma$ if $\nu(x) \perp T_x\Gamma$ and $|\nu(x)| = 1$. In view of the above characterization of $T_x\Gamma$, we then have

$$\nu(x) = \frac{\nabla\phi(x)}{|\nabla\phi(x)|} \quad \text{or} \quad \nu(x) = -\frac{\nabla\phi(x)}{|\nabla\phi(x)|}. \tag{2.4}$$

A $C^1$-hypersurface is called *orientable* if there exists a continuous vector field $\nu : \Gamma \to \mathbb{R}^{n+1}$ such that $\nu(x)$ is a unit normal vector to $\Gamma$ for all $x \in \Gamma$.

The connection between the parametrized surfaces of Section 2.1 and hypersurfaces is given by the following well-known little lemma.

**Lemma 2.2.** Assume that $\Gamma$ is a $C^k$-hypersurface in $\mathbb{R}^{n+1}$. Then for every $x \in \Gamma$ there exists an open set $U \subset \mathbb{R}^{n+1}$ with $x \in U$ and a parametrized $C^k$-surface $X : V \to U \cap \Gamma$ such that $X$ is a bijective map from $V$ onto $U \cap \Gamma$. If $X : V \to U \cap \Gamma$ is a parametrized $C^k$-surface and $\theta \in V$, then there is an open set $\tilde{V} \subset V$ with $\theta \in \tilde{V}$ such that $X(\tilde{V})$ is a $C^k$-hypersurface.

This means that locally we can always work with hypersurfaces. And we may use all the definitions from Section 2.1 for hypersurfaces.

**Definition 2.3.** Let $\Gamma \subset \mathbb{R}^{n+1}$ be a $C^1$-hypersurface and let $f : \Gamma \to \mathbb{R}$ be differentiable at $x \in \Gamma$. We define the tangential gradient of $f$ at $x \in \Gamma$ by

$$\nabla_\Gamma f(x) = \nabla\overline{f}(x) - \nabla\overline{f}(x) \cdot \nu(x)\, \nu(x) = P(x)\nabla\overline{f}(x),$$

where $P(x)_{ij} = \delta_{ij} - \nu_i(x)\nu_j(x)$ $(i, j = 1, \ldots, n+1)$. Here $\overline{f}$ is a smooth extension of $f : \Gamma \to \mathbb{R}$ to an $(n+1)$-dimensional neighbourhood $U$ of the surface $\Gamma$, so that $\overline{f}\big|_\Gamma = f$. $\nabla$ denotes the gradient in $\mathbb{R}^{n+1}$ and $\nu(x)$ is a unit normal at $x$.

https://doi.org/10.1017/S0962492913000056 Published online by Cambridge University Press

The *Laplace–Beltrami operator* applied to a twice differentiable function $f \in C^2(\Gamma)$ is given by

$$\Delta_\Gamma f = \nabla_\Gamma \cdot \nabla_\Gamma f = \sum_{i=1}^{n+1} \underline{D}_i \underline{D}_i f. \tag{2.5}$$

See the proof of Theorem 2.10 in Section 2.3 for the construction of an extension $\overline{f}$. We shall use the notation (as in the above definition)

$$\nabla_\Gamma f(x) = (\underline{D}_1 f(x), \dots, \underline{D}_{n+1} f(x))$$

for the $n+1$ components of the tangential gradient. Note that $\nabla_\Gamma f(x) \cdot \nu(x) = 0$ and hence $\nabla_\Gamma f(x) \in T_x\Gamma$.

Let us show that (2.1) and (2.2) are equivalent to the settings in Definition 2.3. Since the tangential gradient is a tangent vector, $\nabla_\Gamma f \circ X = \sum_{i=1}^n \alpha_i X_{\theta_i}$ with certain scalars $\alpha_j$. We solve this equation for $\alpha_1, \dots, \alpha_n$ by multiplying it by $X_{\theta_k}$, to get

$$F_{\theta_k} = \nabla_\Gamma f \circ X \cdot X_{\theta_k} = \sum_{i=1}^n \alpha_i X_{\theta_i} \cdot X_{\theta_k} = \sum_{i=1}^n \alpha_i g_{ik}. \tag{2.6}$$

For the first equality on the left we have used the fact that, by the chain rule applied to $F(\theta) = f(X(\theta))$, we have $F_{\theta_k} = \sum_{l=1}^n \underline{D}_l f \circ X X_{l\theta_k}$, since $X_{\theta_k}$ is a tangent vector. From (2.6) we infer that $\alpha_l = \sum_{k=1}^n F_{\theta_k} g^{kl}$, and this finally gives (2.2). Now it is easy to derive (2.1).

**Lemma 2.4.** $\nabla_\Gamma f(x)$ only depends on the values of $f$ on $\Gamma \cap U$, where $U \subset \mathbb{R}^{n+1}$ is a neighbourhood of $x$.

*Proof.* It is sufficient to show that $f \equiv 0$ on $\Gamma \cap U$ implies that $\nabla_\Gamma f(x) = 0$. Choose $\gamma : (-\epsilon, \epsilon) \to \mathbb{R}^{n+1}$ such that $\gamma(0) = x, \gamma((-\epsilon, \epsilon)) \subset \Gamma \cap U$ and $\gamma'(0) = \nabla_\Gamma f(x)$. Since $\overline{f}(\gamma(t)) = f(\gamma(t)) = 0$ for all $|t| < \epsilon$, we have

$$0 = \nabla \overline{f}(x) \cdot \gamma'(0) = \big(\nabla_\Gamma f(x) + \nabla \overline{f}(x) \cdot \nu(x)\, \nu(x)\big) \cdot \nabla_\Gamma f(x) = |\nabla_\Gamma f(x)|^2,$$

which implies the result. □

We denote by $C^1(\Gamma)$ the set of functions $f : \Gamma \to \mathbb{R}$, which are differentiable at every point $x \in \Gamma$ and for which $\underline{D}_j f : \Gamma \to \mathbb{R}, j = 1, \dots, n+1$ are continuous. Similarly one can define $C^l(\Gamma)$ $(l \in \mathbb{N})$ provided that $\Gamma$ is a $C^k$-hypersurface with $k \geq l$.

**Definition 2.5.** For $\Gamma \in C^2$ we define

$$\mathcal{H}_{ij} = \underline{D}_i \nu_j \quad (i, j = 1, \dots, n+1). \tag{2.7}$$

It is easily shown that the matrix $\mathcal{H}$ is symmetric and that it possesses an eigenvalue 0 in the normal direction: $\mathcal{H}\nu = 0$. $\mathcal{H}$ is called the *extended*

https://doi.org/10.1017/S0962492913000056 Published online by Cambridge University Press

*Weingarten map.* The restriction of $\mathcal{H}$ to the tangent space is called the Weingarten map.

For $x \in \Gamma$ the quantity

$$H(x) = \mathrm{trace}\mathcal{H}(x) = \sum_{i=1}^{n+1} \mathcal{H}_{ii}(x) \tag{2.8}$$

is the *mean curvature* of $\Gamma$ at the point $x$. It differs from the common definition by a factor of $n$. We note that the eigenvalues $\kappa_1, \ldots, \kappa_n$ of $\mathcal{H}$ (apart from the trivial eigenvalue 0 in the $\nu$-direction) are the *principal curvatures* of $\Gamma$.

Let us have a look at the most simple example. The sphere of radius $R > 0$, $\Gamma = \{x \in \mathbb{R}^{n+1} \mid |x| = R\}$, is given by the level set function $\phi(x) = |x| - R$ for $0 < |x| < \infty$. We may choose

$$\nu = \frac{\nabla\phi}{|\nabla\phi|} = \frac{x}{|x|}$$

and get for $x \in \Gamma$

$$\mathcal{H}_{ij}(x) = \underline{D}_i \nu_j(x) = \underline{D}_i \frac{x_j}{|x|} = \frac{1}{R}\underline{D}_i x_j = \frac{1}{R}(\delta_{ij} - \nu_i\nu_j) = \frac{1}{R}\left(\delta_{ij} - \frac{x_i x_j}{R^2}\right).$$

This matrix has an eigenvalue 0 with eigenvector $\frac{x}{R}$ and $n$ eigenvalues $\kappa_j = \frac{1}{R}$ $(j = 1, \ldots, n)$. The mean curvature of $\Gamma$ is then given as $H = \frac{n}{R}$.

The following result concerning the exchange of tangential derivatives is easily proved.

**Lemma 2.6.** For $\Gamma \in C^2$ and $u \in C^2(\Gamma)$ we have

$$\underline{D}_i\underline{D}_j u - \underline{D}_j\underline{D}_i u = (\mathcal{H}\nabla_\Gamma u)_j \nu_i - (\mathcal{H}\nabla_\Gamma u)_i \nu_j. \tag{2.9}$$

for $i, j = 1, \ldots, n+1$.

### *2.3. Global coordinates*

It is quite convenient to use global coordinates in a neighbourhood of a hypersurface, the so-called Fermi coordinates. This avoids working with charts and atlases (see Section 2.1) when proving results and carrying out the numerical analysis. For this one introduces the *oriented distance function* for $\Gamma$.

**Remark 2.7.** In the context of surface finite elements we will use the oriented distance function only for our analysis and numerical analysis. We will not use it in defining the computational methods. We will not need the oriented distance function for the implementation of our algorithms. It may be of use in *implicit surface* methods.

https://doi.org/10.1017/S0962492913000056 Published online by Cambridge University Press

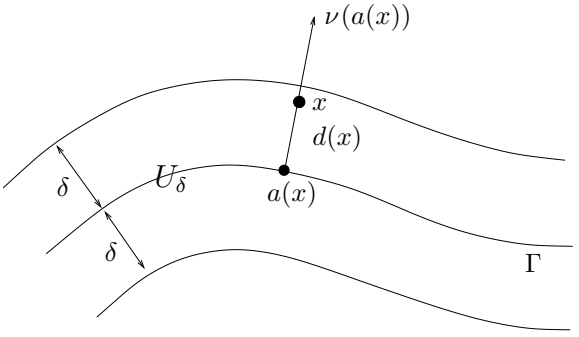



Figure 2.1. Strip $U_\delta$ around the hypersurface $\Gamma$ and normal coordinates $x = a(x) + d(x)\nu(a(x))$.

Assume in the following that $G \subset \mathbb{R}^{n+1}$ is bounded and open with exterior normal $\nu$ and assume that $\Gamma = \partial G$ is a $C^k$-hypersurface ($k \geq 2$). The oriented distance function for $\Gamma$ is defined by

$$d(x) = \begin{cases} \inf_{y\in\Gamma}|x-y| & x \in \mathbb{R}^{n+1} \setminus \bar{G}, \\ -\inf_{y\in\Gamma}|x-y| & x \in G. \end{cases}$$

One easily verifies that $d$ is globally Lipschitz-continuous with Lipschitz constant 1. Since $\partial G$ is a $C^2$-hypersurface, it satisfies both a uniform interior and a uniform exterior sphere condition, which means that for each point $x_0 \in \partial\Omega$ there are balls $B$ and $B'$ such that

$$\bar{B} \cap (\mathbb{R}^{n+1} \setminus \Omega) = \{x_0\}, \quad \bar{B}' \cap \bar{\Omega} = \{x_0\},$$

and the radii of $B$, $B'$ are bounded from below by a positive constant $\delta$ uniformly in $x_0$. With this observation the following lemma is easily proved.

**Lemma 2.8.** We define

$$U_\delta = \big\{x \in \mathbb{R}^{n+1} \mid |d(x)| < \delta\big\}.$$

Then $d \in C^k(U_\delta)$, and for every point $x \in U_\delta$ there exists a unique point $a(x) \in \Gamma$ such that

$$x = a(x) + d(x)\nu(a(x)). \tag{2.10}$$

Moreover, we have that

$$\nabla d(x) = \nu(a(x)), \quad |\nabla d(x)| = 1, \quad \text{for } x \in U_\delta.$$

We also extend the normal constantly in the normal direction: $\nu(x) = \nu(a(x))$ for $x \in U_\delta$. Thus we have introduced a global coordinate system around $\Gamma$. Every point $x \in U_\delta$ can be described by its *Fermi coordinates* (normal coordinates) $d(x)$ and $a(x)$ according to (2.10).

The introduction of global coordinates allows us to work with the well-known co-area formula (Evans 1998).

https://doi.org/10.1017/S0962492913000056 Published online by Cambridge University Press

**Theorem 2.9.** Let $\Gamma(r) = \{x \in \mathbb{R}^{n+1} \mid \mathrm{d}(x) = r\}$ be the parallel surface to $\Gamma = \Gamma(0)$ for $|r| < \delta$. Then

$$\int_{U_\varepsilon} f(x)\,\mathrm{d}x = \int_{-\varepsilon}^{\varepsilon} \int_{\Gamma(r)} f(x)\,\mathrm{d}A(x)\,\mathrm{d}r \tag{2.11}$$

for $f \in C^0(U_\delta)$ and $0 < \varepsilon < \delta$.

We note that this formula changes to

$$\int_{U_\varepsilon} f(x)\,\mathrm{d}x = \int_{-\varepsilon}^{\varepsilon} \int_{\Gamma(r)} f(x)|\nabla\phi(x)|\,\mathrm{d}A(x)\,\mathrm{d}r \tag{2.12}$$

if the surfaces are given by an arbitrary level set function $\phi$ as in (2.3), $\Gamma(r) = \{x \in \mathbb{R}^{n+1} \mid \phi(x) = r\}$, and the strip around $\Gamma$ is taken to be $U_\delta = \{x \in \mathbb{R}^{n+1} \mid |\phi(x)| < \delta\}$. In this case one does not work with parallel surfaces to $\Gamma$.

With the co-area formula one can prove the formula for *integration by parts* on surfaces $\Gamma$.

**Theorem 2.10.** Assume that $\Gamma$ is a hypersurface in $\mathbb{R}^{n+1}$ with smooth boundary $\partial\Gamma$ and that $f \in C^1(\overline{\Gamma})$. Then

$$\int_\Gamma \nabla_\Gamma f\,\mathrm{d}A = \int_\Gamma fH\nu\,\mathrm{d}A + \int_{\partial\Gamma} f\mu\,\mathrm{d}A. \tag{2.13}$$

Here, $\mu$ denotes the co-normal vector which is normal to $\partial\Gamma$ and tangent to $\Gamma$. A compact hypersurface $\Gamma$ does not have a boundary, $\partial\Gamma = \emptyset$, and the last term on the right-hand side vanishes.

Note that in (2.13) $\mathrm{d}A$ in connection with an integral over $\Gamma$ denotes the $n$-dimensional surface measure, while $\mathrm{d}A$ in connection with an integral over $\partial\Gamma$ is the $(n-1)$-dimensional surface measure.

*Proof.* We extend $f$ to the tubular neighbourhood $U_\varepsilon$ of $\Gamma$ by

$$\overline{f}(x) = f(a(x)) \quad (x \in U_\varepsilon).$$

Then the chain rule gives

$$\frac{\partial \overline{f}}{\partial x_j}(x) = \sum_{k=1}^{n+1} \underline{D}_k f(a(x)) \frac{\partial a_k}{\partial x_j}(x).$$

The tangential derivative $\underline{D}_k f$ appears because we have that

$$\frac{\partial a_k}{\partial x_j}(x) = \frac{\partial}{\partial x_j}(x_k - d(x)\nu_k(x)) = \delta_{jk} - \nu_j(x)\nu_k(x) - d(x)\mathcal{H}_{jk}(x),$$

and the matrix $(\tilde{a}_{kj})_{j,k=1,\dots,n+1}$ $(\tilde{a}_{kj} = a_{k,x_j})$ maps any vector into a tangent vector. Thus we have

$$\nabla\overline{f}(x) = (I - d(x)\mathcal{H}(x))\nabla_\Gamma f(a(x)). \tag{2.14}$$

https://doi.org/10.1017/S0962492913000056 Published online by Cambridge University Press

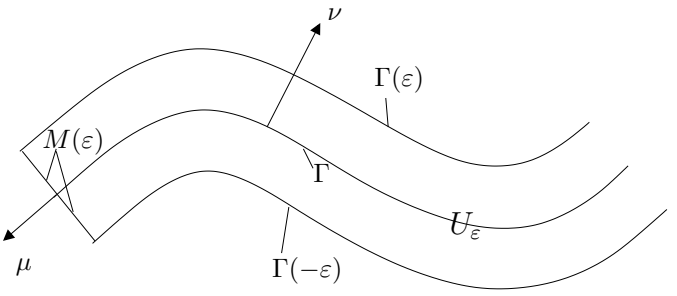



Figure 2.2. Geometric situation around the given surface $\Gamma$. Parallel surfaces $\Gamma(\varepsilon)$, $\Gamma(-\varepsilon)$ and normal $\nu$, co-normal $\mu$.

In particular, we obtain $\nabla\overline{f}(x) = \nabla_\Gamma f(x)$ for $x \in \Gamma$. We apply Gauss's theorem to $\overline{f}$ on $U_\varepsilon$ and get

$$\int_{U_\varepsilon} \nabla\overline{f}(x)\,\mathrm{d}x = \int_{\partial U_\varepsilon} \overline{f}(x)\nu_{\partial U_\varepsilon}(x)\,\mathrm{d}A(x).$$

We have that $\partial U_\varepsilon = \Gamma(\varepsilon) \cup \Gamma(-\varepsilon) \cup M(\varepsilon)$, where $M(\varepsilon) = \{x + r\nu_\Gamma(x) \mid x \in \partial\Gamma, r \in [-\varepsilon, \varepsilon]\}$ (see Figure 2.2). Thus

$$\begin{aligned}\frac{1}{2\varepsilon}\int_{U_\varepsilon} (I - d(x)\mathcal{H}(x))\nabla_\Gamma f(a(x))\,\mathrm{d}x \qquad (2.15)\\ = \frac{1}{2\varepsilon}\bigg(\int_{\Gamma(\varepsilon)} \overline{f}(x)\nu_\Gamma(x)\,\mathrm{d}A(x) - \int_{\Gamma(-\varepsilon)} \overline{f}(x)\nu_\Gamma(x)\,\mathrm{d}A(x)\\ + \int_{M(\varepsilon)} \overline{f}(x)\mu_\Gamma(x)\,\mathrm{d}A(x)\bigg),\end{aligned}$$

with the normal $\nu_\Gamma$ and the co-normal $\mu_\Gamma$ to $\Gamma$, which do not depend on $\varepsilon$. We take the limit $\varepsilon \to 0$ on both sides of this equation. Obviously, for the left-hand side

$$\lim_{\varepsilon\to 0} \frac{1}{2\varepsilon}\int_{U_\varepsilon} (I - d(x)\mathcal{H}(x))\nabla_\Gamma f(a(x))\,\mathrm{d}x = \int_\Gamma \nabla_\Gamma f(x)\,\mathrm{d}A(x).$$

The limit of the first two terms of the right-hand side of (2.15) is given by

$$\frac{\mathrm{d}}{\mathrm{d}\varepsilon}\Big|_{\varepsilon=0} \int_{\Gamma(\varepsilon)} \overline{f}(x)\nu_\Gamma(x)\,\mathrm{d}A(x) = \int_\Gamma f(x)H(x)\nu_\Gamma(x)\,\mathrm{d}A(x),$$

the last equality being the transport theorem in Theorem 5.1 with $v = \nu_\Gamma$. In the proof of that theorem we will not use integration by parts.

https://doi.org/10.1017/S0962492913000056 Published online by Cambridge University Press

For the last term on the right-hand side of (2.15) we have that

$$\lim_{\varepsilon\to 0}\frac{1}{2\varepsilon}\int_{M(\varepsilon)}\overline{f}(x)\mu_\Gamma(x)\,\mathrm{d}A(x)=\int_{\partial\Gamma}f(x)\mu_\Gamma(x)\,\mathrm{d}A(x),$$

because the integrand does not depend on $\varepsilon$. □

The formula for integration by parts on $\Gamma$ leads to the notion of a weak derivative and to the concept of Sobolev spaces on surfaces. Sobolev spaces are the natural spaces for solutions of elliptic partial differential equations. Let $\Gamma\in C^2$ for the following.

For $p\in[1,\infty]$ we let $L^p(\Gamma)$ denote the space of functions $f:\Gamma\to\mathbb{R}$ which are measurable with respect to the surface measure $\mathrm{d}A$ (the $n$-dimensional Hausdorff measure) and have finite norm, where the norm is defined by

$$\|f\|_{L^p(\Gamma)}=\left(\int_\Gamma|f|^p\,\mathrm{d}A\right)^{\frac{1}{p}}$$

for $p<\infty$, and for $p=\infty$ we mean the essential supremum norm.

$L^p(\Gamma)$ is a Banach space and for $p=2$ a Hilbert space. For $1\le p<\infty$ the spaces $C^0(\Gamma)$ and $C^1(\Gamma)$ are dense in $L^p(\Gamma)$.

**Definition 2.11.** A function $f\in L^1(\Gamma)$ has the weak derivative $v_i=\underline{D}_i f\in L^1(\Gamma)$ $(i\in\{1,\dots,n+1\})$ if, for every function $\varphi\in C^1(\Gamma)$ with compact support $\overline{\{x\in\Gamma\mid\varphi(x)\neq 0\}}\subset\Gamma$, we have the relation

$$\int_\Gamma f\underline{D}_i\varphi\,\mathrm{d}A=-\int_\Gamma\varphi v_i\,\mathrm{d}A+\int_\Gamma f\varphi H\nu_i\,\mathrm{d}A.$$

The Sobolev space $H^{1,p}(\Gamma)$ is defined by

$$H^{1,p}(\Gamma)=\left\{f\in L^p(\Gamma)\mid\underline{D}_i f\in L^p(\Gamma),\ i=1,\dots,n+1\right\}$$

with norm

$$\|f\|_{H^{1,p}(\Gamma)}=\left(\|f\|^p_{L^p(\Gamma)}+\|\nabla_\Gamma f\|^p_{L^p(\Gamma)}\right)^{\frac{1}{p}}.$$

For $k\in\mathbb{N}$ we define

$$H^{k,p}(\Gamma)=\left\{f\in H^{k-1,p}(\Gamma)\mid\underline{D}_i v^{(k-1)}\in L^p(\Gamma),i=1,\dots,n+1\right\},$$

where $H^{0,p}(\Gamma)=L^p(\Gamma)$. For $p=2$ we use the notation $H^k(\Gamma)=H^{k,2}(\Gamma)$. We denote by $v^{(l)}$ *all* weak derivatives of order $l$. Then

$$\|v\|_{H^{k,p}(\Gamma)}=\left(\sum_{l=0}^k\|v^{(l)}\|^p_{L^p(\Gamma)}\right)^{\frac{1}{p}}.$$

Note that for the previous definition we have only assumed that $\Gamma\in C^2$. This was done because in the formulation of the weak derivative we used the mean curvature of $\Gamma$.

https://doi.org/10.1017/S0962492913000056 Published online by Cambridge University Press

*2.4. Poincaré's inequality*

For the convenience of the reader we show how the Poincaré inequality for a function with mean value zero on a compact $n$-dimensional hypersurface can be deduced from the Poincaré inequality in $\mathbb{R}^{n+1}$ with the use of global coordinates.

**Theorem 2.12.** Assume that $\Gamma \in C^3$ and $1 \le p < \infty$. Then there is a constant $c$ such that, for every function $f \in H^{1,p}(\Gamma)$ with $\int_\Gamma f \,\mathrm{d}A = 0$, we have the inequality

$$\|f\|_{L^p(\Gamma)} \le c\|\nabla_\Gamma f\|_{L^p(\Gamma)}. \tag{2.16}$$

*Proof.* Clearly it is sufficient to prove the inequality for $L^1$ instead of $L^p$ and it is sufficient to work with smooth functions. Assume that $f \in C^1(\Gamma)$ with $\int_\Gamma f \,\mathrm{d}A = 0$. We extend this function to the tubular neighbourhood $U_\delta$ of the surface $\Gamma$, $\delta$ being sufficiently small, by

$$\overline{f}(x) = f(a(x)), \quad x \in U_\delta.$$

We state the following intermediate lemma.

**Lemma 2.13.** Let $\Gamma \in C^2$ be a compact hypersurface. Then there is a constant $c$, such that for every $0 < \varepsilon < \delta$ we have

$$\left|\frac{1}{2\varepsilon}\int_{U_\varepsilon} \overline{f}(x)\,\mathrm{d}x - \int_\Gamma f(x)\,\mathrm{d}A(x)\right| \le c\varepsilon \int_\Gamma |f(x)|\,\mathrm{d}A(x). \tag{2.17}$$

The proof of this lemma is left to the reader. We note that by the co-area formula from Theorem 2.9 we have

$$\frac{1}{2\varepsilon}\int_{U_\varepsilon} \overline{f}(x)\,\mathrm{d}x = \frac{1}{2\varepsilon}\int_{-\varepsilon}^{\varepsilon}\int_{\Gamma(r)} f(a(x))\,\mathrm{d}A(x)\,\mathrm{d}r$$

with an integrand which does not depend on $\varepsilon$.

We continue with the proof of Theorem 2.12. From (2.17) we get the inequality

$$\begin{aligned}(1-c_1\varepsilon)\int_\Gamma |f(x)|\,\mathrm{d}A(x) &\le \frac{1}{2\varepsilon}\int_{U_\varepsilon} |\overline{f}(x)|\,\mathrm{d}x\\ &\le \frac{1}{2\varepsilon}\int_{U_\varepsilon}\left|\overline{f}(x) - \frac{1}{|U_\varepsilon|}\int_{U_\varepsilon}\overline{f}(y)\,\mathrm{d}y\right|\mathrm{d}x + c_2\left|\frac{1}{|U_\varepsilon|}\int_{U_\varepsilon}\overline{f}(y)\,\mathrm{d}y\right|\\ &\le c_3(\varepsilon)\int_{U_\varepsilon}|\nabla\overline{f}(x)|\,\mathrm{d}x + c_2\left|\frac{1}{|U_\varepsilon|}\int_{U_\varepsilon}\overline{f}(y)\,\mathrm{d}y\right|\end{aligned}$$

https://doi.org/10.1017/S0962492913000056 Published online by Cambridge University Press

by using the Poincaré inequality for $\overline{f}$ on $U_\varepsilon$. We also have that

$$\left|\frac{1}{|U_\varepsilon|}\int_{U_\varepsilon}\overline{f}(x)\,\mathrm{d}x\right| = \frac{2\varepsilon}{|U_\varepsilon|}\left|\frac{1}{2\varepsilon}\int_{U_\varepsilon}\overline{f}(x)\,\mathrm{d}x - \int_\Gamma f(x)\,\mathrm{d}A(x)\right| \leq c_4\varepsilon\int_\Gamma |f(x)|\,\mathrm{d}A(x).$$

Thus we have the estimate

$$(1-c_1\varepsilon-c_4\varepsilon)\int_\Gamma |f(x)|\,\mathrm{d}A(x) \leq c_3(\varepsilon)\int_{U_\varepsilon}|\nabla\overline{f}(x)|\,\mathrm{d}x \leq c_5(\varepsilon)\int_\Gamma |\nabla_\Gamma f(x)|\,\mathrm{d}A(x).$$

For the last estimate we have used that by definition $\frac{\partial\overline{f}}{\partial\nu}=0$. A suitable choice of $\varepsilon>0$ gives the estimate

$$\int_\Gamma |f(x)|\,\mathrm{d}A(x) \leq c\int_\Gamma |\nabla_\Gamma f(x)|\,\mathrm{d}A(x).$$

This is Poincaré's inequality in $L^1(\Gamma)$. For $p>1$ we apply this result to $|f|^p$ instead of $f$, use that $|\nabla_\Gamma|f|^p| = p|f|^{p-1}|\nabla_\Gamma f|$ and the Hölder inequality, and the theorem is proved. □

The formula for integration by parts on surfaces directly implies Green's formula. From Theorem 2.10, using the summation convention that we sum over doubly appearing indices, we have

$$\int_\Gamma \nabla_\Gamma f\cdot\nabla_\Gamma g\,\mathrm{d}A = \int_\Gamma \underline{D}_i f\underline{D}_i g\,\mathrm{d}A = \int_\Gamma \underline{D}_i(f\underline{D}_i g)\,\mathrm{d}A - \int_\Gamma f\underline{D}_i\underline{D}_i g\,\mathrm{d}A$$
$$= \int_\Gamma f\underline{D}_i g H\nu_i\,\mathrm{d}A + \int_{\partial\Gamma} f\underline{D}_i g\mu_i\,\mathrm{d}A - \int_\Gamma f\Delta_\Gamma g\,\mathrm{d}A.$$

Since $\underline{D}_i g\nu_i = \nabla_\Gamma g\cdot\nu = 0$, we have the following theorem.

**Theorem 2.14.**

$$\int_\Gamma \nabla_\Gamma f\cdot\nabla_\Gamma g\,\mathrm{d}A = -\int_\Gamma f\Delta_\Gamma g\,\mathrm{d}A + \int_{\partial\Gamma} f\nabla_\Gamma g\cdot\mu\,\mathrm{d}A. \tag{2.18}$$

## 3. Partial differential equations on surfaces

### *3.1. Elliptic equations on hypersurfaces*

In this section we briefly give the basic ideas for the analysis of elliptic PDEs on hypersurfaces. We assume that $\Gamma$ is a compact and connected hypersurface.

https://doi.org/10.1017/S0962492913000056 Published online by Cambridge University Press

*The Poisson equation*

We begin with the model case of the Poisson equation

$$-\Delta_\Gamma u = f \tag{3.1}$$

on a compact hypersurface $\Gamma$ in $\mathbb{R}^{n+1}$ and thus without boundary. Here $f$ is a given right-hand side or source term which is taken to be from $L^2(\Gamma)$ or more generally from $H^{-1}(\Gamma)$, the dual space of $H^1(\Gamma)$.

A *weak solution* of (3.1) is a function $u \in H^1(\Gamma)$ which satisfies the relation

$$\int_\Gamma \nabla_\Gamma u \cdot \nabla_\Gamma \varphi \,\mathrm{d}A = \int_\Gamma f\varphi \,\mathrm{d}A \tag{3.2}$$

for every test function $\varphi \in H^1(\Gamma)$. Since $\varphi = 1$ is allowed as a test function we have to impose the condition $\int_\Gamma f = 0$ on the right-hand side. If the right-hand side $f$ is a functional only from $H^{-1}(\Gamma)$, then the weak form of the equation reads

$$\int_\Gamma \nabla_\Gamma u \cdot \nabla_\Gamma \varphi \,\mathrm{d}A = \langle f, \varphi \rangle,$$

where the brackets stand for the evaluation of the functional $f$ at the function $\varphi$.

Obviously there is no uniqueness of weak solutions in this case, since every constant is a solution. We will fix the free constant by choosing the mean value of $u$ to vanish. The following theorem can easily be proved.

**Theorem 3.1.** Let $\Gamma \in C^2$ be a compact hypersurface in $\mathbb{R}^{n+1}$ and assume that $f \in H^{-1}(\Gamma)$ with the property $\langle f, 1 \rangle = 0$. Then there exists a unique solution $u \in H^1(\Gamma)$ of (3.2) with $\int_\Gamma u \,\mathrm{d}A = 0$.

The proof is an application of the Lax–Milgram theorem or the Riesz representation theorem. The bilinear form

$$a(u, v) = \int_\Gamma \nabla_\Gamma u \cdot \nabla_\Gamma v \,\mathrm{d}A$$

is a scalar product on the Hilbert space $X = \{u \in H^1(\Gamma) \mid \int_\Gamma u \,\mathrm{d}A = 0\}$ because of Poincaré's inequality (2.16). The right-hand side $f$ was chosen to be in the space $H^{-1}(\Gamma)$ of linear functionals.

Besides the existence of weak solutions the most important ingredient for suitable numerics is the proof of regularity and of *a priori* estimates for solutions of the Poisson equation. We shall show how to prove an *a priori* estimate in the $H^2(\Gamma)$ norm. For this we use the following little lemma, in which we use the usual notational convention for the seminorms $|\cdot|_{H^1(\Gamma)}$ and $|\cdot|_{H^2(\Gamma)}$.

**Lemma 3.2.** Let $\Gamma \in C^2$ and $u \in H^2(\Gamma)$. Then

$$|u|_{H^2(\Gamma)} \leq \|\Delta_\Gamma u\|_{L^2(\Gamma)} + c|u|_{H^1(\Gamma)} \tag{3.3}$$

https://doi.org/10.1017/S0962492913000056 Published online by Cambridge University Press

with the constant $c = \sqrt{\|H\mathcal{H} - 2\mathcal{H}^2\|_{L^\infty(\Gamma)}}$.

*Proof.* By approximation arguments we can assume that $\Gamma \in C^3$ and $u \in C^3(\Gamma)$. We have

$$|u|^2_{H^2(\Gamma)} = \sum_{i,j=1}^{n+1} \int_\Gamma (\underline{D}_i \underline{D}_j u)^2 \,\mathrm{d}A,$$

and with the formula for integration by parts on $\Gamma$ (2.13) in combination with Lemma 2.6 we obtain (using the summation convention)

$$\begin{aligned}
\int_\Gamma \underline{D}_i \underline{D}_j u \underline{D}_i \underline{D}_j u \,\mathrm{d}A &= \int_\Gamma \underbrace{\underline{D}_i \underline{D}_j u \underline{D}_j u H \nu_i}_{=0} \,\mathrm{d}A - \int_\Gamma \underline{D}_i \underline{D}_i \underline{D}_j u \underline{D}_j u \,\mathrm{d}A \\
&= -\int_\Gamma \underline{D}_i \big(\underline{D}_j \underline{D}_i u + \underline{D}_k u(\nu_i \mathcal{H}_{jk} - \nu_j \mathcal{H}_{ik})\big) \underline{D}_j u \,\mathrm{d}A \\
&= -\int_\Gamma \underline{D}_i \underline{D}_j \underline{D}_i u \underline{D}_j u \,\mathrm{d}A - \int_\Gamma \underbrace{\underline{D}_i \underline{D}_k u(\nu_i \mathcal{H}_{jk} - \nu_j \mathcal{H}_{ik}) \underline{D}_j u}_{=0} \,\mathrm{d}A \\
&\quad - \int_\Gamma \underline{D}_k u \underline{D}_j u \underline{D}_i (\nu_i \mathcal{H}_{jk} - \nu_j \mathcal{H}_{ik}) \,\mathrm{d}A \\
&= -\int_\Gamma \underline{D}_i \underline{D}_j \underline{D}_i u \underline{D}_j u \,\mathrm{d}A - \int_\Gamma (H\mathcal{H} - \mathcal{H}^2)_{jk} \underline{D}_j u \underline{D}_k u \,\mathrm{d}A.
\end{aligned}$$

For the remaining third-order term we observe that

$$\begin{aligned}
\int_\Gamma \underline{D}_i \underline{D}_j \underline{D}_i u \underline{D}_j u \,\mathrm{d}A &= \int_\Gamma \underline{D}_j \underline{D}_i \underline{D}_i u \underline{D}_j u + \nu_i \mathcal{H}_{jk} \underline{D}_k \underline{D}_i u \underline{D}_j u \,\mathrm{d}A \\
&= \int_\Gamma \underline{D}_j \Delta_\Gamma u \underline{D}_j u \,\mathrm{d}A - \int_\Gamma (\mathcal{H}^2)_{ij} \underline{D}_i u \underline{D}_j u \,\mathrm{d}A \\
&= -\int_\Gamma (\Delta_\Gamma u)^2 \,\mathrm{d}A - \int_\Gamma (\mathcal{H}^2)_{ij} \underline{D}_i u \underline{D}_j u \,\mathrm{d}A.
\end{aligned}$$

Here we have used the fact that

$$\nu_i \underline{D}_k \underline{D}_i u = \underline{D}_k(\nu_i \underline{D}_i u) - \underline{D}_k \nu_i \underline{D}_i u = -\mathcal{H}_{ik} \underline{D}_i u.$$

Altogether we have shown that

$$\begin{aligned}
|u|^2_{H^2(\Gamma)} &= \|\Delta_\Gamma u\|^2_{L^2(\Gamma)} - \int_\Gamma (H\mathcal{H} - 2\mathcal{H}^2) \nabla_\Gamma u \cdot \nabla_\Gamma u \,\mathrm{d}A \\
&\le \|\Delta_\Gamma u\|^2_{L^2(\Gamma)} + \|H\mathcal{H} - 2\mathcal{H}^2\|_{L^\infty(\Gamma)} \|\nabla_\Gamma u\|^2_{L^2(\Gamma)},
\end{aligned}$$

and this finally proves the estimate (3.3). □

With the help of the previous lemma and standard arguments we arrive at the regularity estimate for the solution of the Poisson equation on a compact hypersurface.

https://doi.org/10.1017/S0962492913000056 Published online by Cambridge University Press

**Theorem 3.3.** Assume that $\Gamma \in C^2$ and that $f \in L^2(\Gamma)$ with $\int_\Gamma f \, \mathrm{d}A = 0$. Then the weak solution from Theorem 3.1 satisfies $u \in H^2(\Gamma)$ and

$$\|u\|_{H^2(\Gamma)} \leq c\|f\|_{L^2(\Gamma)}.$$

For the proof we use the basic estimate (choose $\varphi = u$ in (3.2))

$$|u|_{H^1(\Gamma)} \leq c\|f\|_{L^2(\Gamma)}$$

(for which we use Poincaré's inequality again), together with the PDE pointwise almost everywhere, to obtain

$$|u|_{H^2(\Gamma)} \leq c\|f\|_{L^2(\Gamma)},$$

if the solution has square integrable second derivatives.

The $H^2(\Gamma)$-regularity of $u$ is taken from the theory of linear PDEs on Cartesian domains in $\mathbb{R}^n$. Here the arguments are purely local. For this we parametrize the $C^2$ surface $\Gamma$ according to Lemma 2.2 locally by $X \in C^2(\Omega, \Gamma)$, $X = X(\theta)$ with some open domain $\Omega \subset \mathbb{R}^n$. If we set $U(\theta) = u(X(\theta))$, then $U$ is a weak solution of the linear PDE

$$-\big(g^{kj} U_{\theta_j} \sqrt{g}\big)_{\theta_k} = f \circ X \sqrt{g}$$

on $\Omega$. For the notation see Section 2.1. The coefficients of this PDE are in $C^1(\Omega)$ and the right-hand side is in $L^2(\Omega)$ because by assumption $\Gamma \in C^2$. The well-known regularity result from Cartesian PDEs (see for example Gilbarg and Trudinger 1998) then gives $U \in H^2(\Omega')$ for any $\Omega' \subset\subset \Omega$, and this in turn gives $u \in H^2(\Gamma)$.

*General elliptic PDEs*

In the previous section we have shown how the Poisson equation is solved on a compact surface. The methods are easily extended to general linear elliptic PDEs in divergence form and to boundary value problems (on surfaces with a boundary):

$$-\sum_{i,j=1}^{n+1} \underline{D}_i(a_{ij}\underline{D}_j u) - \sum_{i=1}^{n+1} \underline{D}_i(a_i u) + \sum_{i=1}^{n+1} b_i \underline{D}_i u + cu = f - \sum_{i=1}^{n+1} \underline{D}_i g_i. \quad (3.4)$$

We assume for the given coefficients that

$$a_{ij}, a_i, b_i, c \in L^\infty(\Gamma), g_i \in L^2(\Gamma) \quad (i, j = 1, \ldots, n+1).$$

We also assume that the coefficient vectors $a(x) = (a_1(x), \ldots, a_{n+1}(x))$ and $g(x) = (g_1(x), \ldots, g_{n+1}(x))$ are tangent vectors at $x \in \Gamma$, that is, they lie in $T_x\Gamma$, and that the matrix $\mathcal{A}(x) = (a_{ij}(x))_{i,j=1,\ldots,n+1}$ is symmetric and maps the tangent space $T_x\Gamma$ into itself. We emphasize that the latter

https://doi.org/10.1017/S0962492913000056 Published online by Cambridge University Press

condition implies that in general constant coefficients $a_{ij}$ are not admissible. They have to depend on the $x$-variable. Nevertheless $a_{ij} = \delta_{ij}$ is obviously allowed.

As ellipticity condition we assume a so-called Ladyzhenskaya condition, which says that there exists a number $c_0 > 0$ such that

$$\sum_{i,j=1}^{n+1} a_{ij}\xi_i\xi_j + \sum_{i=1}^{n+1} a_i\xi_0\xi_i + \sum_{i=1}^{n+1} b_i\xi_i\xi_0 + c\xi_0^2 \geq c_0 \sum_{i=1}^{n+1} \xi_i^2,$$

almost everywhere on $\Gamma$ for all $\xi = (\xi_1, \ldots, \xi_{n+1}) \in \mathbb{R}^{n+1}$ with $\xi \cdot \nu = 0$ and all $\xi_0 \in \mathbb{R}$.

With the PDE (3.4) we associate the bilinear form $a$,

$$a(u, \varphi) = \int_\Gamma \sum_{i,j=1}^{n+1} a_{ij} \underline{D}_j u \underline{D}_i \varphi + \sum_{i=1}^{n+1} a_i u \underline{D}_i \varphi + \sum_{i=1}^{n+1} b_i \underline{D}_i u \varphi + cu\varphi \, \mathrm{d}A,$$

and the functional $F$,

$$\langle F, \varphi \rangle = \int_\Gamma f\varphi + \sum_{i=1}^{n+1} g_i \underline{D}_i \varphi \, \mathrm{d}A,$$

for $u, \varphi \in H^1(\Gamma)$, for which we assume $\langle F, 1 \rangle = 0$.

**Theorem 3.4.** Let $\Gamma \in C^2$ be a compact hypersurface. Assume that the coefficients satisfy the above conditions. Then there exists a unique weak solution of (3.4) with $\int_\Gamma u \, \mathrm{d}A = 0$, that is, there exists a unique $u \in H^1(\Gamma)$ such that

$$a(u, \varphi) = \langle F, \varphi \rangle$$

for every $\varphi \in H^1(\Gamma)$.

*Proof.* The proof of this theorem is a direct application of the Lax–Milgram theorem. □

## 4. Triangulated surfaces

In this section we discuss the discretization of surfaces in combination with the discretization of elliptic surface PDEs. The continuous surface $\Gamma$ is replaced by a piecewise polynomial surface; in the most simple case the approximating surface $\Gamma_h$ is a polygonal one. This introduces a geometric error between $\Gamma$ and $\Gamma_h$, which we discuss in Section 4.2. In Section 4.4 we introduce finite element spaces on the discrete surface and discretize the PDEs. This is the surface finite element method (SFEM). The error between the continuous solution and the discrete solution is estimated in natural norms in Section 4.5.

https://doi.org/10.1017/S0962492913000056 Published online by Cambridge University Press

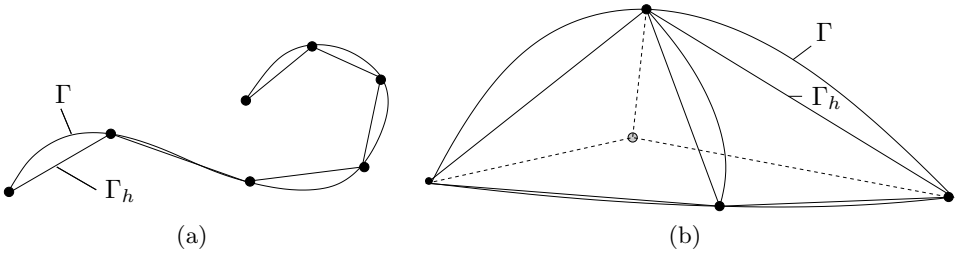



Figure 4.1. (a) Approximation of a smooth curve by a polygonal curve and (b) approximation of a smooth surface by a polygonal surface.

### *4.1. Triangulations*

The smooth $n$-dimensional surface $\Gamma$ ($\partial\Gamma = \emptyset$) is approximated by a surface $\Gamma_h$ which lies in the strip $U_\delta$ (see Lemma 2.8) and which is a Lipschitz surface. The strip can be chosen with locally varying width: see (4.1). In particular, for $n = 1$, $\Gamma_h$ is a polygonal curve, and for $n = 2$, it is a triangulated (and hence polyhedral) surface consisting of triangles. A three-dimensional surface in $\mathbb{R}^4$ consists of tetrahedra.

We assume that the discrete triangulated surface $\Gamma_h$ besides (4.1) has the following properties. $\Gamma_h$ is the union of finitely many non-degenerate (closed) $n$-simplices in $\mathbb{R}^{n+1}$. We let $\mathcal{T}_h$ denote the set of these simplices:

$$\Gamma_h = \bigcup_{T\in\mathcal{T}_h} T.$$

The vertices $X_j$ ($j = 1, \dots, J$) of the simplices are taken to sit on the smooth surface $\Gamma$. For $T, \tilde{T} \in \mathcal{T}_h$, either $T \cap \tilde{T} = \emptyset$ or $T \cap \tilde{T}$ is an $(n-k)$-dimensional side simplex ($k \in \{1, \dots, n\}$) common to both of the simplices $T$ and $\tilde{T}$. For $T \in \mathcal{T}_h$ we denote by $h(T)$ its diameter and by $\rho(T)$ the in-ball radius. Also,

$$h = \max_{T\in\mathcal{T}_h} h(T), \quad \rho = \min_{T\in\mathcal{T}_h} \rho(T).$$

We assume that the quantity

$$\sigma = \max_{T\in\mathcal{T}_h} \sigma(T), \quad \sigma(T) = \frac{h(T)}{\rho(T)}$$

is uniformly bounded independently of $h$.

Note that, by Lemma 2.8, for every simplex $T \subset \Gamma_h$ there is a unique curved simplex $\tilde{T} = a(T) \subset \Gamma$. In order to avoid a global double covering (see Figure 4.2), we assume that for each point $a \in \Gamma$ there is at most one point $x \in \Gamma_h$ with $a = a(x)$. This implies that there is a bijective correspondence between the triangles on $\Gamma_h$ and the induced curvilinear triangles on $\Gamma$.

https://doi.org/10.1017/S0962492913000056 Published online by Cambridge University Press

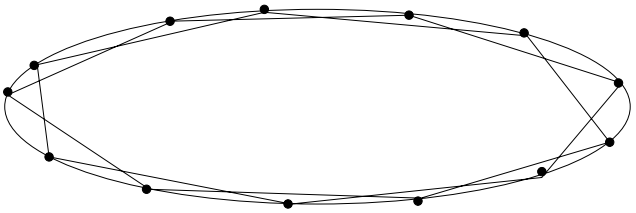


Figure 4.2. Approximation of an ellipse $\Gamma$ by a polygon $\Gamma_h$ violating the simple covering condition.

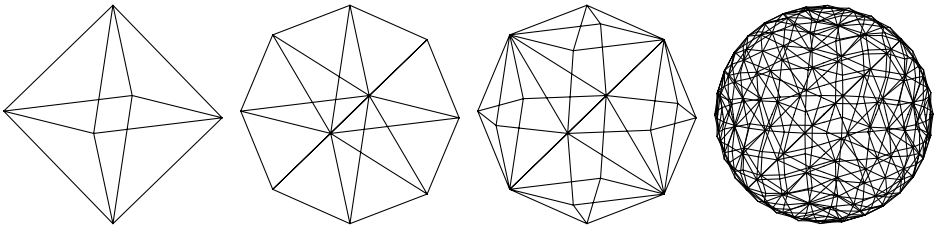



Figure 4.3. Refine and project for the sphere. We start from a macro-triangulation (a) with 6 vertices and 8 triangles, and obtain the first (b), second (c) and sixth (d) refinement. The finest triangulation consists of 258 vertices and 512 triangles. The method of refinement is bisection of triangles.

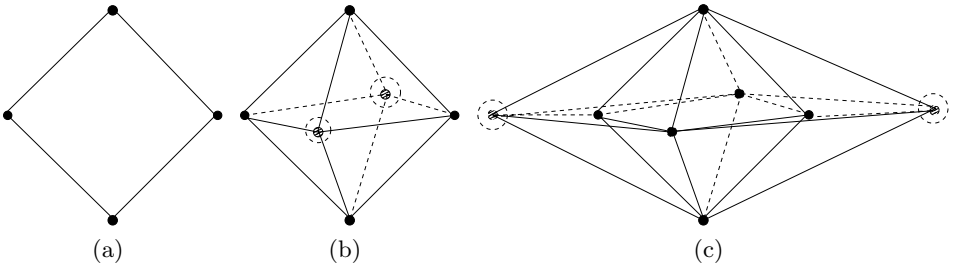



Figure 4.4. Discrete spheres as a macro-triangulation of $S^1$, $S^2$ and $S^3$ (symbolically). We start with the macro-triangulation of $S^1$ (a), embed it into $\mathbb{R}^3$ and add two new vertices (surrounded by circles) to obtain a macro-triangulation of $S^2$ (b). We embed it into $\mathbb{R}^4$ and add new vertices to obtain a macro-triangulation of $S^3$ (c).

https://doi.org/10.1017/S0962492913000056 Published online by Cambridge University Press

For the description of the approximation of surfaces we take the practical point of view. In order to generate triangulated parametric surfaces the two main techniques are as follows.

(1) Construct a macro-triangulation for the given smooth surface in such a way that the coarse discrete surface $\Gamma_h$ is contained in a strip of unique projection around $\Gamma$. Then refine and project the new nodes onto the smooth surface. For an example see Figure 4.3.

(2) Glue together patches (charts). Here one follows the classical differential geometric path. The additional difficulty from the numerical point of view is the joining of two or more different grids.

Both methods can be used to generate a discretization of a standard surface such as a sphere, which can then serve as a parameter domain for the surface to be approximated. One may think of deforming the available discrete surface in order to obtain a new discrete surface. An example of this method is shown in Figure 4.5, where the surface shown is an image of a discretized cylinder.

*Refine and project.* The following can be understood as setting up a macro-triangulation approximating the smooth surface. For this method we use the description introduced in Section 2.3. We assume that $\Gamma$ has only one connected component. We start with a discrete surface $\Gamma_h$ contained in the variable strip $U_\delta$,

$$\Gamma_h \subset U_\delta = \{y + s\nu(y) \mid |s| < \delta(y), y \in \Gamma\}, \tag{4.1}$$

where for a point $y \in \Gamma$ we set

$$\delta(y) = \min\left\{ \left( \max_{i=1,\dots,n} |\kappa_i(y)| \right)^{-1}, \sup_{z\in\Gamma, z\neq y} \frac{L(y,z)}{|y-z|} \right\}$$

with the sectional curvatures $\kappa_i$. $L(y,z)$ denotes the geodesic distance between $y$ and $z$ on $\Gamma$. Just as in Section 2.3, one can show that each point $x \in U_\delta$ can be uniquely projected onto the smooth surface, yielding the decomposition

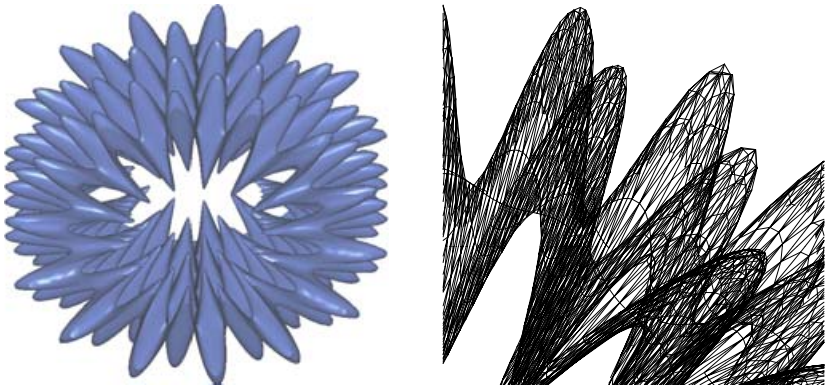
$$x = a(x) + d(x)\nu(a(x)), \quad x \in U_\delta,$$

with $a(x)$ the orthogonal projection of $x$ onto $\Gamma$ and $d(x)$ the oriented distance between $x$ and $\Gamma$. Given a refinement of $\Gamma_h$, a new refined triangulation of $\Gamma$ may be obtained by projecting the new nodes on $\Gamma_h$ onto $\Gamma$.

For any function $\eta$ defined on the discrete surface $\Gamma_h$ we define an extension or lift onto $\Gamma$ by

$$\eta^l(a) = \eta(x(a)), \quad a \in \Gamma, \tag{4.2}$$

https://doi.org/10.1017/S0962492913000056 Published online by Cambridge University Press



(a) (b)

Figure 4.5. (a) A complicated hypersurface $\Gamma$ approximated by a piecewise linear surface. (b) Close-up of the discrete surface $\Gamma_h$.

where, by our assumptions, $x(a)$ is defined as the unique solution of

$$x = a + d(x)\nu(a). \tag{4.3}$$

Furthermore, we understand by $\eta^l(x)$ the constant extension from $\Gamma$ in the normal direction $\nu(a(x))$.

We will use a finite element space

$$S_h = \{\phi_h \in C^0(\Gamma_h) \mid \varphi_h|_T \text{ is linear affine for each } T \in \mathcal{T}_h\}. \tag{4.4}$$

The lifted finite element space is then

$$S_h^l = \{\varphi_h = \phi_h^l \mid \phi_h \in S_h\}. \tag{4.5}$$

### *4.2. Approximation of geometry*

In order to avoid too many technical arguments, we begin with a piecewise linear approximation of a smooth surface $\Gamma \in C^2$ and its geometry. The extension to a higher-order approximation then follows the arguments in the piecewise linear case, and in fact is based upon a piecewise linear approximation.

#### *Piecewise linear approximation of geometry*

In this section we collect estimates for the geometric error which is produced by approximating the smooth surface $\Gamma$ by a discrete surface $\Gamma_h$.

The following technical lemma gives more detailed information about the order of approximation of the geometry.

https://doi.org/10.1017/S0962492913000056 Published online by Cambridge University Press

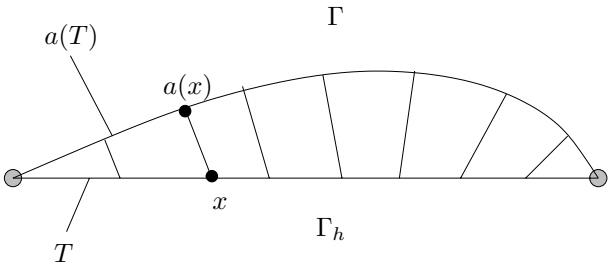



Figure 4.6. A curved 'simplex' $a(T)$ is parametrized over a planar one. Orthogonal projection onto the smooth surface $\Gamma$.

**Lemma 4.1.** Assume $\Gamma$ and $\Gamma_h$ are as above. The map $a : \Gamma_h \to \Gamma$ is bijective. For the oriented distance function to $\Gamma$ we have the estimate

$$\|d\|_{L^\infty(\Gamma_h)} \leq ch^2. \tag{4.6}$$

The quotient, $\delta_h$, between the smooth and discrete surface measures $\mathrm{d}A$, and $\mathrm{d}A_h$, defined by $\delta_h \,\mathrm{d}A_h = \mathrm{d}A$, satisfies

$$\|1 - \delta_h\|_{L^\infty(\Gamma_h)} \leq ch^2. \tag{4.7}$$

Let $P$ and $P_h$ be the projections onto the tangent planes, $P_{ij} = \delta_{ij} - \nu_i\nu_j$, $P_{h,ij} = \delta_{ij} - \nu_{h,i}\nu_{h,j}$, and let

$$R_h = \frac{1}{\delta_h} P(I - d\mathcal{H})P_h(I - d\mathcal{H}), \tag{4.8}$$

$\mathcal{H}_{ij} = d_{x_i x_j} = \nu_{i_{x_j}}$. Then

$$\|(I - R_h)P\|_{L^\infty(\Gamma_h)} \leq ch^2. \tag{4.9}$$

*Proof.* Let $T \in \mathcal{T}_h$ be a simplex of the discrete surface. By assumption it lies in the strip $U_\delta$ (see Lemma 2.8). Without loss of generality we may assume that $T \subset \mathbb{R}^n \times \{0\}$. The corresponding curved triangle $\tilde{T} = a(T)$ is thus parametrized over $T$. Note that the parametrization is not given as a (vertical) graph. This is crucial for all our arguments! See Figure 4.6 for a sketch of the situation.

We let $I_h$ denote the Lagrange interpolation on $T$. Since the vertices of $T$ lie on $\Gamma$, we have that the interpolant $I_h d$ vanishes identically on $T$ and, with the well-known estimates for the Lagrangian interpolation (see Ciarlet 1978), we obtain

$$\|d\|_{L^\infty(T)} = \|d - I_h d\|_{L^\infty(T)} \leq ch^2 |d|_{H^{2,\infty}(T)} \leq ch^2 \|d\|_{C^2(U_\delta)}, \tag{4.10}$$

and similarly, for $j = 1, \ldots, n$,

$$\|\nu_j\|_{L^\infty(T)} = \|d_{x_j}\|_{L^\infty(T)} = \|(d - I_h d)_{x_j}\|_{L^\infty(T)} \leq ch \|d\|_{C^2(U_\delta)}. \tag{4.11}$$

https://doi.org/10.1017/S0962492913000056 Published online by Cambridge University Press

To derive the estimate of the surface elements (4.7), we observe that

$$\mathrm{d}A = \sqrt{D_1^2 + \cdots + D_{n+1}^2}\,\mathrm{d}x_1 \cdots \mathrm{d}x_n$$

while $\mathrm{d}A_h = \mathrm{d}x_1 \cdots \mathrm{d}x_n$, with

$$D_i = (-1)^{n+1+i} \begin{vmatrix} \frac{\partial a_1}{\partial x_1} & \cdots & \frac{\partial a_1}{\partial x_n} \\ \vdots & \vdots & \vdots \\ \frac{\partial a_{i-1}}{\partial x_1} & \cdots & \frac{\partial a_{i-1}}{\partial x_n} \\ \frac{\partial a_{i+1}}{\partial x_1} & \cdots & \frac{\partial a_{i+1}}{\partial x_n} \\ \vdots & \vdots & \vdots \\ \frac{\partial a_{n+1}}{\partial x_1} & \cdots & \frac{\partial a_{n+1}}{\partial x_n} \end{vmatrix}.$$

Now $a_j(x) = x_j - d(x)\nu_j(x)$, and thus for $j,k = 1,\ldots,n$,

$$\frac{\partial a_j}{\partial x_k} = \delta_{jk} - \nu_k(x)\nu_j(x) - d(x)\mathcal{H}_{jk}(x) = P(x)_{jk} + O(h^2), \tag{4.12}$$

since from (4.10) and (4.11) we know that $|\nu_k\nu_j| \le ch^2$ for $j,k = 1,\ldots,n$ and $|d\mathcal{H}_{jk}| \le ch^2$. Similarly, for $j = 1,\ldots,n$,

$$\frac{\partial a_{n+1}}{\partial x_j} = -\nu_{n+1}\nu_j + O(h^2). \tag{4.13}$$

The multilinearity of the determinant, together with (4.12) and (4.13), implies that for $i = 1,\ldots,n$

$$D_i = -\nu_{n+1}\nu_i + O(h^2), \quad D_{n+1} = 1 + O(h^2). \tag{4.14}$$

Then

$$\begin{aligned}\sqrt{D_1^2 + \cdots + D_{n+1}^2} - 1 &= \frac{D_1^2 + \cdots + D_{n+1}^2 - 1}{\sqrt{D_1^2 + \cdots + D_{n+1}^2} + 1} \\ &= \frac{\nu_{n+1}^2(1-\nu_{n+1}^2) + O(h^2)}{\sqrt{D_1^2 + \cdots + D_{n+1}^2} + 1} = O(h^2),\end{aligned}$$

because $\nu_{n+1}^2 = 1 + O(h^2)$. We have proved (4.7).

The proof of (4.9) follows from the previous estimates when we keep in mind that in our situation $\nu_h = e_{n+1}$. Note that by $\nu_h$ we mean the piecewise constant vector defined by the normals to the simplices of $\Gamma_h$. We find that

$$(R_h - I)P = PP_hP - P + O(h^2) = O(h^2),$$

since for a unit vector $z$ we have

$$|(PP_hP - P)z| = |z \cdot \big(\nu_h - (\nu_h \cdot \nu)\nu\big)(\nu_h - (\nu_h \cdot \nu)\nu)| \le ch^2,$$

https://doi.org/10.1017/S0962492913000056 Published online by Cambridge University Press

because from (4.11),

$$|\nu_h - (\nu_h \cdot \nu)\nu| = |e_{n+1} - \nu_{n+1}\nu| = \sqrt{1-\nu_{n+1}^2} = O(h).$$

This proves (4.9). □

In order to compare the norms between functions on $\Gamma_h$ and their lift (4.2) to $\Gamma$ we need the following lemma.

**Lemma 4.2.** Let $\eta : \Gamma_h \to \mathbb{R}$ with lift $\eta^l : \Gamma \to \mathbb{R}$. Then, for the plane $T \subset \Gamma_h$, and smooth curved triangles $\tilde{T} \subset \Gamma$, the following estimates hold if the norms exist. There is a constant $c > 0$ independent of $h$ such that

$$\frac{1}{c}\|\eta\|_{L^2(T)} \le \|\eta^l\|_{L^2(\tilde{T})} \le c\|\eta\|_{L^2(T)}, \tag{4.15}$$

$$\frac{1}{c}\|\nabla_{\Gamma_h}\eta\|_{L^2(T)} \le \|\nabla_\Gamma \eta^l\|_{L^2(\tilde{T})} \le c\|\nabla_{\Gamma_h}\eta\|_{L^2(T)}, \tag{4.16}$$

$$\|\nabla^2_{\Gamma_h}\eta\|_{L^2(T)} \le c\|\nabla^2_\Gamma \eta^l\|_{L^2(\tilde{T})} + ch\|\nabla_\Gamma \eta^l\|_{L^2(\tilde{T})}. \tag{4.17}$$

*Proof.* The proof is contained in Dziuk (1988). Here we only give the main ideas. In the following let $d$ be the distance function with respect to the smooth surface $\Gamma$. By definition (see (4.2))

$$\eta(x) = \eta^l(x - d(x)\nu(x)), \quad x \in \Gamma_h.$$

The chain rule together with the definition of the tangential gradients on smooth and discrete surface, the latter one in a piecewise sense, gives

$$\nabla_{\Gamma_h}\eta(x) = P_h(x)\big(I - d(x)\mathcal{H}(x)\big)\nabla_\Gamma \eta^l(a(x)), \quad x \in \Gamma_h, \tag{4.18}$$

where $P_h$ and $\mathcal{H}$ are as in Lemma 4.1. The results then easily follow from the estimates of that lemma, and in particular the estimate $0 < \frac{1}{c} \le \delta_h \le c < \infty$. □

For later use we list interpolation inequalities which are now available. The lemma was proved in Dziuk (1988) for the gradient. It is easily extended to the $L^2$-estimate.

**Lemma 4.3 (interpolation).** For $n \le 3$ and given $\eta \in H^2(\Gamma)$, there exists a unique $I_h\eta \in S_h^l$ such that

$$\|\eta - I_h\eta\|_{L^2(\Gamma)} + h\|\nabla_\Gamma(\eta - I_h\eta)\|_{L^2(\Gamma)} \le ch^2\big(\|\nabla^2_\Gamma\eta\|_{L^2(\Gamma)} + h\|\nabla_\Gamma\eta\|_{L^2(\Gamma)}\big). \tag{4.19}$$

*Proof.* The interpolant is constructed in an obvious way. Since $\eta \in H^2(\Gamma)$, by Sobolev's embedding it is in $C^0(\Gamma)$ since $\Gamma$ is at most three-dimensional. (Compare with Remark 4.10.) Thus the pointwise linear interpolation $\tilde{I}_h\eta \in X_h$ is well defined. The vertices of $\Gamma_h$ lie on the smooth surface $\Gamma$ and so the nodal values of $\eta$ are well defined for this interpolation. We then lift $\tilde{I}_h\eta$ onto $\Gamma$ by the process $I_h\eta = (\tilde{I}_h\eta)^l$ according to (4.2). □

https://doi.org/10.1017/S0962492913000056 Published online by Cambridge University Press

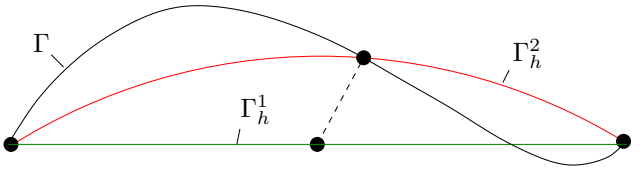



Figure 4.7. Higher-order approximation $\Gamma_h^k$ to $\Gamma$ for $k = 2$.

*Higher-order approximation of geometry*

In the previous subsection we discussed the polygonal approximation of smooth hypersurfaces. The higher-order approximation of the smooth surface $\Gamma$ is based on the piecewise linear approximation and is related to an isoparametric approximation to boundaries in the usual finite element methods. Let

$$\Gamma_h^1 = \bigcup_{T^1 \in \mathcal{T}_h^1} T^1$$

be the piecewise linear approximation of $\Gamma$ from the previous subsection. As shown, the map $a : \Gamma_h^1 \to \Gamma$ is bijective. We denote by $a^k = I_h^k a \in \mathbb{P}_k(T^1)$ the $k$th-order interpolation on the planar simplex $T^1$ at the Lagrange nodes of $T^1$. We then define the $k$th-order discrete surface $\Gamma_h^k$ by

$$\Gamma_h^k = \bigcup_{T^1 \in \mathcal{T}_h^1} a^k(T^1).$$

Figure 4.7 illustrates this definition. Then the next lemma follows from the proof of Lemma 4.1 in combination with the common estimates for the Lagrange interpolation on (flat) simplices: see Demlow (2009).

**Lemma 4.4.** Assume that $\Gamma$ is as in Lemma 4.1 and let $\Gamma_h^k$ be the $k$th-order ($k \geq 1$) approximation described above. Then we have the estimates

$$\|d\|_{L^\infty(\Gamma_h^k)} + \|1 - \delta_h^k\|_{L^\infty(\Gamma_h^k)} + \|(I - R_h^k)P\|_{L^\infty(\Gamma_h^k)} \leq ch^{k+1},$$

where $\delta_h^k$ is the quotient of the surface measures on $\Gamma$ and on $\Gamma_h^k$, $\mathrm{d}A = \delta_h^k \,\mathrm{d}A_h$, and $\delta_h^k R_h^k = P(I - d\mathcal{H})P_h^k(I - d\mathcal{H})$ with the projection $P_h^k = I - \nu_h^k \otimes \nu_h^k$ onto $\Gamma_h^k$ with the normal $\nu_h^k$ of $\Gamma_h^k$.

### *4.3. Discrete charts*

We end this section by adding some information on a discrete differential geometric approach which is consistent with the introduction of parametrized surfaces in Section 2.1. For a complete exposition see Nedelec (1976).

https://doi.org/10.1017/S0962492913000056 Published online by Cambridge University Press

Let $\Gamma$ be given as in Section 2.1 by local charts $(X_i)_{i\in I}$, $X_i \in C^k(V_i, \mathbb{R}^{n+1})$. We assume that already

$$\Gamma = \bigcup_{i\in I} X_i(V_{ih}),$$

with $V_{ih} \subset V_i$ and triangulated domains $V_{ih} \subset \mathbb{R}^n$. We interpolate the smooth parametrization $X_{ih} = I_h X_i$, where $I_h$ is the interpolation from Lemma 4.3 on the polygonal domain $V_{ih}$. We assume that if $U_{ij} = X_{ih}(V_{ih}) \cap X_{jh}(V_{jh}) \neq \emptyset$, then the map $X_{ih}^{-1} \circ X_{jh} : X_{jh}^{-1}(U_{ij}) \to X_{ih}^{-1}(U_{ij})$ is bijective, continuous and piecewise linear. Then the discrete surface is defined by

$$\Gamma_h = \bigcup_{i\in I} X_{ih}(V_{ih}).$$

The advantage of this way to discretize the surface $\Gamma$ is that it allows the approximation of immersions.

### *4.4. The surface finite element method* (SFEM)

In the previous section we constructed and analytically treated an approximation of the smooth surface $\Gamma$ by a discrete surface $\Gamma_h$. For the following the discrete surface is the union of $n$-simplices, $\Gamma_h = \cup_{T\in\mathcal{T}_h} T$. The extension to higher-order approximations is then an extension. For a function $g : \Gamma_h \to \mathbb{R}$ we understand the *tangential gradient* on the discrete surface in the sense of Definition 2.3 as

$$\nabla_{\Gamma_h} g = P_h \nabla g$$

in a piecewise sense, on each simplex. Here $(P_h)ij = \delta_{ij} - \nu_{hi}\nu_{hj}$ $(i, j = 1, \dots, n)$. $\nabla g$ denotes the $(n+1)$-dimensional gradient of a continuation of $g$ orthogonal to the simplex.

In the following we will set up a finite element method on this discrete surface in order to solve PDEs. Because this approach is quite transparent, we treat piecewise linear finite elements on the discrete surface first, and we solve the Poisson equation.

We use the finite element space (see (4.4))

$$S_h = \{\phi_h \in C^0(\Gamma_h) \mid \varphi_h|_T \text{ is linear affine for each } T \in \mathcal{T}_h\}. \tag{4.20}$$

This space is spanned by the nodal basis $\chi_1, \dots, \chi_J$, which is given by

$$\chi_j \in S^h, \quad \chi_j(X_k) = \delta_{jk} \quad (j, k = 1, \dots, J).$$

Here we denote by $X_j \in \Gamma$ the nodes, *i.e.*, the vertices, of the triangulation $\mathcal{T}_h$. Every function $U_h \in S_h$ has the form

$$U_h(x) = \sum_{j=1}^{J} \alpha_j \chi_j(x) \quad (x \in \Gamma_h)$$

https://doi.org/10.1017/S0962492913000056 Published online by Cambridge University Press

with real constants $\alpha_j$ $(j = 1, \dots, J)$.

Associated with the finite element space $S_h$ defined on the discrete surface is the lifted finite element space

$$S_h^l = \{\varphi_h = \phi_h^l \mid \phi_h \in S_h\}. \tag{4.21}$$

Note that $S_h^l$ is a subspace of the continuous space $H^1(\Gamma)$. This space will appear in theoretical considerations only.

*Intermediate remark.* We can define $r$th-order finite element spaces on $k$th-order approximations of the smooth surface: see Lemma 4.4. The finite element space of $r$th order $(r \geq 1)$ on the piecewise linear approximation $\Gamma_h^1$ to $\Gamma$ is given by

$$S_{h,r}^1 = \{\varphi_h \in C^0(\Gamma_h^1) \mid \varphi_h\big|_T \in \mathbb{P}_r(T), T \in \mathcal{T}_h^1\}.$$

The general isoparametric finite element space on $\Gamma_h^k$ is then defined by

$$S_{h,r}^k = \{\varphi_h \in C^0(\Gamma_h^k) \mid \varphi_h \circ a^k \in S_{h,r}^1\}.$$

In the following we will continue to work with piecewise linear finite elements on piecewise linear approximations $\Gamma_h = \Gamma_h^1$ and $S_h = S_{h,1}^1$ with $S_h$ from (4.4), to keep the methods transparent. For more information concerning the higher-order case we refer to Demlow (2009).

**Definition 4.5.** Let $F_h \in L^2(\Gamma_h)$ with the property that $\int_{\Gamma_h} F_h \,\mathrm{d}A_h = 0$. A function $U_h \in S_h$ is a discrete solution of the Poisson equation (3.1) on $\Gamma_h$ if

$$\int_{\Gamma_h} \nabla_{\Gamma_h} U_h \cdot \nabla_{\Gamma_h} \phi_h \,\mathrm{d}A_h = \int_{\Gamma_h} F_h \phi_h \,\mathrm{d}A_h, \tag{4.22}$$

for every discrete test function $\phi_h \in S_h$.

The discrete Poisson equation is a linear system for the solution $U_h = \sum_{j=1}^J \alpha_j \chi_j$. Equation (4.22) is equivalent to

$$\sum_{j=1}^n \mathcal{S}_{kj} \alpha_j = F_k \quad (k = 1, \dots, J),$$

where

$$\mathcal{S}_{kj} = \int_{\Gamma_h} \nabla_{\Gamma_h} \chi_k \cdot \nabla_{\Gamma_h} \chi_j \,\mathrm{d}A_h \quad (k, j = 1, \dots, J)$$

is the stiffness matrix and $F_k = \int_{\Gamma_h} F_h \chi_k \,\mathrm{d}A_h$ $(k = 1, \dots, J)$ is the right-hand side. The linear system then reads

$$\mathcal{S}\alpha = F$$

for $\alpha = (\alpha_1, \dots, \alpha_J)$ and with $F = (F_1, \dots, F_J)$.

https://doi.org/10.1017/S0962492913000056 Published online by Cambridge University Press

First we note that, for solvability of the discrete system, we need the integral over the right-hand side $F_h$ to vanish, because in (4.22) $\phi_h = 1$ is a possible test function. According to the continuous setting the linear system is not uniquely solvable, but solvable only up to additive constants.

**Lemma 4.6.** Assume that the situation is as in Definition 4.5. Then there is a unique discrete solution to the Poisson equation with the property that

$$\int_{\Gamma_h} U_h \,\mathrm{d}A_h = 0.$$

*Proof.* We only have to show uniqueness for a solution. For this we insert $\phi_h = U_h$ as a test function into the homogeneous Poisson equation ((4.22) with $F_h = 0$) and find that $\|\nabla_{\Gamma_h} U_h\|_{L^2(\Gamma_h)} = 0$. This implies that $U_h$ is constant on each simplex of the triangulation separately. Since $U_h \in C^0(\Gamma_h)$, $U_h = c \in \mathbb{R}$ on $\Gamma_h$. Since the integral of $U_h$ over $\Gamma_h$ vanishes, we have that $U_h = 0$ on $\Gamma_h$. □

With respect to the implementation of the method we mention that the method is precisely like a Euclidean method except for the fact that the nodes of the triangulation are $(n+1)$-dimensional. Since the stiffness matrix is assembled in a loop over all simplices and set up by calculating element stiffness matrices for $T \in \mathcal{T}_h$,

$$\mathcal{S}^T_{jk} = \int_T \nabla_{\Gamma_h} \chi^T_j \cdot \nabla_{\Gamma_h} \chi^T_k \,\mathrm{d}A_h \quad (j,k = 1,\dots,n+1),$$

the method is quite simple. Note that the element stiffness matrix is a planar integral. By $\chi^T_k$ we denote the basis function with respect to the $k$th vertex of $T$.

### *4.5. Error analysis*

We begin with an estimate for the geometric error when approximating bilinear forms. The most important bilinear forms are

$$m(u,\varphi) = \int_\Gamma u\varphi \,\mathrm{d}A, \quad a(u,\varphi) = \int_\Gamma \nabla_\Gamma u \cdot \nabla_\Gamma \varphi \,\mathrm{d}A, \tag{4.23}$$

for $u, \varphi \in H^1(\Gamma)$, and the discrete analogues

$$m_h(U_h,\phi_h) = \int_{\Gamma_h} U_h\phi_h \,\mathrm{d}A_h, \quad a_h(U_h,\phi_h) = \int_{\Gamma_h} \nabla_{\Gamma_h} U_h \cdot \nabla_{\Gamma_h} \phi_h \,\mathrm{d}A_h, \tag{4.24}$$

for $U_h, \phi_h \in S_h$.

In the following lemma we bound the geometric perturbation errors in the bilinear forms.

https://doi.org/10.1017/S0962492913000056 Published online by Cambridge University Press

**Lemma 4.7.** For any $(W_h, \phi_h) \in S_h \times S_h$ with corresponding lifts $(w_h, \varphi_h) \in S_h^l \times S_h^l$, the following bounds hold:

$$|m(w_h, \varphi_h) - m_h(W_h, \phi_h)| \leq ch^2 \|w_h\|_{L^2(\Gamma)} \|\varphi_h\|_{L^2(\Gamma)}, \tag{4.25}$$

$$|a(w_h, \varphi_h) - a_h(W_h, \phi_h)| \leq ch^2 \|\nabla_\Gamma w_h\|_{L^2(\Gamma)} \|\nabla_\Gamma \varphi_h\|_{L^2(\Gamma)} \tag{4.26}$$

*Proof.* The bound (4.25) follows by noting that

$$\begin{aligned} &|m(w_h, \varphi_h) - m_h(W_h, \phi_h)| \\ &\quad = \left| \int_\Gamma \left(1 - \frac{1}{\delta_h^l}\right) w_h \varphi_h \right| \leq \left\| 1 - \frac{1}{\delta_h} \right\|_{L^\infty(\Gamma_h)} \|w_h\|_{L^2(\Gamma)} \|\varphi_h\|_{L^2(\Gamma)} \end{aligned}$$

and using Lemma 4.1.

In order to prove (4.26) it is convenient to introduce the notation

$$\mathcal{Q}_h = \frac{1}{\delta_h}(I - d\mathcal{H}) P P_h P (I - d\mathcal{H}) = \frac{1}{\delta_h} P (I - d\mathcal{H}) P_h (I - d\mathcal{H}) P$$

on $\Gamma_h(t)$, and its lifted version, $\mathcal{Q}_h^l$ on $\Gamma$. Using (4.18) we may write on $\Gamma_h$

$$\begin{aligned} &\nabla_{\Gamma_h} W_h \cdot \nabla_{\Gamma_h} \phi_h \\ &\qquad = P_h (I - d\mathcal{H}) \nabla_\Gamma w_h(a) \cdot P_h (I - d\mathcal{H}) \nabla_\Gamma \varphi_h(a) \\ &\qquad = P_h P (I - d\mathcal{H}) \nabla_\Gamma w_h(a) \cdot P_h P (I - d\mathcal{H}) \nabla_\Gamma \varphi_h(a) \\ &\qquad = \delta_h \mathcal{Q}_h \nabla_\Gamma w_h(a) \cdot \nabla_\Gamma \varphi_h(a). \end{aligned}$$

We use the geometry estimate (4.8) from Lemma 4.1 and get the estimate

$$|P - \mathcal{Q}_h| \leq ch^2.$$

Hence the bound (4.26) follows from

$$\begin{aligned} &a(w_h, \varphi_h) - a_h(W_h, \phi_h) \\ &\qquad = \int_\Gamma \nabla_\Gamma w_h \cdot \nabla_\Gamma \varphi_h \, \mathrm{d}A - \int_{\Gamma_h} \delta_h \mathcal{Q}_h \nabla_\Gamma w_h \circ a \cdot \nabla_\Gamma \varphi_h \circ a \, \mathrm{d}A_h \\ &\qquad = \int_\Gamma (P - \mathcal{Q}_h) \nabla_\Gamma w_h \cdot \nabla_\Gamma \varphi_h \, \mathrm{d}A. \end{aligned}$$

Thus we have proved Lemma 4.7. □

**Example 4.8.** As an example of the solution of the Poisson equation on a surface without boundary we take the surface from Figure 4.8. The hypersurface was constructed by mapping a discretization of the unit sphere $S^2$ onto the surface $\Gamma$ by

$$F(y_1, y_2, y_3) = \left(2y_1, y_2, \frac{1}{2} y_3 \left(1 + \frac{1}{2}\sin(2\pi y_1)\right)\right), \quad y = (y_1, y_2, y_3) \in S^2.$$

https://doi.org/10.1017/S0962492913000056 Published online by Cambridge University Press

Table 4.1. Errors and experimental orders of convergence (EOC) for Example 4.8 in the $L^\infty(\Gamma)$, $L^2(\Gamma)$ and $H^1(\Gamma)$ norms.

| $h$ | $E_{L^\infty(\Gamma)}(h)$ | EOC | $E_{L^2(\Gamma)}(h)$ | EOC | $E_{H^1(\Gamma)}(h)$ | EOC |
|---|---|---|---|---|---|---|
| 2.0615 | 0.62256 | – | 0.85015 | – | 0.42326 | – |
| 1.4577 | 0.47755 | 0.76 | 0.78648 | 0.22 | 0.17300 | 2.58 |
| 1.0126 | 0.17590 | 2.74 | 0.20326 | 3.71 | $4.3717\times10^{-2}$ | 3.77 |
| 0.60406 | $4.4493\times10^{-2}$ | 2.66 | $4.5902\times10^{-2}$ | 2.87 | $3.3671\times10^{-2}$ | 0.50 |
| 0.33968 | $1.1708\times10^{-2}$ | 2.31 | $1.0577\times10^{-2}$ | 2.54 | $1.3849\times10^{-2}$ | 1.54 |
| 0.17613 | $2.9819\times10^{-3}$ | 2.08 | $2.6590\times10^{-3}$ | 2.10 | $7.9195\times10^{-3}$ | 0.85 |
| $8.8805\times10^{-2}$ | $7.5899\times10^{-4}$ | 1.99 | $6.6591\times10^{-4}$ | 2.02 | $3.7204\times10^{-3}$ | 1.10 |
| $4.4476\times10^{-2}$ | $1.8974\times10^{-4}$ | 2.00 | $1.6651\times10^{-4}$ | 2.00 | $1.9332\times10^{-3}$ | 0.94 |
| $2.2242\times10^{-2}$ | $4.7476\times10^{-5}$ | 1.99 | $4.1628\times10^{-5}$ | 2.00 | $9.5198\times10^{-4}$ | 1.02 |

The grid is shown in Figure 4.9. The representation of $\Gamma = F(S^2)$ as a hypersurface $\{x \in \mathbb{R}^3 \mid \phi(x) = 0\}$ follows from $y_1^2 + y_2^2 + y_3^2 = 1$ with the level set function

$$\phi(x) = \frac{1}{4}x_1^2 + x_2^2 + \frac{4x_3^2}{(1 + \frac{1}{2}\sin(\pi x_1))^2} - 1.$$

From $\phi$ we calculate the normal $\nu = \frac{\nabla\phi}{|\nabla\phi|}$ of $\Gamma$. As exact solution we choose $u(x) = x_1x_2$ $(x \in \Gamma)$. We then calculate the right-hand side $f$ from $u$ as $f(x) = -\Delta_\Gamma u(x)$ $(x \in \Gamma)$, and after some calculations we get

$$f(x) = 2\nu_1(x)\nu_2(x) + H(x)(x_2\nu_1(x) + x_1\nu_2(x)), \quad x \in \Gamma, \tag{4.27}$$

with the mean curvature $H$ of $\Gamma$. According to (2.8) the mean curvature can be calculated from the formula

$$H = \nabla \cdot \frac{\nabla\phi}{|\nabla\phi|} = \frac{1}{|\nabla\phi|}\sum_{j,k=1}^{3}\left(\delta_{jk} - \frac{\phi_{x_j}\phi_{x_k}}{|\nabla\phi|^2}\right)\phi_{x_jx_k}.$$

Figure 4.10 shows the numerical solution with piecewise linear finite elements to the Poisson equation for the right-hand side $f$ and with mean value equal to zero on $\Gamma$.

In Table 4.1 we show the errors in the norms $E_{L^\infty(\Gamma)}(h) = \|u - u_h\|_{L^\infty(\Gamma)}$, $E_{L^2(\Gamma)}(h) = \|u - u_h\|_{L^2(\Gamma)}$ and $E_{H^1(\Gamma)}(h) = \|\nabla_\Gamma(u - u_h)\|_{L^2(\Gamma)}$. For errors $E(h_1)$ and $E(h_2)$ for the grid sizes $h_1$ and $h_2$, the experimental order of convergence is defined by

$$\mathrm{EOC}(h_1, h_2) = \log\frac{E(h_1)}{E(h_2)}\left(\log\frac{h_1}{h_2}\right)^{-1}.$$

The results confirm the theoretical results from Theorem 4.9.

https://doi.org/10.1017/S0962492913000056 Published online by Cambridge University Press

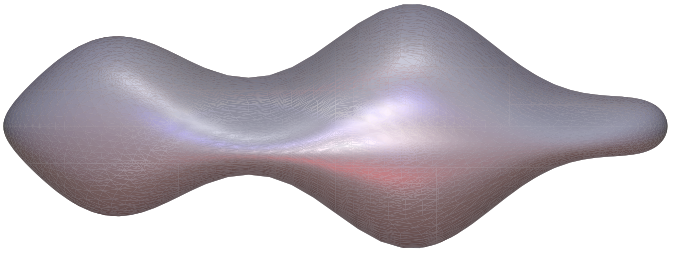


Figure 4.8. The hypersurface for Example 4.8.

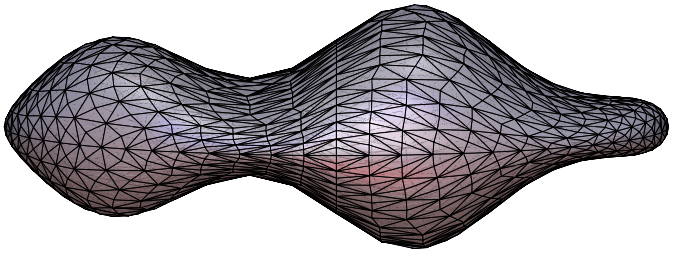


Figure 4.9. Computational grid on the surface from Figure 4.8 obtained after eight bisections of the macro-triangulation.

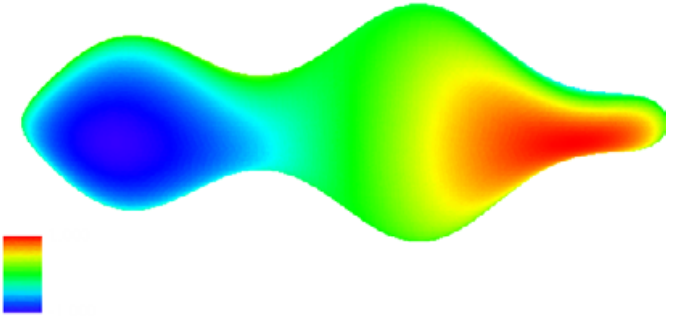


Figure 4.10. Solution $u$ to Example 4.8 on $\Gamma$. Values between $-1$ (blue) and 1 (red).

We now prove the following result on the numerical solution of the Poisson equation by piecewise linear finite elements on a compact connected surface.

**Theorem 4.9.** Assume that $\Gamma$ and $\Gamma_h$ are as above with $n \leq 3$. Let $F_h \in L^2(\Gamma_h)$ with $\int_{\Gamma_h} F_h = 0$. Let $S_h$ be the space of piecewise linear finite elements on the discrete surface $\Gamma_h$ as in (4.4) and $S_h^l$ its lifted version as in (4.21). Then there is a discrete solution of (3.1), $U_h \in S_h$, which is uniquely determined up to a constant,

$$\int_{\Gamma_h} \nabla_{\Gamma_h} U_h \cdot \nabla_{\Gamma_h} \phi_h \,\mathrm{d}A = \int_{\Gamma_h} F_h \phi_h \,\mathrm{d}A \tag{4.28}$$

for all $\phi_h \in S_h$. Fix the free constant by the requirement $\int_{\Gamma_h} U_h = 0$.

https://doi.org/10.1017/S0962492913000056 Published online by Cambridge University Press

The error in the natural norm between the continuous solution $u$ with $\int_\Gamma u = 0$ for $f \in L^2(\Gamma)$, $\int_\Gamma f \,\mathrm{d}A = 0$, from Theorem 3.1 and the lifted discrete solution $u_h = U_h^l$ can be estimated for $h \le h_0$ as follows:

$$\|\nabla_\Gamma(u - u_h)\|_{L^2(\Gamma)} \le ch\|f\|_{L^2(\Gamma)} + c\|f - f_h\|_{L^2(\Gamma)}, \tag{4.29}$$

with $c$ depending on the geometry of $\Gamma$. Here we have set $f_h = F_h^l$.

For the $L^2(\Gamma)$-error we have the estimate

$$\|u - u_h\|_{L^2(\Gamma)} \le ch^2\|f\|_{L^2(\Gamma)} + c\|f - f_h\|_{L^2(\Gamma)}. \tag{4.30}$$

If we choose $F_h$ so that

$$\|f - f_h\|_{L^2(\Gamma)} \le c_f h^2,$$

then

$$\|u - u_h\|_{L^2(\Gamma)} \le ch^2, \quad \|\nabla_\Gamma(u - u_h)\|_{L^2(\Gamma)} \le ch. \tag{4.31}$$

**Remark 4.10.** The assumption that the dimension $n$ of the surface $\Gamma$ is less than or equal to 3 is necessary only for the use of the interpolation inequalities in Lemma 4.3. The error estimates of the theorem are valid for any dimension $n$ if it is guaranteed that the estimates (4.19) hold.

Note that for the $H^1(\Gamma)$ error estimate it is sufficient to require first-order approximation of the right-hand side $f$ by $f_h$.

The proof of this theorem was given in Dziuk (1988). For the convenience of the reader and because the theorem concerns a model problem, we present the proof.

*Proof.* For sufficiently small grid size $h \le h_0$ the discrete bilinear form $a_h$ is coercive. From Lemma 4.7 we get for $\phi_h \in S_h$ and $\varphi_h = \phi_h^l$ with the coercivity of the bilinear form $a$,

$$\begin{aligned} a_h(\phi_h, \phi_h) &\ge a(\varphi_h, \varphi_h) - |a(\varphi_h, \varphi_h) - a_h(\phi_h, \phi_h)| \\ &\ge \|\nabla_\Gamma \varphi_h\|^2_{L^2(\Gamma)} - ch^2\|\nabla_\Gamma \varphi_h\|^2_{L^2(\Gamma)} \qquad (4.32) \\ &\ge \frac{1}{2}\|\nabla_\Gamma \varphi_h\|^2_{L^2(\Gamma)} \qquad (4.33) \end{aligned}$$

for $h \le h_0$.

From the continuous equation (3.2) and the discrete equation (4.28) we have

$$a(u, \varphi) = m(f, \varphi), \quad a_h(U_h, \phi_h) = m_h(F_h, \phi_h) \tag{4.34}$$

for all $\varphi \in H^1(\Gamma)$ and all $\phi_h \in S_h$.

https://doi.org/10.1017/S0962492913000056 Published online by Cambridge University Press

Following the common arguments of the first Strang lemma, we infer from (4.33) and (4.34) for arbitrary $\phi_h \in S_h$, $\varphi_h = \phi_h^l$ that

$$\begin{aligned}
\frac{1}{2}\|\nabla_\Gamma(u_h - \varphi_h)\|^2_{L^2(\Gamma)} &\leq a_h(U_h - \phi_h, U_h - \phi_h) \\
&= a(u - \varphi_h, u_h - \varphi_h) \\
&\quad + a(\varphi_h, u_h - \varphi_h) - a_h(\phi_h, U_h - \phi_h) \\
&\quad - (m(f, u_h - \varphi_h - c) - m_h(F_h, U_h - \phi_h - c)) \\
&= a(u - \varphi_h, u_h - \varphi_h) \\
&\quad + a(\varphi_h, u_h - \varphi_h) - a_h(\phi_h, U_h - \phi_h) \\
&\quad - (m(f, u_h - \varphi_h - c) - m(f_h, u_h - \varphi_h - c)) \\
&\quad - (m(f_h, u_h - \varphi_h - c) - m_h(F_h, U_h - \phi_h - c)).
\end{aligned}$$

Because the mean value of $f$ over $\Gamma$ and the mean value of $F_h$ over $\Gamma_h$ vanish, we were able to smuggle in an arbitrary real constant $c$. We have set $f_h = F_h^l$. So,

$$\begin{aligned}
&\frac{1}{2}\|\nabla_\Gamma(u_h - \varphi_h)\|^2_{L^2(\Gamma)} \\
&\quad \leq \|\nabla_\Gamma(u - \varphi_h)\|_{L^2(\Gamma)}\|\nabla_\Gamma(u_h - \varphi_h)\|_{L^2(\Gamma)} \\
&\qquad + |a(\varphi_h, u_h - \varphi_h) - a_h(\phi_h, U_h - \phi_h)| \\
&\qquad + \|f - f_h\|_{L^2(\Gamma)}\|u_h - \varphi_h - c\|_{L^2(\Gamma)} \\
&\qquad + |m(f_h, u_h - \varphi_h - c) - m_h(F_h, U_h - \phi_h - c)|.
\end{aligned}$$

We continue the estimate with the results from Lemma 4.7 and get

$$\begin{aligned}
&\frac{1}{2}\|\nabla_\Gamma(u_h - \varphi_h)\|^2_{L^2(\Gamma)} \\
&\quad \leq \|\nabla_\Gamma(u - \varphi_h)\|_{L^2(\Gamma)}\|\nabla_\Gamma(u_h - \varphi_h)\|_{L^2(\Gamma)} \\
&\qquad + ch^2\|\nabla_\Gamma\varphi_h\|_{L^2(\Gamma)}\|\nabla_\Gamma(u_h - \varphi_h)\|_{L^2(\Gamma)} \\
&\qquad + \|f - f_h\|_{L^2(\Gamma)}\|u_h - \varphi_h - c\|_{L^2(\Gamma)} \\
&\qquad + ch^2\|f_h\|_{L^2(\Gamma)}\|u_h - \varphi_h - c\|_{L^2(\Gamma)}.
\end{aligned}$$

The choice $c = \frac{1}{|\Gamma|}\int_\Gamma u_h - \varphi_h \,\mathrm{d}A$ allows the application of Poincaré's inequality from Theorem 2.16,

$$\|u_h - \varphi_h - c\|_{L^2(\Gamma)} \leq \tilde{c}\|\nabla_\Gamma(u_h - \varphi_h)\|_{L^2(\Gamma)}.$$

We finally arrive at the estimate

$$\begin{aligned}
&\frac{1}{2}\|\nabla_\Gamma(u_h - \varphi_h)\|_{L^2(\Gamma)} \\
&\quad \leq \|\nabla_\Gamma(u - \varphi_h)\|_{L^2(\Gamma)} + ch^2\|\nabla_\Gamma\varphi_h\|_{L^2(\Gamma)} \\
&\qquad + c\|f - f_h\|_{L^2(\Gamma)} + ch^2\|f\|_{L^2(\Gamma)}.
\end{aligned}$$

https://doi.org/10.1017/S0962492913000056 Published online by Cambridge University Press

We choose $\varphi_h = I_h u$ and use the interpolation estimates from Lemma 4.3:

$$\begin{aligned}\frac{1}{2}&\|\nabla_\Gamma(u_h - I_h u)\|_{L^2(\Gamma)}\\ &\le \big(1+ch^2\big)\|\nabla_\Gamma(u - I_h u)\|_{L^2(\Gamma)} + ch^2\|\nabla_\Gamma u\|_{L^2(\Gamma)}\\ &\qquad + c\|f - f_h\|_{L^2(\Gamma)} + ch^2\|f\|_{L^2(\Gamma)}\\ &\le ch\|u\|_{H^2(\Gamma)} + c\|f - f_h\|_{L^2(\Gamma)} + ch^2\|f\|_{L^2(\Gamma)}.\end{aligned}$$

The *a priori* estimate from Theorem 3.3 now finally gives

$$\|\nabla_\Gamma(u - u_h)\|_{L^2(\Gamma)} \le ch\|f\|_{L^2(\Gamma)} + c\|f - f_h\|_{L^2(\Gamma)},$$

and the estimate (4.29) of the theorem is proved.

The $L^2(\Gamma)$ error estimate follows with the usual Aubin–Nitsche trick. Let $v \in H^2(\Gamma)$ be the solution of the problem

$$-\Delta_\Gamma v = u - u_h - \frac{1}{|\Gamma|}\int_\Gamma u - u_h \,\mathrm{d}A$$

on $\Gamma$ with $\int_\Gamma v \,\mathrm{d}A = 0$. It follows from Theorem 3.3 that

$$\|v\|_{H^2(\Gamma)} \le c\|u - u_h\|_{L^2(\Gamma)}.$$

The PDE for $v$ gives

$$\|u - u_h\|^2_{L^2(\Gamma)} - \frac{1}{|\Gamma|}\left(\int_\Gamma u - u_h \,\mathrm{d}A\right)^2 = -\int_\Gamma (u - u_h)\Delta_\Gamma v \,\mathrm{d}A. \tag{4.35}$$

The right-hand side of this equation is equal to $a(u-u_h, v)$ by Theorem 2.14. Using the results from Lemma 4.7 we have, for $\varphi_h = I_h v \in S_h^l$,

$$\begin{aligned}a(u - u_h, v)&\\ &= a(u - u_h, v - \varphi_h) + a(u - u_h, \varphi_h)\\ &= a(u - u_h, v - \varphi_h) + m(f, \varphi_h)\\ &\qquad - m_h(F_h, \phi_h) - (a(u_h, \varphi_h) - a_h(U_h, \phi_h))\\ &\le \|\nabla_\Gamma(u - u_h)\|_{L^2(\Gamma)}\|\nabla_\Gamma(v - \varphi_h)\|_{L^2(\Gamma)}\\ &\qquad + c(\|f - f_h\|_{L^2(\Gamma)} + h^2\|f_h\|_{L^2(\Gamma)})\|\nabla_\Gamma\varphi_h\|_{L^2(\Gamma)}\\ &\qquad + ch^2\|\nabla_\Gamma u_h\|_{L^2(\Gamma)}\|\nabla_\Gamma\varphi_h\|_{L^2(\Gamma)}\\ &\le c\big(h^2\|f\|_{L^2(\Gamma)} + \|f - f_h\|_{L^2(\Gamma)}\big)\|v\|_{H^2(\Gamma)}\\ &\le c\big(h^2\|f\|_{L^2(\Gamma)} + \|f - f_h\|_{L^2(\Gamma)}\big)\|u - u_h\|_{L^2(\Gamma)}.\end{aligned}$$

For the left-hand side of (4.35) we observe the following:

$$\begin{aligned}\frac{1}{|\Gamma|}&\left(\int_\Gamma u - u_h \,\mathrm{d}A\right)^2 = cm(u - u_h, 1)^2 = cm(u_h, 1)^2\\ &= c(m(u_h, 1) - m_h(U_h, 1))^2 \le ch^4\big(\|u\|^2_{L^2(\Gamma)} + \|u - u_h\|^2_{L^2(\Gamma)}\big).\end{aligned}$$

https://doi.org/10.1017/S0962492913000056 Published online by Cambridge University Press

But then

$$(1 - ch^4)\|u - u_h\|^2_{L^2(\Gamma)} \leq ch^4\|f\|^2_{L^2(\Gamma)} + c\big(h^2\|f\|_{L^2(\Gamma)} + \|f - f_h\|_{L^2(\Gamma)}\big)\|u - u_h\|_{L^2(\Gamma)}.$$

This finally gives the estimate (4.30) for $h \leq h_0$. □

### *4.6. Other methods on discrete surfaces*

First note that the use of surface finite elements for solving parabolic equations on stationary surfaces follows rather naturally from the developments in this section (Dziuk and Elliott 2007*b*). Higher-order finite element spaces for elliptic equations were analysed in Demlow (2009), an adaptive finite element method for stationary surfaces was considered in Demlow and Dziuk (2007), and coupling of surface and bulk elliptic equations was analysed in Elliott and Ranner (2013).

A discontinuous Galerkin surface finite element method was considered by Dedner, Madhavan and Stinner (2013). An extension of the idea of the surface finite element method (SFEM) is to use surface finite volumes. An analysis of elliptic equations using general meshes is given in Ju and Du (2009) and Ju, Tian and Wang (2009). A method for parabolic equations on stationary surfaces using logically Cartesian grids is presented in Calhoun and Helzel (2009). See also Berger, Calhoun, Helzel and Leveque (2009) for conservation laws on the sphere.

## 5. Partial differential equations on moving surfaces

Quite often we have to solve PDEs which live on a moving surface or interface. We refer to examples in Section 10. In this chapter we will treat the most basic linear PDE on an evolving surface. The motion of the surface will be prescribed. The geometry will be described in Section 5.1. It will be important to use the space–time structure of the given geometry. We will describe in Section 5.2 how the standard conservation law can be derived. In Section 5.3 we will work with moving triangulated surfaces and use them to discretize the heat equation on a moving surface.

### *5.1. The geometry of moving surfaces*

For each $t \in [0,T]$, let $\Gamma(t)$ be a compact hypersurface oriented by the normal vector field $\nu(\cdot,t)$ and $\Gamma_0 = \Gamma(0)$. We assume that there exists a map $G(\cdot,t) : \Gamma_0 \to \Gamma(t)$, $G \in C^1([0,T], C^2(\Gamma_0))$, such that $G(\cdot,t)$ is a diffeomorphism from $\Gamma_0$ to $\Gamma(t)$, and we define the velocity of $\Gamma(t)$ by

$$v(G(\cdot,t),t) = \frac{\partial G}{\partial t}(\cdot,t),$$

https://doi.org/10.1017/S0962492913000056 Published online by Cambridge University Press

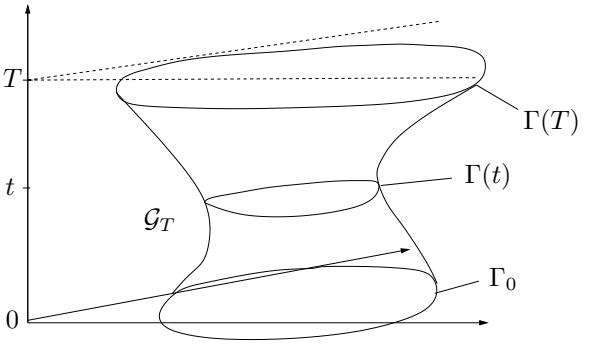



Figure 5.1. Space–time surface $\mathcal{G}_T$ for the dimension $n = 1$. Here each $\Gamma(t)$ is a curve.

$G(\cdot, 0) = \mathrm{Id}$. We assume that $v(\cdot, t) \in C^2(\Gamma(t))$. The normal velocity of $\Gamma$ is then defined by $v_\nu = v \cdot \nu \nu$.

We use the appropriate time derivative, that is,

$$\partial^\bullet f = \frac{\partial f}{\partial t} + v \cdot \nabla f. \tag{5.1}$$

Obviously this derivative only depends on values of the function $f$ on $\mathcal{G}_T$. It is quite often convenient to work with the space–time surface (see Figure 5.1)

$$\mathcal{G}_T = \bigcup_{t\in[0,T]} \Gamma(t) \times \{t\}. \tag{5.2}$$

Note that for a function $f : \mathcal{G}_T \to \mathbb{R}$ the time derivative $\frac{\partial f}{\partial t}$ and the spatial derivatives $\nabla f$ do not make sense separately.

*Leibniz formulae, transport theorems*

The following formulae for the differentiation of time-dependent surface integrals are called *transport formulae*, and are proved in Dziuk and Elliott (2007*a*, 2012).

**Theorem 5.1.** Let $\mathcal{M}(t)$ be an evolving surface with normal velocity $v_\nu$. Let $v_\tau$ be a tangential velocity field on $\mathcal{M}(t)$. Let the boundary $\partial\mathcal{M}(t)$ evolve with the velocity $v = v_\nu + v_\tau$. Assume that f is a function such that all the following quantities exist. Then

$$\frac{\mathrm{d}}{\mathrm{d}t} \int_{\mathcal{M}(t)} f \,\mathrm{d}A = \int_{\mathcal{M}(t)} \partial^\bullet f + f \,\nabla_\Gamma \cdot v \,\mathrm{d}A. \tag{5.3}$$

*Proof.* Let $\Omega \subset \mathbb{R}^n$ be open and let $X = X(\theta, t)$, $\theta \in \Omega$, $X(\cdot, t) : \Omega \to U \cap \Gamma$ be a local regular parametrization of the open portion $U \cap \Gamma$ of the surface $\Gamma$ which evolves so that $X_t = v(X(\theta, t), t)$. The induced metric $(g_{ij})_{i,j=1,\dots,n}$ is given by $g_{ij} = X_{\theta_i} \cdot X_{\theta_j}$ with determinant $g = \det(g_{ij})$. Let $(g^{ij}) = (g_{ij})^{-1}$.

https://doi.org/10.1017/S0962492913000056 Published online by Cambridge University Press

See also Section 2.1. Define

$$F(\theta,t) = f(X(\theta,t),t) \quad \text{and} \quad \mathcal{V}(\theta,t) = v(X(\theta,t),t).$$

Then, with the Euler relation for the derivative of the determinant,

$$\frac{\partial}{\partial t}\sqrt{g} = \sqrt{g}\sum_{i,j=1}^{n} g^{ij} X_{\theta_i}\cdot\mathcal{V}_{\theta_j},$$

we have the following proof of (5.3):

$$\begin{aligned}\frac{\mathrm{d}}{\mathrm{d}t}\int_{\Gamma\cap U} f\,\mathrm{d}A &= \frac{\mathrm{d}}{\mathrm{d}t}\int_{\Omega} F\sqrt{g}\,\mathrm{d}\theta = \int_{\Omega}\frac{\partial F}{\partial t}\sqrt{g} + F\frac{\partial\sqrt{g}}{\partial t}\,\mathrm{d}\theta\\ &= \int_{\Omega}\left(\frac{\partial f}{\partial t}(X,\cdot) + \nabla f(X,\cdot)\cdot X_t\right)\sqrt{g} + f(X,\cdot)\sqrt{g}\sum_{i,j=1}^{n} g^{ij}X_{\theta_i}\cdot\mathcal{V}_{\theta_j}\,\mathrm{d}\theta\\ &= \int_{\Gamma\cap U}\dot{f} + f\nabla_\Gamma\cdot v\,\mathrm{d}A,\end{aligned}$$

where in the last step we used that $\mathcal{V} = X_t$ and that the tangential divergence of $v$ is given by

$$(\nabla_\Gamma\cdot v)(X,\cdot) = \sum_{i,j=1}^{n} g^{ij}X_{\theta_i}\cdot\mathcal{V}_{\theta_j}.$$

The theorem is proved. □

We give transport formulae for the time derivative of the most important bilinear forms $m$, $a$ and $g$ given by

$$\begin{aligned} m(\phi(\cdot,t),\psi(\cdot,t)) &= \int_{\Gamma(t)}\phi(x,t)\psi(x,t)\,\mathrm{d}A(x),\\ a(\phi(\cdot,t),\psi(\cdot,t)) &= \int_{\Gamma(t)}\mathcal{A}(\cdot,t)\nabla_{\Gamma(t)}\phi(\cdot,t)\cdot\nabla_{\Gamma(t)}\psi(\cdot,t)\,\mathrm{d}A(x),\\ g(v;\phi(\cdot,t),\psi(\cdot,t)) &= \int_{\Gamma(t)}\phi(x,t)\psi(x,t)\nabla_\Gamma\cdot v(x,t)\,\mathrm{d}A(x).\end{aligned}$$

Note that these bilinear forms now explicitly depend on time too. But instead of writing, say, $m(t,\phi(\cdot,t),\psi(\cdot,t))$, we suppress the explicit dependence on $t$. It will always be clear from the arguments $\phi$ and $\psi$ at which time the bilinear form has to be evaluated.

**Lemma 5.2.** For $\varphi,\psi\in H^1(\mathcal{G}_T)$, we have

$$\frac{\mathrm{d}}{\mathrm{d}t}m(\varphi,\psi) = m(\partial^\bullet\varphi,\psi) + m(\varphi,\partial^\bullet\psi) + g(v;\varphi,\psi) \tag{5.4}$$

https://doi.org/10.1017/S0962492913000056 Published online by Cambridge University Press

and

$$\frac{\mathrm{d}}{\mathrm{d}t}a(\varphi,\psi) = a(\partial^\bullet\varphi,\psi) + a(\varphi,\partial^\bullet\psi) + b(v;\varphi,\psi), \tag{5.5}$$

with the bilinear form

$$b(v;\varphi,\psi) = \int_\Gamma \mathcal{B}(v)\nabla_\Gamma\varphi\cdot\nabla_\Gamma\psi\,\mathrm{d}A. \tag{5.6}$$

With the deformation tensor

$$D(v)_{ij} = \frac{1}{2}\sum_{k=1}^{n+1}(\mathcal{A}_{ik}(\nabla_\Gamma)_k v_j + \mathcal{A}_{jk}(\nabla_\Gamma)_k v_i) \quad (i,j=1,\dots,n+1)$$

and the tensor

$$\mathcal{B}(v) = \partial^\bullet\mathcal{A} + \nabla_\Gamma\cdot v\,\mathcal{A} - 2D(v), \tag{5.7}$$

we have the formula

$$\frac{\mathrm{d}}{\mathrm{d}t}\int_{\mathcal{M}(t)}\mathcal{A}\nabla_\Gamma f\cdot\nabla_\Gamma g\,\mathrm{d}A = \tag{5.8}$$
$$\int_{\mathcal{M}(t)}\mathcal{A}\nabla_\Gamma\partial^\bullet f\cdot\nabla_\Gamma g + \mathcal{A}\nabla_\Gamma f\cdot\nabla_\Gamma\partial^\bullet g\,\mathrm{d}A + \int_{\mathcal{M}(t)}\mathcal{B}(v)\nabla_\Gamma f\cdot\nabla_\Gamma g\,\mathrm{d}A.$$

For the convenience of the reader we derive the transport formula for Dirichlet's integral,

$$\int_\Gamma |\nabla_\Gamma f|^2\,\mathrm{d}A,$$

for a time-dependent surface. We continue to use the notation of the previous proof. The generalization to the more general case in Lemma 5.2 then follows easily. We first observe that we have

$$|(\nabla_\Gamma f)(X,\cdot)|^2 = \sum_{i,j=1}^n g^{ij}F_{\theta_i}F_{\theta_j}, \tag{5.9}$$

so that

$$\frac{1}{2}\frac{\mathrm{d}}{\mathrm{d}t}\int_{\Gamma\cap U}|\nabla_\Gamma f|^2\,\mathrm{d}A = \int_\Omega\sqrt{g}\sum_{i,j=1}^n g^{ij}F_{\theta_i}F_{\theta_j t}\,\mathrm{d}\theta$$
$$+\frac{1}{2}\int_\Omega\sqrt{g}\sum_{i,j=1}^n g_t^{ij}F_{\theta_i}F_{\theta_j}\,\mathrm{d}\theta + \frac{1}{2}\int_\Omega\sqrt{g}\sum_{i,j,k,l=1}^n g^{ij}g^{kl}X_{\theta_k}\cdot\mathcal{V}_{\theta_l}F_{\theta_i}F_{\theta_j}\,\mathrm{d}\theta.$$

https://doi.org/10.1017/S0962492913000056 Published online by Cambridge University Press

An easy calculation shows that

$$g^{ij}_t = -\sum_{k,l=1}^{n} g^{ik}g^{jl}g_{kl,t} = -\sum_{k,l=1}^{n} g^{ik}g^{jl}(X_{\theta_k}\cdot X_{\theta_l})_t$$
$$= -\sum_{k,l=1}^{n} g^{ik}g^{jl}(\mathcal{V}_{\theta_k}\cdot X_{\theta_l} + X_{\theta_k}\cdot \mathcal{V}_{\theta_l}),$$

and we arrive at

$$\frac{1}{2}\frac{\mathrm{d}}{\mathrm{d}t}\int_{\Gamma\cap U} |\nabla_\Gamma f|^2 \,\mathrm{d}A = \int_{\Gamma\cap U} \nabla_\Gamma f\cdot\nabla_\Gamma \partial^\bullet f \,\mathrm{d}A$$
$$- \int_{\Gamma\cap U}\sum_{i,j=1}^{n} \underline{D}_i v_j \underline{D}_i f \underline{D}_j f \,\mathrm{d}A + \frac{1}{2}\int_{\Gamma\cap U} |\nabla_\Gamma f|^2 \nabla_\Gamma\cdot v \,\mathrm{d}A.$$

The formula (5.8) for $\mathcal{A} = I$ then follows by polarization.

### *5.2. Conservation and diffusion on moving surfaces*

*Conservation law*

Let $u$ be the density of a scalar quantity on $\Gamma(t)$ (for example mass per unit area $n = 2$ or mass per unit length $n = 1$). We suppose there is a surface flux $q$. The basic conservation law we wish to consider can be formulated for an arbitrary portion $\mathcal{M}(t)$ of $\Gamma(t)$, which is the image of a portion $\mathcal{M}(0)$ of $\Gamma(0)$ evolving with the prescribed velocity $v = v_\nu$. In the following we write $\partial^\circ u$ for the material time derivative of $u$ with respect to this purely normal velocity:

$$\partial^\circ u = u_t + v_\nu\cdot\nabla u.$$

$\partial^\circ u$ is sometimes known as the *normal time derivative* (Cermelli, Fried and Gurtin 2005).

The conservation law is that for every $\mathcal{M}(t)$

$$\frac{\mathrm{d}}{\mathrm{d}t}\int_{\mathcal{M}(t)} u \,\mathrm{d}A = -\int_{\partial\mathcal{M}(t)} q\cdot\mu \,\mathrm{d}A, \tag{5.10}$$

where $\partial\mathcal{M}(t)$ is the boundary of $\mathcal{M}(t)$ (a curve if $n = 2$ and the end points of a curve if $n = 1$) and $\mu$ is the co-normal on $\partial\mathcal{M}(t)$. Thus $\mu$ is the unit normal to $\partial\mathcal{M}(t)$ pointing out of $\mathcal{M}(t)$ and tangential to $\Gamma(t)$. The surface flux is denoted by $q$. Observe that components of $q$ normal to $\mathcal{M}$ do not contribute to the flux, so we may assume that $q$ is a tangent vector.

With the use of integration by parts, (2.13), we obtain

$$\int_{\partial\mathcal{M}(t)} q\cdot\mu \,\mathrm{d}A = \int_{\mathcal{M}(t)} \nabla_\Gamma\cdot q \,\mathrm{d}A - \int_{\mathcal{M}(t)} q\cdot\nu H \,\mathrm{d}A = \int_{\mathcal{M}(t)} \nabla_\Gamma\cdot q \,\mathrm{d}A.$$

https://doi.org/10.1017/S0962492913000056 Published online by Cambridge University Press

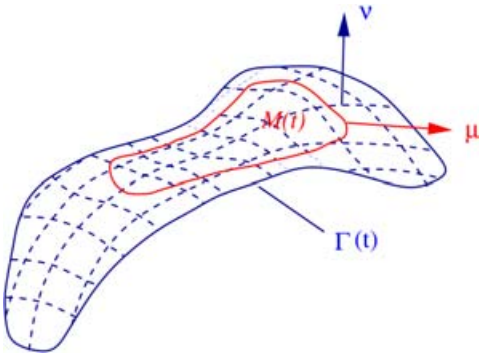



Figure 5.2. Conservation on a moving surface. Moving surface $\Gamma(t)$ and subset $M(t)$ with co-normal $\mu$.

On the other hand, by the transport formula (5.3) we have

$$\frac{\mathrm{d}}{\mathrm{d}t}\int_{\mathcal{M}(t)} u\,\mathrm{d}A = \int_{\mathcal{M}(t)} \partial^\circ u + u\nabla_\Gamma \cdot v_\nu\,\mathrm{d}A,$$

so that

$$\int_{\mathcal{M}(t)} \partial^\circ u + u\,\nabla_\Gamma \cdot v_\nu + \nabla_\Gamma \cdot q\,\mathrm{d}A = 0,$$

which implies the pointwise conservation law

$$\partial^\circ u + u\,\nabla_\Gamma \cdot v_\nu + \nabla_\Gamma \cdot q = 0. \tag{5.11}$$

This may also be written as

$$u_t + V\frac{\partial u}{\partial \nu} + HVu + \nabla_\Gamma \cdot q = 0, \tag{5.12}$$

where $V = v_\nu \cdot \nu$; see also Stone (1990).

We wish to consider a diffusive flux $q_d = -\mathcal{A}\nabla_\Gamma u$ and an advective flux $q_a = uv_\tau$, where $v_\tau$ is an advective tangential velocity field, that is, $v_\tau \cdot \nu = 0$, so that

$$q = q_d + q_a = -\mathcal{A}\nabla_\Gamma u + uv_\tau.$$

Then we arrive at the PDE

$$\partial^\bullet u + u\,\nabla_\Gamma \cdot v - \nabla_\Gamma \cdot (\mathcal{A}\nabla_\Gamma u) = 0. \tag{5.13}$$

In the following we assume that $\mathcal{A}$ is a sufficiently smooth symmetric $(n+1)\times(n+1)$ matrix which maps the tangent space of $\Gamma$ at each point into itself and is positive definite on the tangent space, that is,

$$\mathcal{A}\xi \cdot \xi \geq c_0|\xi|^2 \quad \text{for all } \xi \in \mathbb{R}^{m+1},\ \xi \cdot \nu = 0, \tag{5.14}$$

with some constant $c_0 > 0$. For the definition of a solution we assume that

https://doi.org/10.1017/S0962492913000056 Published online by Cambridge University Press

the elements of $\mathcal{A}$ belong to $L^\infty(\mathcal{G}_T)$. A weak solution of the PDE (5.13) is a function $u \in H^1(\mathcal{G}_T)$ that satisfies the equation

$$\frac{\mathrm{d}}{\mathrm{d}t}\int_{\Gamma(t)} u\varphi \,\mathrm{d}A + \int_{\Gamma(t)} \mathcal{A}\nabla_\Gamma u \cdot \nabla_\Gamma \varphi \,\mathrm{d}A = \int_{\Gamma(t)} u\partial^\bullet \varphi \,\mathrm{d}A \tag{5.15}$$

almost everywhere on $(0,T)$, where $\varphi$ is an arbitrary test function defined on the space–time surface $\mathcal{G}_T$.

In Dziuk and Elliott (2007*a*) we proved the existence of a weak solution.

**Theorem 5.3.** Assume that the initial data $u_0 \in H^1(\Gamma_0)$, where $\Gamma_0 = \Gamma(0)$. Then there exists a unique weak solution $u \in H^1(\mathcal{G}_T)$ of the PDE (5.13), that is, equation (5.15) is satisfied for almost every $t \in (0,T)$, which satisfies the initial condition $u(\cdot,0) = u_0$ on $\Gamma_0$. Furthermore, if $\mathcal{A}$ and $v \in C^1(\mathcal{G}_T)$, the solution satisfies the energy estimates

$$\sup_{(0,T)} \|u\|^2_{L^2(\Gamma)} + \int_0^T \|\nabla_\Gamma u\|^2_{L^2(\Gamma)} \,\mathrm{d}t \le c\|u_0\|^2_{L^2(\Gamma_0)}, \tag{5.16}$$

$$\int_0^T \|\partial^\bullet u\|^2_{L^2(\Gamma)} \,\mathrm{d}t + \sup_{(0,T)} \|\nabla_\Gamma u\|^2_{L^2(\Gamma)} \le c\|u_0\|^2_{H^1(\Gamma_0)}, \tag{5.17}$$

where $c = c(\mathcal{A}, v, \mathcal{G}_T, T)$.

*Proof.* For the convenience of the reader we include a proof of the *a priori* estimates. For (5.16) we set $\varphi = u$ in (5.15) and, using Lemma 5.2, we get

$$\frac{\mathrm{d}}{\mathrm{d}t} m(u,u) + a(u,u) = m(u,\partial^\bullet u) = \frac{1}{2}\frac{\mathrm{d}}{\mathrm{d}t} m(u,u) - \frac{1}{2} g(v;u,u).$$

This gives

$$\frac{1}{2}\frac{\mathrm{d}}{\mathrm{d}t} m(u,u) + a(u,u) + \frac{1}{2} g(v;u,u) = 0,$$

and with a Gronwall argument this implies (5.16).

For (5.17) we use (5.4). The weak equation (5.15) implies

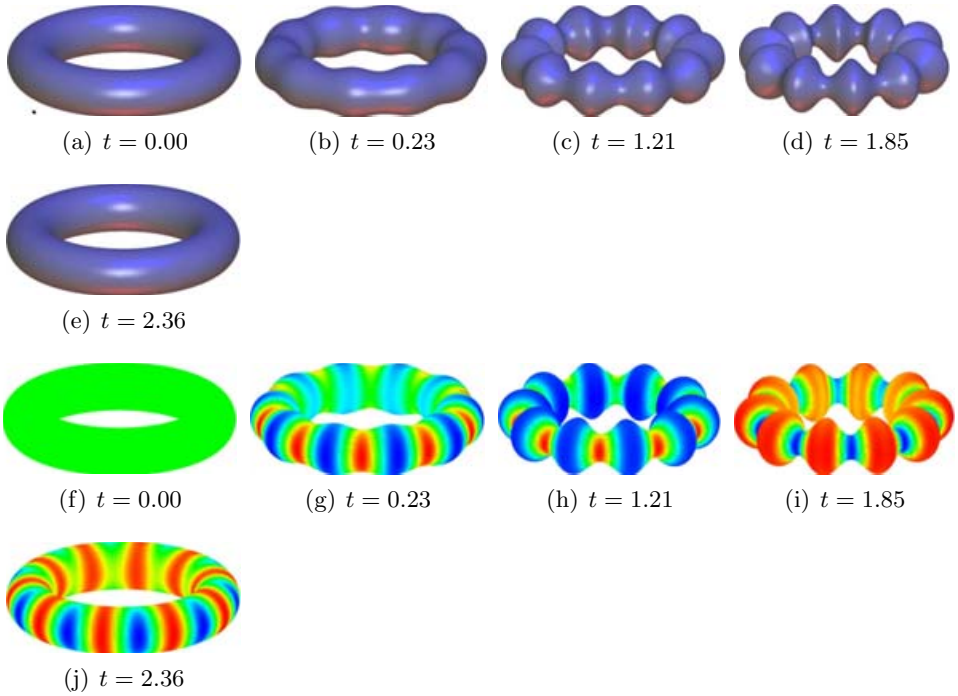
$$m(\partial^\bullet u, \varphi) + g(v;u,\varphi) + a(u,\varphi) = 0.$$

We insert $\varphi = \partial^\bullet u$ and get from (5.5)

$$m(\partial^\bullet u, \partial^\bullet u) + g(v;u,\partial^\bullet u) + \frac{1}{2}\frac{\mathrm{d}}{\mathrm{d}t} a(u,u) - \frac{1}{2} b(v;u,u) = 0.$$

Standard arguments then lead to (5.17). □

https://doi.org/10.1017/S0962492913000056 Published online by Cambridge University Press



(a) $t = 0.00$ (b) $t = 0.23$ (c) $t = 1.21$ (d) $t = 1.85$

(e) $t = 2.36$

(f) $t = 0.00$ (g) $t = 0.23$ (h) $t = 1.21$ (i) $t = 1.85$

(j) $t = 2.36$

Figure 5.3. (a–e) Deformation of a torus and (f–j) solution of equation (5.13). Colours indicate the magnitude of the solution. There was no source term. The surface is deformed and reaches the initial form of a round torus again at time $t = 2.36$. The initial value was constant: $u_0 = 10.0$ (green at $t = 0.00$). The solution at final time $t = 2.36$ is due purely to geometric motion.

For $\varphi, \psi \in H^1(\Gamma)$ we use the bilinear forms

$$a(\varphi(\cdot,t),\psi(\cdot,t)) = \int_{\Gamma(t)} \mathcal{A}(\cdot,t)\nabla_\Gamma\varphi(\cdot,t)\cdot\nabla_\Gamma\psi(\cdot,t)\,\mathrm{d}A, \tag{5.18}$$

$$m(\varphi(\cdot,t),\psi(\cdot,t)) = \int_{\Gamma(t)} \varphi(\cdot,t)\psi(\cdot,t)\,\mathrm{d}A, \tag{5.19}$$

$$g(v(\cdot,t);\varphi(\cdot,t),\psi(\cdot,t)) = \int_{\Gamma(t)} \varphi(\cdot,t)\psi(\cdot,t)\nabla_\Gamma\cdot v(\cdot,t)\,\mathrm{d}A. \tag{5.20}$$

Using this notation, the weak form (5.15) of the PDE (5.13) becomes

$$\frac{\mathrm{d}}{\mathrm{d}t}m(u,\varphi) + a(u,\varphi) = m(u,\partial^\bullet\varphi). \tag{5.21}$$

Of course, the variational problem may be posed on the initial surface $\Gamma_0$. This would lead to non-constant coefficients even with $\mathcal{A} = \mathcal{I}$. It would also require knowledge of the map $G$ in Section 5.1 which we choose to avoid.

https://doi.org/10.1017/S0962492913000056 Published online by Cambridge University Press

*5.3. Discretization*

*Evolving triangulated surfaces*

The smooth evolving surface $\Gamma(t)$ ($\partial\Gamma(t) = \emptyset$) is approximated by an evolving triangulated surface

$$\Gamma_h(t) \subset U_\delta(t) \quad (\partial\Gamma_h(t) = \emptyset),$$

which for each $t$ is polygonal and is smooth in time. $U_\delta(t)$ is as in Lemma 2.8. Let us suppose for simplicity that $\delta$ does not depend on time. We assume that every surface $\Gamma(t)$ is approximated as described in Section 4.2. So, $\Gamma_h(t)$ is homeomorphic to $\Gamma(t)$ for every $t \in [0,T]$. $U_\delta(t)$ is a neighbourhood in $\mathbb{R}^{n+1}$ of $\Gamma(t)$ such that for each $x \in U_\delta(t)$ there is a unique $a(x,t) \in \Gamma(t)$ which is the normal projection of $x$ onto $\Gamma(t)$, and $x = a(x,t) + d(x,t)\nu(a(x,t),t)$, where $d(x,t)$ is the oriented distance function with respect to $\Gamma(t)$. We have that

$$\Gamma_h(t) = \bigcup_{E(t)\in\mathcal{T}_h(t)} E(t)$$

with the admissible triangulation $\mathcal{T}_h(t)$ as in Section 4.1. We suppose that the maximum diameter of the simplices in $\mathcal{T}_h(t)$ is bounded uniformly in time by $h$. Note that for each $E(t) \subset \Gamma_h(t)$ there is a unique $\tilde{E}(t) \subset \Gamma(t)$, $\tilde{E}(t) = a(E(t),t)$, whose edges are the unique projections of the side simplices of $E(t)$ onto $\Gamma(t)$. This induces an exact 'triangulation' of $\Gamma(t)$ with curved simplices.

As in Section 4.2, we consider triangulated surfaces for which the vertices $X_j(t)$ ($j = 1,\dots,J$) of the simplices sit on $\Gamma(t)$ so that $\Gamma_h(t)$ is an interpolation. Furthermore, we advect the nodes in the tangential direction with the advective velocity $v_\tau$, as well as keeping them on the surface using the normal velocity $v_\nu$, so that with $v = v_\nu + v_\tau$

$$\frac{\mathrm{d}X_j}{\mathrm{d}t}(t) = v(X_j(t),t) \quad (j = 1,\dots,J). \tag{5.22}$$

As discrete analogues of the bilinear forms (5.18), (5.19) and (5.20), we define for $\phi_h(\cdot,t), W_h(\cdot,t) \in S_h(t)$

$$a_h(\phi_h(\cdot,t), W_h(\cdot,t)) = \sum_{E(t)\in\mathcal{T}_h(t)} \int_{E(t)} \mathcal{A}^{-l}(\cdot,t)\nabla_{\Gamma_h}\phi_h(\cdot,t)\cdot\nabla_{\Gamma_h}W_h(\cdot,t)\,\mathrm{d}A_h,$$

$$m_h(\phi_h(\cdot,t), W_h(\cdot,t)) = \int_{\Gamma_h(t)} \phi_h(\cdot,t)W_h(\cdot,t)\,\mathrm{d}A_h,$$

$$g_h(V_h(\cdot,t);\phi_h(\cdot,t), W_h(\cdot,t)) = \int_{\Gamma_h(t)} \phi_h(\cdot,t)W_h(\cdot,t)\nabla_{\Gamma_h}\cdot V_h(\cdot,t)\,\mathrm{d}A_h.$$

We keep in mind that the forms explicitly depend on $t$.

https://doi.org/10.1017/S0962492913000056 Published online by Cambridge University Press

*Evolving finite element spaces*

As in the stationary case in Section 4.4, we use piecewise linear finite elements. But now they live on the evolving discrete surface $\Gamma_h(t)$. We use the lift of functions from (4.2). This has two purposes. First we use the lift from $\Gamma_h(t)$ to $\Gamma(t)$ in order to define extensions of our finite element space, which allows an error analysis of the discretization on the smooth surface $\Gamma(t)$. Second, since the numerical method is based upon integration of finite element functions upon $\Gamma_h(t)$, we define approximations of the data, $\mathcal{A}$, given on $\Gamma(t)$ using $\mathcal{A}^{-l}$.

**Definition 5.4.** For each $t$ and $t^n = n\tau$, $\tau > 0$, we define the finite element spaces

$$S_h(t) = \big\{\phi_h(\cdot,t) \in C^0(\Gamma_h(t)) \mid \phi_h(\cdot,t)|_{E(t)} \text{ is linear affine for each } E(t) \in \mathcal{T}_h(t)\big\},$$

$$S_h^l(t) = \big\{\varphi_h(\cdot,t) = \phi_h(\cdot,t)^l \mid \phi_h(\cdot,t) \in S_h(t)\big\},$$

$$S_h^n = S_h(t^n), \quad S_h^{n,l} = S_h^l(t^n).$$

For each $\varphi_h \in S_h^l\big(\varphi_h^n \in S_h^{n,l}\big)$ there is a unique $\phi_h \in S_h\big(\phi_h^n \in S_h^n\big)$ such that

$$\varphi_h = \phi_h^l\big(\varphi_h^n = \phi_h^{n,l}\big).$$

By $\chi_1, \dots, \chi_J$ we denote the nodal basis of $S_h$.

### *5.4. Evolving surface finite element method* (ESFEM)

There is an astonishingly simple extension of the Leibniz formulae from Theorem 5.1 and Lemma 5.2 to the case of discrete surfaces. We formulate this as follows.

A discrete material velocity, $V_h$, for $x = X(t) \in \Gamma_h(t)$ on the surface $\Gamma_h(t)$ is defined by

$$\dot X(t) = V_h(X(t),t), \quad V_h(x,t) = I_h v(x,t) := \sum_{j=1}^{N} \dot X_j(t)\chi_j(x,t), \tag{5.23}$$

and an associated discrete material velocity, $v_h$, for $Y(t) = a(X(t),t)$ on $\Gamma(t)$ is defined by

$$\dot Y(t) = v_h(Y(t),t) = \frac{\partial a}{\partial t}(X(t),t) + V_h(X(t),t)\cdot\nabla a(X(t),t). \tag{5.24}$$

Note that (i) edges of $\tilde E(t)$ (which are the projections onto $\Gamma(t)$ of $E(t) \subset \Gamma_h(t)$) evolve with the material velocity $v_h(\cdot,t)$, and (ii) the discrete material velocity $v_h$ is *not* the interpolation of $v$ in $S_h^l(t)$.

https://doi.org/10.1017/S0962492913000056 Published online by Cambridge University Press

In analogy to (5.1), we define the *discrete material derivatives* on $\Gamma_h(t)$ and $\Gamma(t)$ element-by-element via the equations

$$\partial_h^\bullet \phi_h|_{E(t)} := (\phi_{ht} + V_h \cdot \nabla \phi_h)|_{E(t)}, \tag{5.25}$$

$$\partial_h^\bullet \varphi_h|_{e(t)} := (\varphi_{ht} + v_h \cdot \nabla \varphi_h)|_{e(t)}. \tag{5.26}$$

With these discrete material derivatives we can formulate one of the main properties of ESFEM.

**Lemma 5.5 (transport property of the basis functions).** The basis functions satisfy the *transport property* that

$$\partial_h^\bullet \chi_j = 0, \quad \partial_h^\bullet \chi_j^l = 0. \tag{5.27}$$

*Proof.* We prove the property for the discrete material derivative of the basis functions on the discrete surface which follows from the definition of the nodal basis. Take a simplex $E(t) \in \mathcal{T}_h(t)$ with $X_k(t) \in \partial E(t)$. We have that $\chi_j(X_k(t), t) = \delta_{jk}$. The time derivative of this equation gives

$$\frac{\partial \chi_j}{\partial t}(X_k(t), t) + \nabla \chi_j(X_k(t), t) \cdot \frac{\mathrm{d}X_k}{\mathrm{d}t}(t) = 0$$

where the gradient is taken on $E(t)$. Since by definition

$$V_h(X_k(t), t) = \frac{\mathrm{d}X_k}{\mathrm{d}t}(t),$$

it follows that $\partial_h^\bullet \chi_j(X_k(t), t) = 0$. Since $\chi_j$ (and $\partial_h^\bullet \chi_j$ too) is a linear polynomial on $E(t)$ this then implies $\partial_h^\bullet \chi_j = 0$. Using $\chi_j(x, t) = \chi_j^l(a(x, t), t)$ and the definition of the projection $a(\cdot, t)$, we find that

$$\begin{aligned} 0 = \partial_h^\bullet \chi_j &= (\chi_{j\,t} + V_h \cdot \nabla \chi_j) \\ &= (\chi_{j\,t}^l + (a_t + (V_h \cdot \nabla) a) \cdot \nabla \chi_j^l)(a, \cdot) = \partial_h^\bullet \chi_j^l(a, \cdot). \end{aligned}$$ □

We can now formulate the transport theorem on the discrete evolving surface. This is possible because in the proof, which is similar to the proofs of Theorem 5.1 and Lemma 5.2, we do not use integration by parts.

**Lemma 5.6.** Let $\Gamma_h(t)$ be an evolving admissible triangulation with material velocity $V_h$. Then

$$\frac{\mathrm{d}}{\mathrm{d}t} \int_{\Gamma_h(t)} f \, \mathrm{d}A_h = \int_{\Gamma_h(t)} \partial_h^\bullet f + f \, \nabla_{\Gamma_h} \cdot V_h \, \mathrm{d}A_h. \tag{5.28}$$

For $\phi \in S_h(t), W_h \in S_h(t)$,

$$\frac{\mathrm{d}}{\mathrm{d}t} m_h(\phi, W_h) = m_h(\partial_h^\bullet \phi, W_h) + m_h(\phi, \partial_h^\bullet W_h) + g_h(V_h; \phi, W_h),$$

$$\frac{\mathrm{d}}{\mathrm{d}t} a_h(\phi, W_h) = a_h(\partial_h^\bullet \phi, W_h) + a_h(\phi, \partial_h^\bullet W_h) + b_h(V_h; \phi, W_h),$$

https://doi.org/10.1017/S0962492913000056 Published online by Cambridge University Press

with the bilinear form

$$b_h(V_h;\phi,W_h)=\sum_{E(t)\in\mathcal{T}_h(t)}\int_{E(t)}\mathcal{B}_h(V_h)\nabla_{\Gamma_h}\phi\cdot\nabla_{\Gamma_h}W_h\,\mathrm{d}A_h, \tag{5.29}$$

where

$$\mathcal{B}_h(V_h)=\partial_h^\bullet\mathcal{A}^{-l}+\nabla_{\Gamma_h}\cdot V_h\,\mathcal{A}^{-l}-2D_h(V_h),$$

$$D_h(V_h)_{ij}=\frac{1}{2}\sum_{k=1}^{n+1}\big(\mathcal{A}^{-l}_{ik}(\nabla_{\Gamma_h})_kV_{hj}+\mathcal{A}^{-l}_{jk}(\nabla_{\Gamma_h})_kV_{hi}\big),\quad i,j=1,\dots,n+1.$$

Let $\Gamma(t)$ be an evolving surface decomposed into curved elements $\tilde{E}(t)$ whose edges move with velocity $v_h$. Then

$$\frac{\mathrm{d}}{\mathrm{d}t}\int_{\Gamma(t)}f\,\mathrm{d}A=\int_{\Gamma(t)}\partial_h^\bullet f+f\,\nabla_{\Gamma_h}\cdot v_h\,\mathrm{d}A. \tag{5.30}$$

For $\varphi(\cdot,t),w(\cdot,t),\partial_h^\bullet\varphi(\cdot,t),\partial_h^\bullet w(\cdot,t)\in H^1(\Gamma(t))$,

$$\frac{\mathrm{d}}{\mathrm{d}t}m(\varphi,w)=m(\partial_h^\bullet\varphi,w)+m(\varphi,\partial_h^\bullet w)+g(v_h;\varphi,w), \tag{5.31}$$

$$\frac{\mathrm{d}}{\mathrm{d}t}a(\varphi,w)=a(\partial_h^\bullet\varphi,w)+a(\varphi,\partial_h^\bullet w)+b(v_h;\varphi,w). \tag{5.32}$$

**Remark 5.7.** The continuous surface moves with the smooth velocity $v$; the discrete surface moves with the piecewise linear velocity $V_h$. If we project the discrete surface onto the continuous one by $a(\cdot,t)$, then this induces another velocity on (of) the smooth surface, which we call $v_h$.

From the smoothness of $\Gamma$ and $\mathcal{A}$ and the fact that $V_h$ is the interpolant of the smooth velocity $v$, we have that

$$\|\nabla_{\Gamma_h}V_h\|_{L^\infty(\Gamma_h)}+\|\mathcal{B}_h(V_h)\|_{L^\infty(\Gamma_h)}\le c$$

uniformly in time.

We are now in a position to cleanly formulate a discretization of the continuous PDE (5.15).

**Definition 5.8 (ESFEM).** Given $U_{h0}\in S_h(0)$, determine $U_h\in S_h^T$,

$$S_h^T=\big\{\phi_h\in C^0(\mathcal{G}_T^h)\mid\partial_h^\bullet\phi_h\in C^0(\mathcal{G}_T^h)\text{ and }\phi_h(\cdot,t)\in S_h(t)\ \forall t\in[0,T]\big\},$$

such that for all $\phi_h\in S_h^T$ and all $t\in(0,T]$,

$$\frac{\mathrm{d}}{\mathrm{d}t}m_h(U_h,\phi_h)+a_h(U_h,\phi_h)=m_h(U_h,\partial_h^\bullet\phi_h),\ U_h(\cdot,0)=U_{h0}. \tag{5.33}$$

$U_h$ is then called a discrete solution of (5.15) with initial value $U_{h0}$.

https://doi.org/10.1017/S0962492913000056 Published online by Cambridge University Press

Using the transport property Lemma 5.5, it follows that this definition is equivalent to

$$\frac{\mathrm{d}}{\mathrm{d}t} m_h(U_h, \chi_j) + a_h(U_h, \chi_j) = 0, \quad U_h(\cdot, 0) = U_{h0}, \tag{5.34}$$

for all $j = 1, \dots, J$.

Setting $\mathcal{M}(t)$ to be the evolving mass matrix

$$\mathcal{M}(t)_{jk} = \int_{\Gamma_h(t)} \chi_j \chi_k \, \mathrm{d}A_h,$$

$\mathcal{S}(t)$ to be the evolving stiffness matrix

$$\mathcal{S}(t)_{jk} = \int_{\Gamma_h(t)} \mathcal{A}^{-l} \nabla_{\Gamma_h} \chi_j \cdot \nabla_{\Gamma_h} \chi_k \, \mathrm{d}A_h,$$

and $U_h = \sum_{j=1}^{J} \alpha_j \chi_j$, $\alpha = (\alpha_1, \dots, \alpha_J)$, we arrive at the following simple version of the finite element approximation:

$$\frac{\mathrm{d}}{\mathrm{d}t}(\mathcal{M}(t)\alpha) + \mathcal{S}(t)\alpha = 0, \tag{5.35}$$

which does not explicitly involve the velocity of the surface.

Since the mass matrix $\mathcal{M}(t)$ is uniformly positive definite for $t \in [0, T]$ and the stiffness matrix $\mathcal{S}(t)$ is positive semidefinite, we get existence and uniqueness of the semidiscrete finite element solution.

Observe that our method and analysis includes the case of advection–diffusion on a stationary surface in which $v_\nu = 0$ and the vertices are moved with the tangential velocity $v_\tau$. Moreover, note that the numerical method simply requires knowledge of the location of the vertices of the triangulation and avoids knowledge of the map $G$ in Section 5.1. This is of particular advantage in applications where an approximate triangulated surface is often calculated as part of the solution process.

**Lemma 5.9.** There exists a unique solution of (5.33). The lifted discrete solution $u_h = U_h^l$, $u_{h0} = U_{h0}^l$, satisfies the *a priori* bounds

$$\sup_{(0,T)} \|u_h\|^2_{L^2(\Gamma)} + \int_0^T \|\nabla_\Gamma u_h\|^2_{L^2(\Gamma)} \, \mathrm{d}t \le c \|u_{h0}\|^2_{L^2(\Gamma(0))}, \tag{5.36}$$

$$\int_0^T \|\partial_h^\bullet u_h\|^2_{L^2(\Gamma)} \, \mathrm{d}t + \sup_{(0,T)} \|\nabla_\Gamma u_h\|^2_{L^2(\Gamma)} \le c \|u_{h0}\|^2_{H^1(\Gamma(0))}. \tag{5.37}$$

The proof of this lemma is done similarly to the proof of Theorem 5.3 but now with the use of Lemma 5.6.

https://doi.org/10.1017/S0962492913000056 Published online by Cambridge University Press

*5.5. Error analysis of ESFEM*

With the help of the formulae from Lemma 5.6 we have proved the following error estimates for the evolving surface finite element method in Dziuk and Elliott (2007*a*, 2013).

**Theorem 5.10 (convergence).** Let $u$ be a sufficiently smooth solution of (5.15) satisfying

$$\int_0^T \|u\|^2_{H^2(\Gamma)} + \|\partial^\bullet u\|^2_{H^2(\Gamma)}\,\mathrm{d}t < \infty, \tag{5.38}$$

and let $u_h(\cdot,t) = U_h^l(\cdot,t)$, $t \in [0,T]$, be the spatially discrete solution from Lemma 5.9 with initial data $u_{h0} = U_{h0}^l$ satisfying

$$\|u(\cdot,0) - u_{h0}\|_{L^2(\Gamma(0))} \le ch^2.$$

Then the error estimates

$$\sup_{t\in(0,T)} \|u(\cdot,t) - u_h(\cdot,t)\|_{L^2(\Gamma(t))} \le ch^2 \tag{5.39}$$

and

$$\int_0^T \|u(\cdot,t) - u_h(\cdot,t)\|^2_{H^1(\Gamma(t))}\,\mathrm{d}t \le ch^2$$

hold for $h \le h_0$ with a constant $c$ independent of $h$ but depending on the norms (5.38) and on the geometry of $\mathcal{G}_T$.

Under suitable assumptions on $\mathcal{G}_T$, $\mathcal{A}$, $v$ and $u_0$ it can be shown that (5.38) holds: see Dziuk and Elliott (2007*a*).

*5.6. Time discretization*

Let $N$ be a positive integer and set $\tau = T/N$. For each $n \in \{0,\dots,N\}$ set $t^n = n\tau$. For a discrete time sequence $f^n$, $n \in \{0,\dots,N\}$, we use the notation

$$\partial_\tau f^n = \frac{1}{\tau}(f^{n+1} - f^n).$$

For the time-discrete case we introduce a suitable material derivative. Assume that $\phi_h^n \in S_h^n$, $\phi_h^n = \sum_{j=1}^J \phi_j^n \chi_j^n$ with the lift

$$\varphi_h^n = \sum_{j=1}^J \phi_j^n \chi_j^{n,l} \in S_h^{n,l}.$$

Then we define

$$\partial_h^\bullet \phi_h^n = \sum_{j=1}^J \partial_\tau \phi_j^n \chi_j^n \in S_h^n, \quad \partial_h^\bullet \varphi_h^n = \sum_{j=1}^J \partial_\tau \phi_j^n \chi_j^{n,l} \in S_h^{n,l}. \tag{5.40}$$

We write the fully discrete scheme in the following form.

https://doi.org/10.1017/S0962492913000056 Published online by Cambridge University Press

**Algorithm 5.11.** Given $U_h^0 \in S_h^0$, find

$$U_h^n \in S_h^n, \quad n \in \{1, \dots, N\}$$

such that for all $\phi_h^n \in S_h^n$ and $\phi_h^{n+1} \in S_h^{n+1}$ and $n \in \{0, \dots, N-1\}$

$$\partial_\tau m_h(U_h^n, \phi_h^n) + a_h(U_h^{n+1}, \phi_h^{n+1}) = m_h(U_h^n, \partial_h^\bullet \phi_h^n). \tag{5.41}$$

Let us discuss the matrix–vector form of this fully discrete scheme. Choosing $\phi_h^n = \chi_i^n$ in (5.41), it follows that this definition is *equivalent* to

$$\partial_\tau m_h(U_h^n, \chi_i^n) + a_h(U_h^{n+1}, \chi_i^{n+1}) = 0 \tag{5.42}$$

for all $i = 1, \dots, J$.

Setting $\mathcal{M}(t), \mathcal{M}^n$ to be the time-dependent mass matrices

$$\mathcal{M}(t)_{jk} = \int_{\Gamma_h(t)} \chi_j(\cdot,t)\chi_k(\cdot,t)\,\mathrm{d}A_h, \quad \mathcal{M}^n = \mathcal{M}(t^n),$$

$(j,k = 1, \dots, J)$, and $\mathcal{S}(t), \mathcal{S}^n$ to be the time-dependent stiffness matrices

$$\mathcal{S}(t)_{jk} = \int_{\Gamma_h(t)} \mathcal{A}^{-l}(\cdot,t)\nabla_{\Gamma_h}\chi_j(\cdot,t) \cdot \nabla_{\Gamma_h}\chi_k(\cdot,t)\,\mathrm{d}A_h, \quad \mathcal{S}^n = \mathcal{S}(t^n),$$

we arrive at the following simple version of the fully discrete finite element approximation:

$$\partial_\tau(\mathcal{M}^n\alpha^n) + \mathcal{S}^{n+1}\alpha^{n+1} = 0.$$

Equivalently,

$$(\mathcal{M}^{n+1} + \tau\mathcal{S}^{n+1})\alpha^{n+1} = \mathcal{M}^n\alpha^n, \tag{5.43}$$

where

$$U_h^{n+1} = \sum_{j=1}^{N} \alpha_j^{n+1}\chi_j^{n+1}$$

has to be determined as the solution of the sparse system of linear equations (5.43). Since for each $n$ the mass matrix $\mathcal{M}^n$ is uniformly positive definite and the stiffness matrix $\mathcal{S}^n$ is positive semidefinite, we get existence and uniqueness of the discrete finite element solution.

We show how to prove stability for the fully discrete scheme. This is the fully discrete analogue of the continuous estimates (5.16) and (5.17). In the lemma below we use the notation $U_h^L$ and $u_h^L$ to denote linear interpolations in time of the time level values $U_h^n$ and $u_h^n$, $n = 0, 1, 2, \dots, N$. Note that the material derivatives are piecewise constant in time and we indicate in the natural way which constants are to be used in the sums.

https://doi.org/10.1017/S0962492913000056 Published online by Cambridge University Press

**Lemma 5.12.** The fully discrete solution $U_h^k$ with lift

$$u_h^k = (U_h^k)^l \quad (k = 0, \dots, N)$$

satisfies the following *a priori* bounds for $\tau \le \tau_0$:

$$|U_h^n|^2_{L^2(\Gamma_h(t^n))} + \tau \sum_{k=1}^{n} |\nabla_{\Gamma_h} U_h^k|^2_{L^2(\Gamma_h(t^k))} \le c|U_h^0|^2_{L^2(\Gamma_h(0))},$$

$$|u_h^n|^2_{L^2(\Gamma(t^n))} + \tau \sum_{k=1}^{n} |\nabla_{\Gamma} u_h^k|^2_{L^2(\Gamma(t^k))} \le c|u_h^0|^2_{L^2(\Gamma(0))},$$

$$\tau \sum_{k=0}^{n-1} |\partial_h^\bullet U_h^L(\cdot, t^{k+1} - 0)|^2_{h,k} + |\nabla_{\Gamma_h} U_h^n|^2_{L^2(\Gamma_h(t^n))} \le c\big(|U_h^0|^2_{L^2(\Gamma_h(0))} + |\nabla_{\Gamma_h} U_h^0|^2_{L^2(\Gamma_h(0))}\big),$$

$$\tau \sum_{k=0}^{n-1} |\partial_h^\bullet u_h^L(\cdot, t^{k+1} - 0)|^2_{k} + |\nabla_{\Gamma} u_h^n|^2_{L^(\Gamma(t^n))} \le c\big(|u_h^0|^2_{L^2(\Gamma(0))} + |\nabla_{\Gamma} u_h^0|^2_{L^2(\Gamma(0))}\big).$$

The constants depend on the data of the problem including the final time $T$.

In Dziuk and Elliott (2012) we proved the following error estimate for the fully discrete scheme.

**Theorem 5.13.** Let $u$ be a sufficiently smooth solution of (5.13), and assume that

$$\|u_0 - u_h^0\|_{L^2(\Gamma_0)} \le ch^2. \tag{5.44}$$

Let $u_h^k = (U_h^k)^l$ $(k = 0, \dots, N)$ be the lift of the solution of the fully discrete scheme (5.41). Then for $0 < \tau \le \tau_0$ and $0 < h \le h_0$ we have the error bounds

$$\|u(\cdot, t^n) - u_h^n\|^2_{L^2(\Gamma(t^n))} + h^2 \tau \sum_{k=1}^{n} \|\nabla_\Gamma u(\cdot, t^k) - \nabla_\Gamma u_h^k\|^2_{L^2(\Gamma(t^k))} \le c(\tau^2 + h^4) \tag{5.45}$$

for all $n \in \{0, \dots, N\}$, with a constant $c$ which is independent of $\tau$ and $h$. Note that $c, h_0$ and $\tau_0$ depend on the data of the problem.

We close this section with an example from Dziuk and Elliott (2007*a*).

**Example 5.14.** The example confirms the theoretical results. We solve the PDE

$$\partial^\bullet u + u \nabla_\Gamma \cdot v - \Delta_\Gamma u = f \tag{5.46}$$

https://doi.org/10.1017/S0962492913000056 Published online by Cambridge University Press

Table 5.1. Errors and experimental orders of convergence (EOC) for the example (5.46), (5.47).

| $h(T)$ | $L^\infty(L^\infty)$ | EOC | $L^\infty(L^2)$ | EOC | $L^2(H^1)$ | EOC |
|---|---|---|---|---|---|---|
| 0.82737 | 0.095488 | – | 0.15424 | – | 0.29287 | – |
| 0.43422 | 0.057944 | 0.77 | 0.097788 | 0.71 | 0.17507 | 0.80 |
| 0.21939 | 0.018764 | 1.65 | 0.033083 | 1.59 | 0.074327 | 1.26 |
| 0.10994 | 0.0050819 | 1.89 | 0.0089784 | 1.89 | 0.033367 | 1.16 |
| 0.055007 | 0.0013038 | 1.97 | 0.0022950 | 1.97 | 0.016053 | 1.06 |

on the moving surface

$$\Gamma(t) = \left\{ x \in \mathbb{R}^3 \mid \frac{x_1^2}{1 + 0.25 \sin t} + x_2^2 + x_3^2 = 1 \right\}. \tag{5.47}$$

As the exact solution of the PDE we have chosen the function $u(x,t) = \mathrm{e}^{-6t} x_1 x_2$ and calculated the right-hand side $f$ from the PDE. We then calculated the following errors from the exact solution and the computed solution for the time interval $[0,T]$ with $T = 2$:

$$L^\infty(L^\infty) = \sup_{(0,T)} \|u - u_h\|_{L^2(\Gamma)}, \quad L^\infty(L^2) = \sup_{(0,T)} \|u - u_h\|_{L^2(\Gamma)},$$

$$L^2(H^1) = \left( \int_0^T \|\nabla_\Gamma (u - u_h)\|^2_{L^2(\Gamma)} \,\mathrm{d}t \right)^{\frac{1}{2}}.$$

In our computations we have chosen $\tau = h^2$ in order to reveal the quadratic convergence in the $L^2$ norm.

For a more appealing computational example see Figure 5.3.

### *5.7. ALE ESFEM*

Another definition of an evolving hypersurface $\Gamma(t)$ is the zero level set of a time-dependent level set function $\phi : \mathcal{U} \times (0,T) \to \mathbb{R}$, where $\mathcal{U}$ is an open set in $\mathbb{R}^3$ so that

$$\Gamma(t) = \{ x \in \mathcal{U} \mid \phi(x,t) = 0 \}$$

and $\nabla \phi(x,t) \neq 0,\ x \in \Gamma(t)$. For such a hypersurface we define the oriented normal $\nu$ and the normal velocity $V$ by

$$\nu(x,t) = \frac{\nabla \phi(x,t)}{|\nabla \phi(x,t)|}, \quad V(x,t) = -\frac{\phi_t(x,t)}{|\nabla \phi(x,t)|}.$$

https://doi.org/10.1017/S0962492913000056 Published online by Cambridge University Press

See Section 7.5 for a complete discussion. Thus moving a point $P_0 \in \Gamma(0)$ by the velocity

$$\dot{P} = V(P,\cdot)\nu(P,\cdot) + v_\tau^a(P,\cdot), \quad P(0) = P_0,$$

where $v_\tau^a$ is an arbitrary tangential velocity field satisfying $v_\tau^a(x,t)\cdot\nu(x,t) = 0$, keeps $P(t)$ on the surface $\Gamma(t)$ because

$$\frac{\mathrm{d}}{\mathrm{d}t}\phi(P(t),t) = \nabla\phi(P(t),t)\cdot\dot{P}(t) + \phi_t(P(t),t) = 0.$$

Thus we may recover the description in Section 5.1 of a moving hypersurface: $G : \Gamma(0)\times(0,T) \to \Gamma(t)$ so that

$$\Gamma(t) = \{x = G(P_0,t) \mid P_0 \in \Gamma(0)\} \quad \text{and} \quad G_t\cdot\nu = V.$$

Choices for a tangential velocity $v_\tau^a$ include the following.

- Frequently in mathematical models there is a material velocity $v = v_\nu + v_\tau$. For example, this might arise when the hypersurface is a fluid–material interface, and choosing $P_t(t) = v(P(t),t)$, $P(0) = P_0 \in \Gamma_0$ implies that points $P(t)$ evolve as material points. In this case there is a natural physical tangential velocity and one may wish to use the material velocity to define the map. For example, this is the case when using ESFEM for the advection–diffusion equation.

- In applications it may be that the hypersurface is determined by a geometric evolution law for which there is a natural partial differential equation which evolves a parametrization. For example, the solution of the equation

  $$X_t - \frac{1}{|X_\theta|}\left(\frac{X_\theta}{|X_\theta|}\right)_\theta = 0$$

  for the parametrization $X = X(\theta,t)$ of a closed curve ($X(\theta+2\pi,t) = X(\theta,t)$, $\theta\in[0,2\pi]$) defines motion by curvature, called curve shortening flow, for which the solution $\Gamma(t) = X([0,2\pi],t)$ moves in a normal direction. On the other hand the equation

  $$X_t - \frac{X_{\theta\theta}}{|X_\theta|^2} = 0$$

  evolves a closed planar curve in the normal direction with velocity given by the curvature, but has a tangential velocity defined by the equation.

- It may be that we wish to choose a tangential velocity in such a way as to yield a *nice* map $G$ and thus a nice grid.

https://doi.org/10.1017/S0962492913000056 Published online by Cambridge University Press

As an example, consider the triangulated surfaces in Figure 5.4. These are interpolations of a hypersurface defined as the zero level set of (*cf.* Barreira *et al.* 2011, Elliott and Styles 2012)

$$\phi(x,t) = x_1^2 + x_2^2 + a(t)^2 G(x_3^2/L(t)^2) - a(t)^2,$$

where $G(s) = 200s(s - 199/200)$, $a(t) = 0.1 - 0.04\sin(2\pi t)$ and $L(t) = 1 + 0.5\sin(\pi t)$. The triangulated surfaces in plots (b), (d) and (f) are obtained using pure normal motion for the position of the triangle vertices, while those in plots (a), (c) and (e) have a non-zero tangential velocity. Plots (a,b) show the initial triangulated surface, which is the same in each case.

From this figure we see that although both sets of surfaces are interpolations which evolve from the same mesh, the difference between the two meshes is quite pronounced. In particular, the nodes of the triangulated surface on the left, where tangential motion is present, are quite uniformly distributed over the surface, while the nodes of the triangulated surface on the left are very coarsely separated over some parts of the surface.

This is an example which suggests that when evolving triangulations it may be useful to use an arbitrary tangential velocity rather than using a material velocity. This arbitrary tangential velocity may be used to generate a *good* triangulation of the surface. This motivates the arbitrary Lagrangian Eulerian evolving surface finite element method (ALE ESFEM). The goal is to solve the advection–diffusion equation (5.13) numerically. In this approach the surface $\Gamma_h(t)$ interpolates $\Gamma(t)$ in such a way that the velocity of the vertices may not be the material velocity associated with the equation (5.13), so that the nodes move with a velocity $V_h^M \neq V_h = I_h v$ (see also Section 5.4). It follows that since

$$\partial_M^\bullet \chi_i = \frac{\partial \chi_i}{\partial t} + V_h^M \cdot \nabla \chi_i = 0, \quad \text{for all} \quad i \in \{1, \dots, J\},$$

the nodal basis functions, $\chi_i(\cdot,t)$ $(i = 1 \dots J)$, of $S^h(\Gamma_h(t))$ satisfy the transport property

$$\partial_h^\bullet \chi_i = (V_h - V_h^M) \cdot \nabla \chi_i.$$

This leads to the following discretization of (5.13) with $\mathcal{A} = I$:

$$\frac{\mathrm{d}}{\mathrm{d}t} \int_{\Gamma_h(t)} U_h \chi_i \,\mathrm{d}A_h + \int_{\Gamma_h(t)} \nabla_{\Gamma_h} U_h \cdot \nabla_{\Gamma_h} \chi_i \,\mathrm{d}A_h = \int_{\Gamma_h(t)} U_h (V_h - V_h^M) \cdot \nabla_{\Gamma_h} \chi_i \,\mathrm{d}A_h$$

for all $i = 1, \dots, J$.

For a fully discrete approximation one can use a fully implicit time discretization.

https://doi.org/10.1017/S0962492913000056 Published online by Cambridge University Press

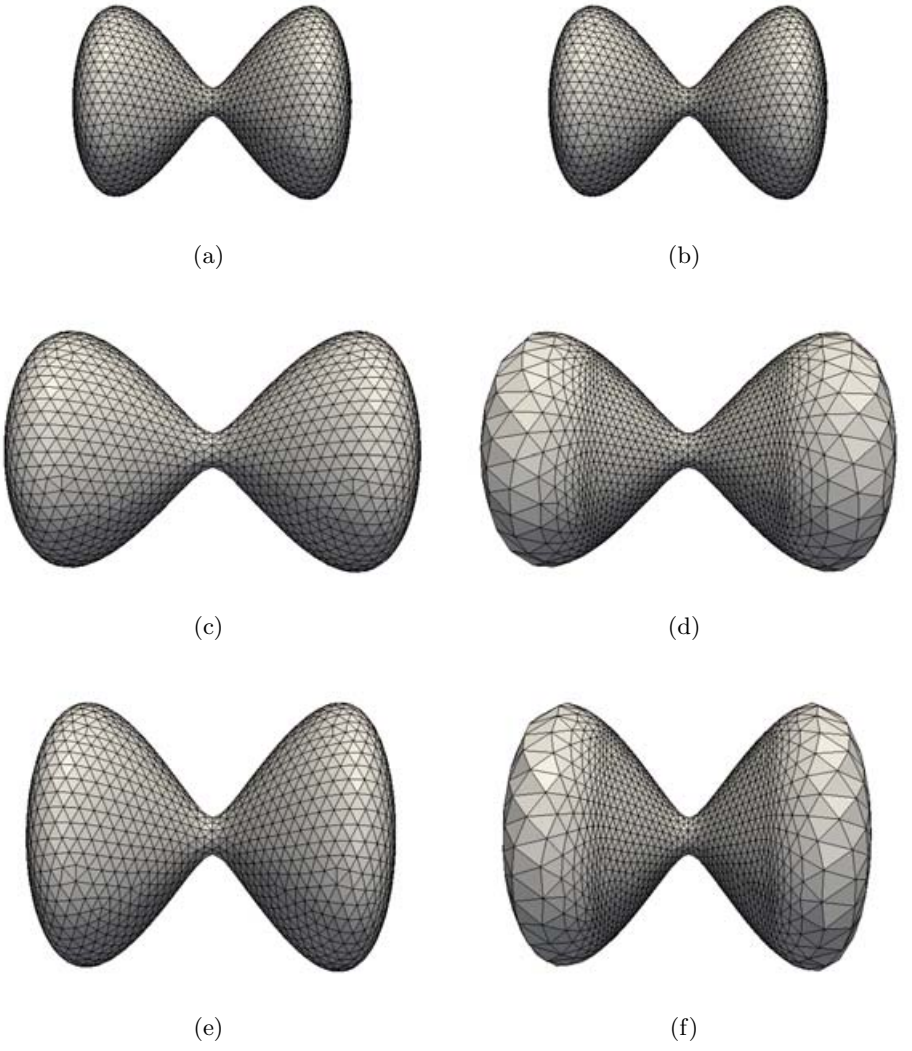


Figure 5.4. Interpolated triangulated surfaces evolving from the same mesh. Vertices (a), (c) and (e) have a tangential and normal velocity whereas vertices (b), (d) and (f) evolve with only a normal velocity.

https://doi.org/10.1017/S0962492913000056 Published online by Cambridge University Press

**Algorithm 5.15.** Given $\Gamma_h^{m-1}$, $\Gamma_h^m$ and $U_h^{m-1} \in S_h^{m-1}$, find $U_h^m \in S_h^m$ such that

$$\frac{1}{\tau}\int_{\Gamma_h^m} U_h^m \chi_h^m \,\mathrm{d}A_h - \frac{1}{\tau}\int_{\Gamma_h^{m-1}} U_h^{m-1}\chi_h^{m-1}\,\mathrm{d}A_h + \int_{\Gamma_h^m} \nabla_{\Gamma_h^m} U_h^m \cdot \nabla_{\Gamma_h^m}\chi_h^m \,\mathrm{d}A_h$$
$$+ \int_{\Gamma_h^m} (V_h^{M,m} - V_h^m) U_h^m \cdot \nabla_{\Gamma_h^m}\chi_h^m \,\mathrm{d}A_h = 0, \quad \text{for all } \chi_h^m \in S_h^m.$$

Here $V_h^{M,m} = \sum_{i=1}^J \dot{X}_i^m \chi_i^m$ and $V_h^m = V_h(\cdot, m\tau)$.

The key difference between the two methods is that in the ESFEM method the normal velocity of the surface and the advective velocity do not explicitly appear in the discretization. The numerical method only requires knowledge of the position of the vertices and there is no advective term to consider in the discretization. On the other hand, in the ALE ESFEM an advective velocity term appears explicitly in the discretization. If $\dot{X}_i^m = v(X_i^m, m\tau)$ then the ALE ESFEM reduces to ESFEM.

We refer to Elliott and Styles (2012) for examples suggesting the possible accuracy advantages of using the ALE version of ESFEM. It may be of particular value when the surface evolution is coupled to the equation on the surface and the surface has to be approximated in some way. The numerical methods of Barrett, Garcke and Nürnberg (2007, 2008*a*, 2008*b*) for geometric surface evolution yield arbitrary tangential velocities which often yield good mesh properties. This has been exploited for various applications by Elliott and Stinner (2012), Elliott *et al.* (2012) and Elliott and Styles (2012).

## 6. More surface PDEs

### *6.1. Nonlinear conservation and diffusion on a stationary surface*

Let us turn to more realistic equations for conservation and diffusion on a surface. We follow Dziuk and Elliott (2007*b*) and begin with the derivation from Section 5.2 for a stationary surface $\Gamma$.

*Conservation.* $u = u(x,t)$ ($x \in \Gamma$, $t \in [0,T]$) is the density of a scalar quantity on $\Gamma$. The basic conservation law we wish to consider can be formulated for an arbitrary portion $\mathcal{M}$ of $\Gamma$ using a surface flux $q$. The law is that, for every $\mathcal{M}$,

$$\frac{\mathrm{d}}{\mathrm{d}t}\int_{\mathcal{M}} u \,\mathrm{d}A = -\int_{\partial\mathcal{M}} q \cdot \mu \,\mathrm{d}A, \tag{6.1}$$

where $\partial\mathcal{M}$ is the boundary of $\mathcal{M}$ and $\mu$ is the co-normal on $\partial\mathcal{M}$. Using the divergence theorem Theorem 2.10 and the fact that without loss of

https://doi.org/10.1017/S0962492913000056 Published online by Cambridge University Press

generality $q$ is a tangential vector, we obtain as in Section 5.2

$$u_t + \nabla_\Gamma \cdot q = 0 \quad \text{on } \Gamma. \tag{6.2}$$

We take $q$ to be the diffusive flux with respect to a scalar function $w$ on $\Gamma$,

$$q = -\mathcal{A}\nabla_\Gamma w, \tag{6.3}$$

where $\mathcal{A}$ is a positive semidefinite symmetric mobility tensor with the property that it maps the tangent space into itself at every point of $\Gamma$; see also (5.14). This leads to the equation

$$u_t - \nabla_\Gamma \cdot (\mathcal{A}\nabla_\Gamma w) = 0 \quad \text{on } \Gamma. \tag{6.4}$$

If the surface has no boundary, $\partial\Gamma = \emptyset$, then there is no need for boundary conditions. This would be the case if $\Gamma$ is the bounding surface of a domain. On the other hand, if $\partial\Gamma$ is non-empty then we may impose boundary conditions similar to the flat case. For example, we may impose the homogeneous Dirichlet boundary condition

$$u = 0 \quad \text{on } \partial\Gamma.$$

or the no-flux condition

$$\mathcal{A}\nabla_\Gamma w \cdot \mu = 0 \quad \text{on } \partial\Gamma.$$

The variational form is obtained in the standard way by multiplying equation (6.4) by an arbitrary test function $\varphi \in H^1(\Gamma)$ and integrating over $\Gamma$. Using (2.10) we obtain

$$\int_\Gamma u_t \varphi \,\mathrm{d}A + \int_\Gamma \mathcal{A}\nabla_\Gamma w \cdot \nabla_\Gamma \varphi \,\mathrm{d}A = 0. \tag{6.5}$$

Of course, for parabolic equations we have to impose an initial condition $u(\cdot, 0) = u_0$ on $\Gamma$ with given $u_0$. In the following we will not mention this condition when it is obviously required. Note that for arbitrary tensor $\mathcal{A}$ this variational equation implies

$$u_t - \nabla_\Gamma \cdot (P\mathcal{A}P\nabla_\Gamma w) = 0 \quad \text{on } \Gamma \tag{6.6}$$

with the projection $P$ onto $\Gamma$. Note that, in general, constant coefficient tensors $\mathcal{A}$ will not satisfy the assumption that $\mathcal{A}$ maps the tangent space into itself and $P$ will not be the constant coefficient. Finally we note that this is indeed a conservation equation by taking $\varphi = 1$ in (6.5), which yields the conservation equation

$$\frac{\mathrm{d}}{\mathrm{d}t} \int_\Gamma u \,\mathrm{d}A = 0.$$

*Linear diffusion.* The heat equation on surfaces is obtained by setting $w = u$ and $\mathcal{A} = I$, where $I$ is the identity tensor,

$$u_t - \Delta_\Gamma u = 0. \tag{6.7}$$

https://doi.org/10.1017/S0962492913000056 Published online by Cambridge University Press

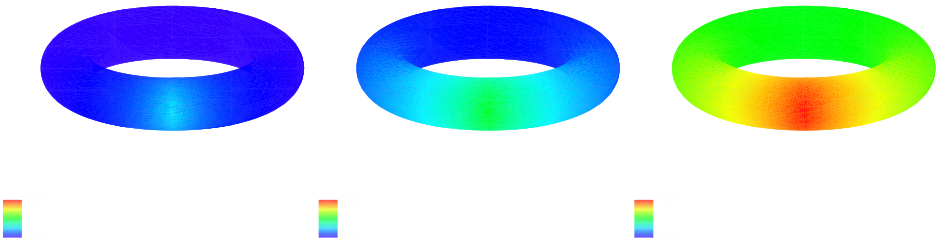


Figure 6.1. Heating up a torus. Solution of the inhomogeneous heat equation (6.8) with right-hand side (6.10) at three successive times. The colouring indicates the magnitude of the solution. The colours range between blue (0.0) and red (5.0).

This can be generalized in obvious ways. For example, an inhomogeneous variable coefficient parabolic equation is

$$u_t - \sum_{i,j=1}^{n+1} \underline{D}_i(a_{ij}\underline{D}_j u) = f, \tag{6.8}$$

where $\mathcal{A} = (a_{ij}(x,t))_{i,j=1,\dots,n+1}$ with a symmetric matrix $\mathcal{A}$ which satisfies (5.14).

We show an example of the inhomogeneous heat equation from Dziuk and Elliott (2007*b*).

**Example 6.1.** In Figure 6.1 we display the solution at three successive times of (6.8) with $\mathcal{A} = \mathcal{I}$ on the torus,

$$\Gamma = \left\{ x \in \mathbb{R}^3 \mid \left( \sqrt{x_1^2 + x_2^2} - 1 \right)^2 + x_3^2 = \frac{1}{16} \right\}, \tag{6.9}$$

with the right-hand side being a regularized version of the characteristic function

$$f(x,t) = 100\,\chi_G(x), \quad x \in \Gamma, \tag{6.10}$$

with $G = \{x \in \Gamma \mid |x - (0,1,0)| < 0.25\}$ and with initial value $u_0 = 0$.

*Nonlinear diffusion.* We find the nonlinear diffusion equation

$$u_t - \nabla_\Gamma \cdot (g(u)\nabla_\Gamma u) = 0$$

by setting

$$w = f(u) \quad \text{and} \quad \mathcal{A} = m(u)I$$

for given continuous functions $f$ and $m$, where

$$g(u) = m(u)f'(u)$$

and $g$ is positive if $f$ is monotone increasing and $m$ is positive. Clearly, by using suitable choices one recovers linear diffusion and the porous medium equation on a stationary surface $\Gamma$.

https://doi.org/10.1017/S0962492913000056 Published online by Cambridge University Press

*Parabolic surface p-Laplace equation.* Setting $w = u$ and, for $1 < p < \infty$, $\mathcal{A} = |\nabla_\Gamma u|^{p-2} I$ yields the parabolic surface $p$-Laplace equation

$$u_t - \nabla_\Gamma \cdot (|\nabla_\Gamma u|^{p-2} \nabla_\Gamma u) = 0.$$

This is $L^2(\Gamma)$-gradient flow for the energy

$$E_p(u) = \frac{1}{p} \int_\Gamma |\nabla_\Gamma u|^p \, \mathrm{d}A.$$

*Total variation flow.* We obtain a singular degenerate equation by setting $w = u$ and taking $\mathcal{A} = |\nabla_\Gamma u|^{-1} I$ which leads (formally) to the surface total variation flow

$$u_t - \nabla_\Gamma \cdot \frac{\nabla_\Gamma u}{|\nabla_\Gamma u|} = 0.$$

Variants of this equation may be useful in processing images on curved surfaces.

*Fourth-order linear diffusion.* The choice $w = -\Delta_\Gamma u$ leads to the fourth-order linear diffusion equation

$$u_t + \nabla_\Gamma \cdot (\mathcal{A} \nabla_\Gamma \Delta_\Gamma u) = 0.$$

An error analysis of the surface finite element approximation of this equation using the splitting into two second-order equations (Elliott, French and Milner 1989) was carried out by Dziuk and Elliott (2007*b*).

*Surface Cahn–Hilliard equation.* Setting

$$w = -\epsilon \Delta_\Gamma u + \frac{1}{\epsilon} \psi'(u),$$

where $\psi : \mathbb{R} \to \mathbb{R}$ is typically a double-well potential, for example the classical quartic potential

$$\psi(u) = \frac{1}{4}(1 - u^2)^2$$

leads to the fourth-order Cahn–Hilliard equation

$$u_t + \nabla_\Gamma \cdot \left( \mathcal{A} \nabla_\Gamma \left( \epsilon \Delta_\Gamma u - \frac{1}{\epsilon} \psi'(u) \right) \right) = 0.$$

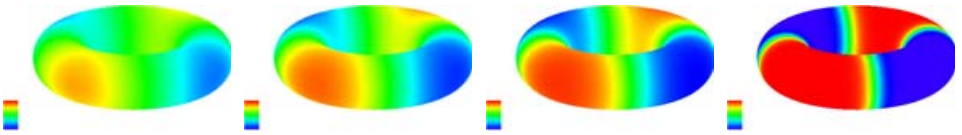
*Surface Allen–Cahn equation.* This is an example of an equation not in conservation form. $L^2(\Gamma)$-gradient flow for the energy functional

$$E(v) = \int_\Gamma \frac{\epsilon}{2} |\nabla_\Gamma v|^2 + \frac{\psi(v)}{\epsilon} \, \mathrm{d}A \tag{6.11}$$

($\epsilon > 0$) leads to

$$\epsilon u_t - \epsilon \Delta_\Gamma u - \frac{1}{\epsilon} \psi'(u) = 0. \tag{6.12}$$

https://doi.org/10.1017/S0962492913000056 Published online by Cambridge University Press



(a) $t = 0.0$ (b) $t = 0.0045$ (c) $t = 0.009$ (d) $t = 0.36$

Figure 6.2. Solution of the surface Allen–Cahn equation on a thick torus.

Here the double-well potential $\psi$ gives the classical Allen–Cahn equation on a surface $\Gamma$. Note that the Cahn–Hilliard equation may be interpreted as an $H^{-1}(\Gamma)$-gradient flow for this energy functional.

In Figure 6.2 we show the results of the numerical solution of the surface Allen–Cahn equation on a torus with initial data

$$u_0(x) = \frac{x_1 x_2}{\sqrt{x_1^2 + x_2^2 + x_3^2}}.$$

We observe the evolution to a pattern on the torus which consists of regions where the solution is close to $-1$ (blue) and regions where the solution is close to 1 (red) with a transition region of width $\varepsilon$. We have chosen $\varepsilon = 0.1$.

### *6.2. Level set equations on surfaces*

We have in mind the evolution, on the fixed surface $\Gamma$ in $\mathbb{R}^3$, of a closed curve $\mathcal{C}(t)$ which is evolving in the *intrinsic* normal direction $\nu_g$ with a velocity $V_g$. The curve $\mathcal{C}(t)$ is given by the zero level set on $\Gamma$ of $u(\cdot, t)$ and

$$\nu_g = \frac{\nabla_\Gamma u}{|\nabla_\Gamma u|}, \quad \kappa_g = \nabla_\Gamma \cdot \frac{\nabla_\Gamma u}{|\nabla_\Gamma u|}, \quad V_g = -\frac{u_t}{|\nabla_\Gamma u|}.$$

Using surface gradient notation, it is straightforward to define analogues of various geometric level set equations in the flat case to level set equations on surfaces.

*Level set geodesic mean curvature flow.* In the case that the the velocity $V_g$ is given by minus its geodesic curvature $\kappa_g$, we formulate the level set equation

$$u_t - |\nabla_\Gamma u| \, \nabla_\Gamma \cdot \frac{\nabla_\Gamma u}{|\nabla_\Gamma u|} = 0.$$

Figure 6.3 shows how circles on a dumbbell-shaped surface move under geodesic mean curvature flow. The surface $\Gamma$ is given as the image of the sphere, $\Gamma = F(S^2)$, under the map $F(x) = (x_1, \eta(x)x_2, \eta(x)x_3)$ with

$$\eta(x) = \sqrt{1 - x_1^2}\sqrt{1 - 0.8(1 - x_1^2)^2}/\sqrt{x_2^2 + x_3^2}$$

https://doi.org/10.1017/S0962492913000056 Published online by Cambridge University Press

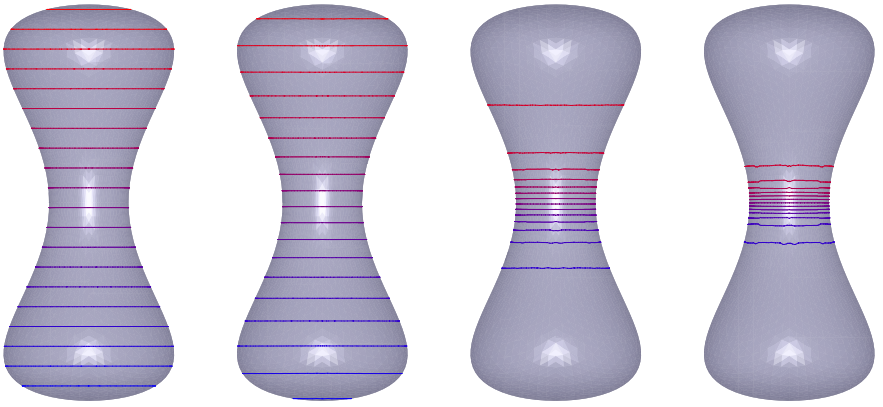


Figure 6.3. Geodesic curve shortening flow on a dumbbell. Initial circles either shrink to a point or to a geodesic during the evolution.

for $x \in S^2$. The initial function is $u_0(x) = x_1 - 0.25$. In Figure 6.3 we display all the level lines $\{x \in \Gamma \mid u(x,t) = c\}$ for $c$ between $-1.05$ and $1.25$ with intervals of 0.2. This example is taken from Dziuk and Elliott (2007*b*).

We observe that circles shrink and either move to the centre of the dumbbell's neck or shrink to round points at the extreme ends of the dumbbell. In this computation of geodesic curve shortening flow we regularized the equation by replacing $|\nabla_\Gamma u|$ by $\sqrt{\varepsilon^2 + |\nabla_\Gamma u|^2}$, and we have taken the parameter $\varepsilon$ proportional to the grid size $h$.

*Level set surface active contours.* We formulate the level set equation

$$u_t - |\nabla_\Gamma u| \nabla_\Gamma \cdot \left( f \frac{\nabla_\Gamma u}{|\nabla_\Gamma u|} \right) = 0, \tag{6.13}$$

where $f = (1 + |\nabla_\Gamma I_\sigma|^2)^{-1}$. Here typically $I_\sigma$ is a smoothing of an image which is essentially a characteristic function with sharp edges. The evolution of the zero level set curve $\mathcal{C}(t)$ is designed to detect the edge.

*Anisotropic geodesic level set mean curvature flow.* Anisotropic geodesic mean curvature flow on the given surface $\Gamma$ may be formulated by the level set equation

$$\mu(\nabla_\Gamma u) u_t - |\nabla_\Gamma u| \nabla_\Gamma \cdot (D\gamma(\nabla_\Gamma u)) = 0,$$

where $\gamma : \mathbb{R}^{n+1} \setminus \{0\} \to (0, \infty)$, $\gamma(0) = 0$, is an anisotropy function, smooth and positively homogeneous of degree one. Here $D\gamma$ denotes the gradient of $\gamma$. $\mu$ is a positive and 0-homogeneous function.

*Level set geodesic surface diffusion.* The evolution, on the fixed surface $\Gamma$ in $\mathbb{R}^3$, of a closed curve $\mathcal{C}(t)$ which is evolving in the 'intrinsic' normal direction $\nu_g$ with a velocity $V$ given by the geodesic Laplacian of the geodesic

https://doi.org/10.1017/S0962492913000056 Published online by Cambridge University Press

curvature $\kappa_g$ may be formulated as the level set equation

$$u_t - \nabla_\Gamma \cdot (|\nabla_\Gamma u|(\mathcal{I} - \nu_g \otimes \nu_g)\nabla_\Gamma w) = 0, \quad w = \nabla_\Gamma \cdot \frac{\nabla_\Gamma u}{|\nabla_\Gamma u|}.$$

*Level set geodesic Willmore flow.* Now suppose the zero level set of $u$ is the curve $\mathcal{C}(t)$ constrained to lie on $\Gamma$, which evolves according to $L^2$ gradient flow for the energy $\mathcal{E}_\mathcal{C} = \frac{1}{2}\int_\mathcal{C} \kappa_g^2$. The level set equation is then

$$\begin{aligned} u_t + |\nabla_\Gamma u| \nabla_\Gamma \cdot \left( \frac{1}{|\nabla_\Gamma u|}(I - \nu_g \otimes \nu_g)\nabla_\Gamma w \right) \\ + \frac{1}{2}|\nabla_\Gamma u| \nabla_\Gamma \cdot \left( \frac{w^2}{|\nabla_\Gamma u|^2} \frac{\nabla_\Gamma u}{|\nabla_\Gamma u|} \right) = 0, \\ w + |\nabla_\Gamma u| \, \nabla_\Gamma \cdot \frac{\nabla_\Gamma u}{|\nabla_\Gamma u|} = 0. \end{aligned}$$

Note that in these last two examples the equations are fourth-order in space but have been written as two coupled second-order equations, and that the definition of $w$ is different in each case.

### *6.3. The Jenner equation*

This PDE was derived by the authors during a stay at Jenner (California, USA). It is a linear wave equation on a moving surface. Starting with a given moving surface $\Gamma(t)$, $t \in [0, T]$, as in Section 5.1, we define the action integral

$$E(u) = \frac{1}{2}\int_0^T \int_{\Gamma(t)} (\partial^\bullet u)^2 - |\nabla_\Gamma u|^2 \, \mathrm{d}A \, \mathrm{d}t,$$

where we have used the material derivative from (5.1). We use the principle of stationary action and, for the first variation in the direction of $\varphi : \mathcal{G}_T \to \mathbb{R}$, vanishing in a neighbourhood of $\partial\mathcal{G}_T$, find that

$$0 = \langle E'(u), \varphi \rangle = \frac{\mathrm{d}}{\mathrm{d}\varepsilon}\Big|_{\varepsilon=0} E(u + \varepsilon\varphi) = \int_0^T \int_{\Gamma(t)} \partial^\bullet \varphi \partial^\bullet u - \nabla_\Gamma \varphi \cdot \nabla_\Gamma u \, \mathrm{d}A \, \mathrm{d}t.$$

Let us derive the PDE in classical form. For this we use the Leibniz formula from Theorem 5.1 together with integration by parts on $\Gamma$ from Theorem 2.10, and obtain

$$\begin{aligned} 0 &= \int_0^T \int_{\Gamma(t)} \partial^\bullet \varphi \partial^\bullet u - \nabla_\Gamma \varphi \cdot \nabla_\Gamma u \, \mathrm{d}A \, \mathrm{d}t \\ &= \int_0^T \int_{\Gamma(t)} \partial^\bullet (\varphi \partial^\bullet u) \, \mathrm{d}A \, \mathrm{d}t - \int_0^T \int_{\Gamma(t)} \varphi(\partial^\bullet \partial^\bullet u - \Delta_\Gamma u) \, \mathrm{d}A \, \mathrm{d}t \end{aligned}$$

https://doi.org/10.1017/S0962492913000056 Published online by Cambridge University Press

$$= \int_0^T \frac{\mathrm{d}}{\mathrm{d}t} \int_{\Gamma(t)} \varphi \partial^\bullet u \,\mathrm{d}A\,\mathrm{d}t - \int_0^T \int_{\Gamma(t)} \varphi \partial^\bullet u \nabla_\Gamma \cdot v \,\mathrm{d}A\,\mathrm{d}t$$
$$- \int_0^T \int_{\Gamma(t)} \varphi(\partial^\bullet \partial^\bullet u - \Delta_\Gamma u)\,\mathrm{d}A\,\mathrm{d}t$$
$$= - \int_0^T \int_{\Gamma(t)} \varphi(\partial^\bullet \partial^\bullet u + \partial^\bullet u \nabla_\Gamma \cdot v - \Delta_\Gamma u)\,\mathrm{d}A\,\mathrm{d}t.$$

The outcome is a linear wave equation on the moving surface $\Gamma$, the Jenner equation

$$\partial^\bullet \partial^\bullet u + \partial^\bullet u \nabla_\Gamma \cdot v - \Delta_\Gamma u = 0$$

on $\mathcal{G}_T$, and one has to add suitable initial conditions

$$u(\cdot, 0) = u_0, \quad \partial^\bullet u(\cdot, 0) = u_1 \quad \text{on } \Gamma(0).$$

Discretizations of this PDE in space and time have been studied in Lubich and Mansour (2012).

### *6.4. First-order conservation laws on moving surfaces*

One parametrizes the flux $q$ in the conservation law

$$\partial^\bullet u + u \nabla_\Gamma \cdot v + \nabla_\Gamma \cdot q = 0$$

by some nonlinear vector-valued function

$$q = f(x, u), \quad f = (f_1, \ldots, f_{n+1}),$$

where $f(x, s) \cdot \nu(x) = 0$ for all $x \in \Gamma(t)$ and all $s \in \mathbb{R}$ (see also (5.11)). Thus the nonlinearity $f$ *has* to depend on the spatial variable $x$. In order to obtain bounded weak solutions to the conservation law, one has to assume that $f$ is divergence-free with respect to $x$, $\nabla_\Gamma \cdot f(\cdot, s) = 0$ for all $s \in \mathbb{R}$. This then leads to the scalar conservation law

$$\partial^\bullet u + u \nabla_\Gamma \cdot v + \sum_{j=1}^{n+1} \frac{\partial f_j}{\partial u}(\cdot, u) \underline{D}_j u = 0 \tag{6.14}$$

on $\mathcal{G}_T$, and one has to impose the initial condition $u(\cdot, 0) = u_0$ on $\Gamma(0)$.

Using the parabolic regularization

$$\partial^\bullet u^\varepsilon + u^\varepsilon \nabla_\Gamma \cdot v + \sum_{j=1}^{n+1} \frac{\partial f_j}{\partial u}(\cdot, u^\varepsilon) \underline{D}_j u^\varepsilon - \varepsilon \nabla_\Gamma \cdot (\mathcal{A} \nabla_\Gamma u^\varepsilon) = 0,$$

Dziuk, Kröner and Müller (2012) prove existence and uniqueness for an entropy solution of (6.14). The PDE is discretized using the finite volume method.

https://doi.org/10.1017/S0962492913000056 Published online by Cambridge University Press

### *6.5. Coupling of surface and bulk equations*

In applications (see Section 10) one frequently encounters the coupling of surface and bulk processes. A model problem concerns the coupling of diffusion within a bulk domain to diffusion on the surface. Let $\Gamma$ be the boundary of a bounded open domain in $\mathbb{R}^{n+1}$. Consider the coupled linear system to find $u\colon \Omega \times [0,T] \to \mathbb{R}$ and $v\colon \Gamma \times [0,T] \to \mathbb{R}$ such that

$$\begin{aligned} u_t - \Delta u + u &= f \quad \text{in } \Omega, \\ (\alpha u - \beta v) + \frac{\partial u}{\partial \nu} &= 0 \quad \text{on } \Gamma, \\ v_t - \Delta_\Gamma v + v + \frac{\partial u}{\partial \nu} &= g \quad \text{on } \Gamma. \end{aligned}$$

Here we assume that $\alpha$ and $\beta$ are given positive constants and $f$ and $g$ are known functions on $\Omega$ and $\Gamma$ respectively.

In applications it may be that one has nonlinear equations or a nonlinear coupling equation or time-dependent domains $\Omega(t)$ and $\Gamma(t)$. Such equations arise in the modelling of surfactants on fluid interfaces (see references cited in Section 10.2) and also in the study of diffusion within biological cells (Novak *et al.* 2007).

## 7. PDEs on implicit surfaces

The idea of this section is based on formulating a partial differential equation on a domain in the ambient bulk space which is equivalent to solving the surface equation on all level set hypersurfaces of a prescribed function $\phi$: see Bertalmío *et al.* (2001). In order to do this we define $\phi$-surface gradients by using a projection of the gradient in $\mathbb{R}^{n+1}$ onto the level surfaces of $\phi$. These $\phi$-surface gradients are used to define weak forms of surface elliptic operators and so generate weak formulations of surface elliptic and parabolic equations. The resulting elliptic operators are degenerate because the surface gradient is always tangential to the level surfaces and thus orthogonal to the normal. In Section 8 we describe approximation of the resulting degenerate equations by the finite element method.

### *7.1. $\phi$-surface gradients, calculus and function spaces*

We follow the development in Dziuk and Elliott (2008), Burger (2009) and Deckelnick, Dziuk, Elliott and Heine (2010). Suppose that $\Omega \subset \mathbb{R}^{n+1}$ is a bounded domain with a Lipschitz boundary and let $\phi \in C^2(\bar{\Omega})$ satisfy $\nabla\phi(x) \neq 0$, for $x \in \bar{\Omega}$. We say that $\phi$ is a non-degenerate level set function. For $r \in \mathbb{R}$ we denote by $\Gamma(r)$ the $r$-level set of $\phi$ given by

$$\Gamma(r) = \{x \in \Omega \mid \phi(x) = r\}.$$

https://doi.org/10.1017/S0962492913000056 Published online by Cambridge University Press

It is a $C^2$-hypersurface if $\Gamma(r) \neq \emptyset$: see Section 2.2. We recall that $\nu : \bar{\Omega} \to \mathbb{R}^{n+1}$and $H_\phi : \bar{\Omega} \to \mathbb{R}$, given by

$$\nu(x) = \frac{\nabla\phi(x)}{|\nabla\phi(x)|}, \quad H_\phi(x) = \sum_{j=1}^{n+1} \nu_{j,x_j}(x), \quad x \in \Omega,$$

when restricted to $\Gamma(r)$, are the unit normal field and the mean curvature of $\Gamma(r)$ respectively. Finally, we associate a $\phi$-gradient with a differentiable function $f : \Omega \to \mathbb{R}$:

$$\nabla_\phi f(x) = \nabla f(x) - (\nabla f(x) \cdot \nu(x))\, \nu(x), \quad x \in \Omega.$$

Note that this is simply the tangential gradient (Definition 2.3) on level set surfaces since

$$(\nabla_\phi f)\big|_{\Gamma(r)} = \nabla_{\Gamma(r)} f\big|_{\Gamma(r)}$$

if $\Gamma(r) \neq \emptyset$. We may rewrite the $\phi$-projected gradient in the following way:

$$\nabla_\phi f = P_\phi \nabla f, \quad P_\phi = I - \nu \otimes \nu.$$

It may be used to construct degenerate elliptic operators. For example, the $\phi$-Laplacian applied to $f$ is given by

$$\Delta_\phi f = \nabla_\phi \cdot \nabla_\phi f.$$

Degeneracy of this PDE is a consequence of $P_\phi \nu = 0$.

**Lemma 7.1 ($\phi$-integration by parts).** Let $\Omega, \phi$ be as above and let $f \in H^{1,1}(\Omega)$. Then

$$\int_\Omega \nabla_\phi f |\nabla\phi| \,\mathrm{d}x = \int_\Omega f H_\phi \nu |\nabla\phi| \,\mathrm{d}x + \int_{\partial\Omega} f(\nu_{\partial\Omega} - (\nu \cdot \nu_{\partial\Omega})\nu)|\nabla\phi| \,\mathrm{d}A,$$

where $\nu_{\partial\Omega}$ denotes the unit outer normal to $\partial\Omega$.

Let $f \in H^{1,2}(\Omega), g \in H^{1,2}(\Omega)^{n+1}$. Then

$$\int_\Omega \nabla_\phi \cdot (fg)|\nabla\phi| \,\mathrm{d}x = \int_\Omega f H_\phi g \cdot \nu |\nabla\phi| \,\mathrm{d}x + \int_{\partial\Omega} fg \cdot \big(\nu_{\partial\Omega} - (\nu \cdot \nu_{\partial\Omega})\nu\big)|\nabla\phi| \,\mathrm{d}A. \tag{7.1}$$

The boundary terms in the integration by parts formulae above disappear when $\nu = \nu_{\partial\Omega}$.

For a proof see Dziuk and Elliott (2008). The following lemma is proved in Deckelnick *et al.* (2010).

**Lemma 7.2.** Let $g : \Omega \to \mathbb{R}^{n+1}$ be a differentiable vector field with $g \cdot \nu = 0$ in $\Omega$. Then

$$\nabla_\phi \cdot g = \frac{1}{|\nabla\phi|} \nabla \cdot \big(g\,|\nabla\phi|\big) \quad \text{in } \Omega.$$

https://doi.org/10.1017/S0962492913000056 Published online by Cambridge University Press

In order to formulate variational problems we introduce some function spaces. To begin we define weak surface derivatives. For a function

$$f \in L^1_{\mathrm{loc}}(\Omega),\ i \in \{1,\dots,n+1\},$$

we say that $g = \nabla_\phi f$ weakly if $g \in L^1_{\mathrm{loc}}(\Omega, \mathbb{R}^{n+1})$, and

$$\int_\Omega f\, \nabla_\phi \zeta |\nabla\phi|\,\mathrm{d}x = -\int_\Omega g\,\zeta\,|\nabla\phi|\,\mathrm{d}x - \int_\Omega f\,\zeta\, H_\phi \nu\,|\nabla\phi|\,\mathrm{d}x \tag{7.2}$$

for all $\zeta \in C_0^\infty(\Omega)$. It is not difficult to see that (7.2) is equivalent to

$$\int_\Omega f\,(\nabla_\phi\zeta)_i\,\mathrm{d}x = -\int_\Omega (\nabla_\phi f)_i\,\zeta\,\mathrm{d}x + \int_\Omega f\,\zeta(h_i - H_\phi\nu_i)\,\mathrm{d}x \tag{7.3}$$

for all $\zeta \in C_0^\infty(\Omega)$, where $h_i = \nu_{i,x_j}\nu_j$ $(i = 1,\dots,n+1)$. For $1 \le p \le \infty$ we define

$$H^{1,p}_\phi(\Omega) = \{f \in L^p(\Omega) \mid \nabla_\phi f \in L^p(\Omega)^{n+1}\},$$

which we equip with the norm

$$\|f\|_{H^{1,p}_\phi(\Omega)} = \left(\int_\Omega |f|^p + |\nabla_\phi f|^p\,\mathrm{d}x\right)^{\frac{1}{p}}$$

for $p < \infty$ with the usual modification in the case $p = \infty$. Similarly we define the spaces $H^{k,p}_\phi(\Omega)$ for $k \in \mathbb{N}, k \ge 2$. Further, let $H^{0,p}_\phi(\Omega) = L^p(\Omega)$. We note that the spaces $H^{k,2}_\phi(\Omega)$ are Hilbert spaces.

In implicit approaches to surface equations a possible choice for the level set function $\phi$ is the signed distance function $d$ to $\Gamma$ (if it is available) and in that case $|\nabla\phi| = |\nabla d| = 1$ on $\Omega$.

### *7.2. $\phi$-elliptic equation*

In this section we prove existence and regularity for solutions of a model equation. We consider the implicit surface equation

$$-\Delta_\phi u + cu = f \quad \text{in } \Omega.$$

It is convenient to consider domains $\Omega$ with the special form

$$\Omega = \{x \in \mathbb{R}^{n+1} \mid \alpha < \phi(x) < \beta\}, \quad -\infty < \alpha < \beta < \infty \tag{7.4}$$

and recall that $\Gamma(r) = \{x \in \Omega \mid \phi(x) = r\}$ is the $r$-level set of $\phi$. We suppose that $\Gamma(\alpha)$ and $\Gamma(\beta)$ are closed hypersurfaces so that $\Omega$ is an annular domain.

Let $\Omega, \phi$ be as above and assume that $f \in L^2(\Omega), c \in L^\infty(\Omega)$ with $c \ge \bar{c}$ a.e. in $\Omega$ where $\bar{c}$ is a positive constant.

Using Lemma 7.2 we may rewrite the equation in the form

$$-\nabla\cdot\big(P_\phi \nabla u\,|\nabla\phi|\big) + cu\,|\nabla\phi| = f\,|\nabla\phi| \quad \text{in } \Omega. \tag{7.5}$$

https://doi.org/10.1017/S0962492913000056 Published online by Cambridge University Press

Multiplying by a test function, integrating over $\Omega$ and using integration by parts leads to the following variational problem: find $u \in H^{1,2}_{\phi}(\Omega)$ such that

$$\int_\Omega \nabla_\phi u \cdot \nabla_\phi \varphi \, |\nabla \phi| \, \mathrm{d}x + \int_\Omega c u \varphi |\nabla \phi| \, \mathrm{d}x = \int_\Omega f \varphi |\nabla \phi| \, \mathrm{d}x \tag{7.6}$$

for all $\varphi \in H^{1,2}_{\phi}(\Omega)$. Note that the boundary term vanishes because the unit outer normal to $\partial\Omega$ points in the direction of $\nabla\phi$. It is clear from the developments above (see also Burger 2009) that (7.6) has a unique solution $u \in H^{1,2}_{\phi}(\Omega)$. The next result gives a characterization of functions in $H^{1,p}_{\phi}(\Omega)$ in terms of the spaces $H^{1,p}(\Gamma(r))$ (see Definition 2.11). Again from Deckelnick *et al.* (2010) we have the following result.

**Lemma 7.3.** Let $1 < p < \infty$, $u \in L^p(\Omega)$ and let $\Omega$ be of the form (7.4). Then $u \in H^{1,p}_{\phi}(\Omega)$ if and only if $u|_{\Gamma(r)} \in H^{1,p}(\Gamma(r))$ for almost all $r \in (\alpha, \beta)$ and the map $r \mapsto \|u\|_{H^{1,p}(\Gamma(r))}$ $(r \in (\alpha, \beta))$ is in $L^p(\alpha, \beta)$.

Using the co-area formula, (2.12), one can show that $u|_{\Gamma(r)}$ is the weak solution of

$$-\Delta_\Gamma u + cu = f \quad \text{on } \Gamma(r)$$

for almost all $r \in (\alpha, \beta)$. Since $f \in L^2(\Gamma(r))$ for almost all $r \in (\alpha, \beta)$, the regularity theory for elliptic partial differential equations on surfaces (see Theorem 3.3) implies that $u \in H^{2,2}(\Gamma(r))$ for almost all $r \in (\alpha, \beta)$ and

$$\|u\|_{H^{2,2}(\Gamma(r))} \leq c \|f\|_{L^2(\Gamma(r))}.$$

Hence,

$$\int_\alpha^\beta \|u\|^2_{H^{2,2}(\Gamma(r))} \, \mathrm{d}r \leq c \int_\alpha^\beta \|f\|^2_{L^2(\Gamma(r))} \, \mathrm{d}r = c \int_\Omega |f|^2 |\nabla \phi| \, \mathrm{d}x < \infty,$$

so that Lemma 7.3 implies that $u \in H^{2,2}_{\phi}(\Omega)$ with

$$\|u\|_{H^{2,2}_{\phi}(\Omega)} \leq c \|f\|_{L^2(\Omega)},$$

and we have proved the following theorem.

**Theorem 7.4.** Let $\Omega \subset \mathbb{R}^{n+1}$ satisfy (7.4) with $\phi \in C^2(\overline{\Omega})$, $\nabla\phi \neq 0$ on $\overline{\Omega}$. Then there exists a unique solution $u \in H^{2,2}_{\phi}(\Omega)$ of equation (7.6) and

$$\|u\|_{H^{2,2}_{\phi}(\Omega)} \leq c \|f\|_{L^2(\Omega)}.$$

Further regularity results may be obtained. The following example comes from Deckelnick *et al.* (2010).

https://doi.org/10.1017/S0962492913000056 Published online by Cambridge University Press

**Theorem 7.5.** In addition to the assumptions of Theorem 7.4, suppose that $\phi \in C^3(\overline{\Omega})$ and that the coefficients satisfy

$$\frac{\partial c}{\partial \nu} \in L^\infty(\Omega) \quad \text{and} \quad \frac{\partial f}{\partial \nu} \in L^2(\Omega).$$

Then $\frac{\partial u}{\partial \nu} \in H^{2,2}_\phi(\Omega')$ for all $\Omega' \subset\subset \Omega$, and

$$\left\| \frac{\partial u}{\partial \nu} \right\|_{H^{2,2}_\phi(\Omega')} \leq c \left( \|f\|_{L^2(\Omega)} + \left\| \frac{\partial f}{\partial \nu} \right\|_{L^2(\Omega)} \right).$$

The constant $c$ depends on $\Omega, \Omega', \phi, \bar{c}$ and $c$.

Note that for a smooth function $g : \mathbb{R} \to \mathbb{R}$ we have that $u = g(\phi)$ is $\phi$-harmonic, that is, $\Delta_\phi u = 0$.

### *7.3. $\phi$-parabolic equation*

*Conservation and diffusion.* We begin with describing a model for conservation and diffusion on level surfaces (see Dziuk and Elliott 2008). This is exactly analogous to the case of a single hypersurface (see Sections 5.2 and 6.1) and we proceed accordingly.

Let $\phi : \Omega \to \mathbb{R}$ be a prescribed non-degenerate level set function and let $\mathcal{Q} : \Omega \to \mathbb{R}^{n+1}$ be a given flux. Then the conservation law we consider is

$$\frac{\mathrm{d}}{\mathrm{d}t} \int_R |\nabla \phi| u \,\mathrm{d}x = - \int_{\partial R} \mathcal{Q} \cdot \nu_{\partial R} \,\mathrm{d}A$$

for each subdomain $R$ of $\Omega$ where $\nu_R$ is the outward unit normal to $\partial R$. In particular we consider a flux of the form

$$\mathcal{Q} = |\nabla \phi| \; q_\phi,$$

where $q_\phi : \Omega \to \mathbb{R}^{n+1}$ is a flux satisfying

$$q_\phi \cdot \nu = 0. \tag{7.7}$$

Since

$$\frac{\mathrm{d}}{\mathrm{d}t} \int_R |\nabla \phi| u \,\mathrm{d}x = \int_R u_t |\nabla \phi| \,\mathrm{d}x$$

and

$$\int_{\partial R} q_\phi \cdot \nu_{\partial R} |\nabla \phi| \,\mathrm{d}x = \int_R \nabla_\phi \cdot q_\phi |\nabla \phi| \,\mathrm{d}x, \tag{7.8}$$

where we have used $\phi$-integration by parts ((7.1), (7.7)), it follows that

$$\int_R (u_t + \nabla_\phi \cdot q_\phi) |\nabla \phi| \,\mathrm{d}x = 0$$

for every subdomain $R$, which implies the partial differential equation

$$u_t + \nabla_\phi \cdot q_\phi = 0 \quad \text{in } \Omega.$$

https://doi.org/10.1017/S0962492913000056 Published online by Cambridge University Press

For the constitutive law, in a similar way to Section 6.1 we take $q_\phi$ to be a diffusive flux given by

$$q_\phi = -\mathcal{A}\nabla_\phi w, \tag{7.9}$$

where $w$ is a field variable which will be defined in terms of $u$ by a another constitutive relation. Again it is natural to take $\mathcal{A}$ to be a symmetric diffusion tensor with the property $\mathcal{A}\nu^\perp \cdot \nu = 0$ for every tangent vector $\nu^\perp$, that is, $\nu^\perp \cdot \nu = 0$, and for which there exists a $c_0 > 0$ such that

$$z \cdot \mathcal{A}z \geq c_0 z \cdot z, \quad \text{for all } z \in \mathbb{R}^{n+1},\ z \cdot \nu = 0.$$

Thus we obtain the diffusion equation

$$u_t - \nabla_\phi \cdot (\mathcal{A}\nabla_\phi w) = 0 \quad \text{on } \Omega. \tag{7.10}$$

Throughout the following we assume the initial condition $u(\cdot, 0) = u_0(\cdot)$.

Observe that (7.10) can be written as

$$u_t - P_\phi \nabla \cdot (\mathcal{A}P_\phi \nabla w) = 0,$$

which can be seen (for $w = u$) to be a degenerate parabolic equation because $P_\phi$ has a zero eigenvalue in the normal direction $\nu$.

The variational form is then obtained by multiplying equation (7.10) by a test function $\eta$ and also by $|\nabla\phi|$, and then integrating to obtain

$$\int_\Omega (u_t - \nabla_\phi \cdot (\mathcal{A}\nabla_\phi w))\, \eta\, |\nabla\phi| \,\mathrm{d}x = 0.$$

Integration by parts (7.1), together with the observation that $\mathcal{A}\nabla_\phi w \cdot \nu = 0$, gives

$$\int_\Omega \mathcal{A}\nabla_\phi w \cdot \nabla_\phi \eta |\nabla\phi| \,\mathrm{d}x = -\int_\Omega \nabla_\phi \cdot \mathcal{A}\nabla_\phi w \eta |\nabla\phi| \,\mathrm{d}x + \int_{\partial\Omega} \mathcal{A}\nabla_\phi w \cdot \nu_{\partial\Omega} \eta |\nabla\phi| \,\mathrm{d}A.$$

In order to proceed we need a boundary condition for $w$ on $\partial\Omega$. It is natural to impose the zero flux condition

$$|\nabla\phi| \mathcal{A}\nabla_\phi w \cdot \nu_{\partial\Omega} = 0 \quad \text{on } \partial\Omega$$

and obtain the equivalent variational equation

$$\int_\Omega u_t \eta |\nabla\phi| \,\mathrm{d}x + \int_\Omega \mathcal{A}\nabla_\phi w \cdot \nabla_\phi \eta |\nabla\phi| \,\mathrm{d}x = 0, \quad \text{for all } \eta \in H^{1,2}_\phi(\Omega). \tag{7.11}$$

The solution of the equation satisfies conservation on each level surface. Let $\xi : \mathbb{R} \to \mathbb{R}$ be an arbitrary smooth function and set $\eta = \xi(\phi)$. Since $\nabla_\phi \eta = \xi'(\phi)\nabla_\phi \phi = 0$, we find the conservation equation

$$\frac{\mathrm{d}}{\mathrm{d}t} \int_\Omega u \xi(\phi) |\nabla\phi| \,\mathrm{d}x = 0.$$

https://doi.org/10.1017/S0962492913000056 Published online by Cambridge University Press

It follows from the co-area formula that

$$\int_{\inf_\Omega \phi}^{\sup_\Omega \phi} \xi(r) \left( \int_{\Gamma(r)} u \, \mathrm{d}A \right) \mathrm{d}r = \int_{\inf_\Omega \phi}^{\sup_\Omega \phi} \xi(r) \left( \int_{\Gamma(r)} u_0 \, \mathrm{d}A \right) \mathrm{d}r$$

from which we infer that on each level surface $\Gamma(r) = \{x \mid \phi(x) = r\}$ of $\phi$ we have conservation,

$$\int_{\Gamma(r)} u \, \mathrm{d}A = \int_{\Gamma(r)} u_0 \, \mathrm{d}A.$$

*Diffusion in a layered medium.* Observing that

$$\nabla_\phi \cdot \tau = \frac{1}{|\nabla \phi|} \nabla \cdot (|\nabla \phi| \tau), \quad \text{for all } \tau \cdot \nu = 0,$$

we can rewrite the diffusion equation (7.10) as

$$|\nabla \phi| u_t = \nabla \cdot (\mathcal{A}_\phi \nabla w),$$

where $\mathcal{A}_\phi = |\nabla \phi| \mathcal{A} P_\phi$. Thus we may view (7.10) as the usual diffusion equation in $\mathbb{R}^{n+1}$ with very special forms of the diffusivity tensor and mass density. Since there is no diffusion in directions normal to the level surfaces of $\phi$, we might interpret this as a diffusion equation for a stratified material whose layers are infinitesimally thin, tangential to the level surfaces of $\phi$, and insulated from each other.

*$\phi$-heat equation.* Setting $w = u$ and $\mathcal{A} = I$, we find the $\phi$-heat equation on all level surfaces of $\phi$:

$$u_t - \Delta_\phi u = 0.$$

The initial value problem for (7.11) becomes

$$\int_\Omega u_t \eta |\nabla \phi| \, \mathrm{d}x + \int_\Omega \nabla_\phi u \cdot \nabla_\phi \eta |\nabla \phi| \, \mathrm{d}x = 0 \quad \text{for all } \eta \in H^{1,2}_\phi(\Omega), \tag{7.12}$$

$$u(\cdot, 0) = u_0. \tag{7.13}$$

Setting $g(r) = \frac{1}{|\Gamma(r)|} \int_{\Gamma(r)} u_0 \, \mathrm{d}x$, we have that in the case of no-flux boundary conditions the long-time steady-state solution is $u_\infty = g(\phi)$.

Let $u$ be a weak solution of (7.12) and (7.13). Then, choosing $\eta = u$ leads to

$$\frac{1}{2} \frac{\mathrm{d}}{\mathrm{d}t} \int_\Omega u^2 |\nabla \phi| \, \mathrm{d}x + \int_\Omega |\nabla_\phi u|^2 |\nabla \phi| \, \mathrm{d}x = 0$$

and choosing $\eta = u_t$ leads to

$$\int_\Omega u_t^2 |\nabla \phi| \, \mathrm{d}x + \frac{1}{2} \frac{\mathrm{d}}{\mathrm{d}t} \int_\Omega |\nabla_\phi u|^2 |\nabla \phi| \, \mathrm{d}x = 0.$$

https://doi.org/10.1017/S0962492913000056 Published online by Cambridge University Press

*7.4. Examples of $\phi$-equations*

It is straightforward to generate analogues of well-known equations.

*Fourth-order linear diffusion.* Setting $w = -\Delta_\phi u$ leads to the fourth-order linear diffusion equation

$$u_t + \nabla_\phi \cdot (\mathcal{A} \nabla_\phi \Delta_\phi u) = 0.$$

*Nonlinear diffusion.* Setting $w = f(u)$ and $\mathcal{A} = m(u)I$, we find the nonlinear diffusion equation

$$u_t - \nabla_\phi \cdot (K(u) \nabla_\phi u) = 0,$$

where $K(u) = m(u) f'(u)$. Linear diffusion and the porous medium equation on level sets are recovered by suitable choices of $f$ and $m$.

*Parabolic surface p-Laplacian equation.* Setting $w = u$ and $\mathcal{A} = |\nabla_\phi u|^{p-2} I$ for $p > 1$ yields the parabolic surface $p$-Laplacian equation

$$u_t - \nabla_\phi \cdot (|\nabla_\phi u|^{p-2} \nabla_\phi u) = 0,$$

which is gradient flow for the energy

$$E_p(u) = \frac{1}{p} \int_\Omega |\nabla_\phi u|^p |\nabla \phi| \, \mathrm{d}x.$$

*$\phi$-Cahn–Hilliard equation.* Setting

$$w = -\epsilon \Delta_\phi u + \frac{1}{\epsilon} \psi'(u),$$

where $\psi$ is a double-well potential (*e.g.*, $\psi(u) = \frac{1}{4}(u^2 - 1)^2$), leads to the fourth-order Cahn–Hilliard equation on level sets:

$$u_t + \nabla_\phi \cdot \mathcal{A} \nabla_\phi \left( \epsilon \Delta_\phi u - \frac{1}{\epsilon} \psi'(u) \right) = 0.$$

*$\phi$-Allen–Cahn equation.* Consideration of the $L^2$ gradient flow for the gradient energy functional,

$$E(v) = \int_\Omega \left\{ \frac{\epsilon}{2} |\nabla_\phi v|^2 + \frac{1}{\epsilon} \psi(v) \right\} |\nabla \phi| \, \mathrm{d}x,$$

leads to an Allen–Cahn equation:

$$\epsilon u_t = \epsilon \Delta_\phi u - \frac{1}{\epsilon} \psi'(u).$$

*7.5. Eulerian approach to parabolic equations on moving surfaces*

We follow the development in Dziuk and Elliott (2010).

https://doi.org/10.1017/S0962492913000056 Published online by Cambridge University Press

*Notation*

It is straightforward to extend the previous notation for fixed implicit surfaces to moving surfaces by using a time-dependent smooth level set function $\phi = \phi(x,t)$ $x \in \mathbb{R}^{n+1}$, $t \in [0,T]$. In particular, we suppose that for some $k \geq 3$ and some $0 < \alpha < 1$, $\phi \in C^1([0,T], C^{k,\alpha}(\overline{\Omega}))$. Thus, for each $t \in [0,T]$, $T > 0$, we let $\Gamma(t)$ be a compact smooth orientable hypersurface (without boundary) in $\mathbb{R}^{n+1}$ so that

$$\Gamma(t) = \{x \in \Omega \mid \phi(x,t) = 0\},$$

where $\Omega$ is a bounded domain in $\mathbb{R}^{n+1}$ with Lipschitz boundary $\partial\Omega$. In what follows we assume that $\phi$ satisfies the non-degeneracy condition $\nabla\phi \neq 0$ on $\Omega \times (0,T)$. We assume that $\partial\Omega \bigcap \Gamma(t)$ is empty and set $\nu_{\partial\Omega}$ to be the unit outward pointing normal to $\partial\Omega$. We set $\Omega_T = \Omega \times (0,T)$.

The orientation of $\Gamma(t)$ is set by taking the normal $\nu$ to $\Gamma$ to be in the direction of increasing $\phi$, yielding the normal vector field

$$\nu(x,t) = \frac{\nabla\phi(x,t)}{|\nabla\phi(x,t)|},$$

so that the normal $\nu_\Gamma$ to $\Gamma(t)$ is equal to $\nu|_{\Gamma(t)}$ and the normal velocity $V$ of $\Gamma$ is given by

$$V(x,t) = -\frac{\phi_t(x,t)}{|\nabla\phi(x,t)|}.$$

*The material derivative and Leibniz formulae*

Let $v : \Omega_T \to \mathbb{R}^{n+1}$ be a prescribed velocity field which has the decomposition

$$v = V\nu + v_\tau$$

into a normal velocity field $V = v \cdot \nu$ and a tangential velocity field $v_\tau$ orthogonal to $\nu$ and thus tangential to all level surfaces of $\phi$. We use the standard notation for the material derivative of a scalar function $f = f(x,t)$ defined on $\Omega_T$:

$$\partial^\bullet f = \frac{\partial f}{\partial t} + v \cdot \nabla f.$$

In particular, we note that $\partial^\bullet f$ restricted to a given level surface

$$\Gamma(r) = \{(x,t) \mid x \in \Omega, t \in (0,T), \phi(x,t) = r\}$$

depends only on the values of $f$ on that level surface in space–time.

It is convenient to note that

$$\nabla_\phi \cdot v = VH_\phi + \nabla_\phi \cdot v_\tau$$

and

$$\nabla_\phi \cdot v = \mathrm{trace}(P_\phi \nabla v).$$

https://doi.org/10.1017/S0962492913000056 Published online by Cambridge University Press

We have the following version of the transport formula, Theorem 5.1.

**Lemma 7.6 (implicit surface transport formula).** Let $\phi$ be a level set function and let $f$ be an arbitrary function defined on $\Omega_T$ such that the following quantities exist. Then

$$\frac{\mathrm{d}}{\mathrm{d}t}\int_\Omega f|\nabla\phi|\,\mathrm{d}x = \int_\Omega (\partial^\bullet f + f\nabla_\phi\cdot v)|\nabla\phi|\,\mathrm{d}x - \int_{\partial\Omega} f\, v\cdot\nu_{\partial\Omega}|\nabla\phi|\,\mathrm{d}A. \tag{7.14}$$

*Proof.* Since $\partial_t|\nabla\phi| = \nu\cdot\nabla\phi_t$, a straightforward calculation yields

$$\frac{\mathrm{d}}{\mathrm{d}t}\int_\Omega f|\nabla\phi|\,\mathrm{d}x = \int_\Omega f_t|\nabla\phi| + f\nu\cdot\nabla\phi_t\,\mathrm{d}x.$$

Integration by parts on the second term in the integrand above gives

$$\frac{\mathrm{d}}{\mathrm{d}t}\int_\Omega f|\nabla\phi|\,\mathrm{d}x = \int_\Omega |\nabla\phi|(f_t + V\nabla f\cdot\nu + fv\cdot\nu H_\phi)\,\mathrm{d}x - \int_{\partial\Omega} f\nu\cdot\nu_{\partial\Omega}V|\nabla\phi|\,\mathrm{d}A.$$

The $\phi$-divergence theorem (7.1) gives

$$\int_\Omega fv\cdot\nu H_\phi|\nabla\phi|\,\mathrm{d}x = \int_\Omega \nabla_\phi\cdot(fv)|\nabla\phi|\,\mathrm{d}x - \int_{\partial\Omega} fv\cdot(\nu_{\partial\Omega} - \nu\cdot\nu_{\partial\Omega}\nu)|\nabla\phi|\,\mathrm{d}A,$$

and observing that

$$V\nabla f\cdot\nu + \nabla_\phi\cdot(fv) = v\cdot\nabla f + f\nabla_\phi\cdot v$$

yields the desired result. □

*Eulerian conservation and diffusion on moving surfaces*

Let $\phi : \Omega_T \to \mathbb{R}$ be a prescribed non-degenerate level set function. Let $Q : \Omega_T \to \mathbb{R}^{n+1}$ be a given flux. Then the Eulerian conservation law we consider is

$$\frac{\mathrm{d}}{\mathrm{d}t}\int_R u|\nabla\phi|\,\mathrm{d}x = -\int_{\partial R}(Q + |\nabla\phi|uv)\cdot\nu_{\partial R}\,\mathrm{d}A$$

for each subdomain $R$ of $\Omega$, where $\nu_{\partial R}$ is the outward unit normal to $\partial R$. In particular, we consider a flux of the form

$$Q = |\nabla\phi|q_\phi,$$

where $q_\phi : \Omega_T \to \mathbb{R}^{n+1}$ is a flux satisfying

$$q_\phi\cdot\nu = 0. \tag{7.15}$$

https://doi.org/10.1017/S0962492913000056 Published online by Cambridge University Press

It follows by the implicit surface transport formula (7.14) that

$$\frac{\mathrm{d}}{\mathrm{d}t}\int_R u|\nabla\phi|\,\mathrm{d}x = \int_R (\partial^\bullet u + u\nabla_\phi\cdot v)|\nabla\phi|\,\mathrm{d}x - \int_{\partial R} uv\cdot\nu_{\partial R}|\nabla\phi|\,\mathrm{d}A$$

and by $\phi$-integration by parts and (7.15) that

$$\int_{\partial R} q_\phi\cdot\nu_{\partial R}|\nabla\phi|\,\mathrm{d}A = \int_R \nabla_\phi\cdot q_\phi|\nabla\phi|\,\mathrm{d}x.$$

It follows that

$$\int_R |\nabla\phi|(\partial^\bullet u + u\nabla_\phi\cdot v + \nabla_\phi\cdot q_\phi)\,\mathrm{d}x = 0$$

for every subdomain $R$, which implies the partial differential equation

$$\partial^\bullet u + u\nabla_\phi\cdot v + \nabla_\phi\cdot q_\phi = 0 \quad \text{in } \Omega_T.$$

Taking $q_\phi$ to be the diffusive flux $q_\phi = -\mathcal{A}\nabla_\phi u$ leads to the diffusion equation

$$\partial^\bullet u + u\nabla_\phi\cdot v - \nabla_\phi\cdot(\mathcal{A}\nabla_\phi u) = 0. \tag{7.16}$$

Here $\mathcal{A}\geq 0$ again is a symmetric mobility tensor with the property that it maps the tangent space $\mathcal{T} = \{\nu^\perp\in\mathbb{R}^{n+1} \mid \nu\cdot\nu^\perp = 0\}$ into itself. Observe that (7.16) is a linear degenerate parabolic equation because $P_\phi$ has a zero eigenvalue in the normal direction $\nu$.

Another form of this PDE is

$$u_t + V\frac{\partial u}{\partial\nu} + \nabla_\phi\cdot(uv_\tau) + VH_\phi u - \nabla_\phi\cdot(\mathcal{A}\nabla_\phi u) = 0. \tag{7.17}$$

A variational form of (7.16) is obtained in the standard way. In order to proceed we need a boundary condition for $u$ on $\partial\Omega$. For convenience here, we impose the zero flux condition

$$|\nabla\phi|\mathcal{A}\nabla_\phi u\cdot\nu_{\partial\Omega} = 0 \quad \text{on } \partial\Omega\times(0,T) \tag{7.18}$$

and assume that

$$v\cdot\nu_{\partial\Omega} = 0 \quad \text{on } \partial\Omega\times(0,T). \tag{7.19}$$

For each level surface of $\phi$ we multiply equation (7.16) by a test function $\eta$ and by $|\nabla\phi|$ to give

$$\int_\Omega (\partial^\bullet u + u\nabla_\phi\cdot v - \nabla_\phi\cdot(\mathcal{A}\nabla_\phi u))\eta|\nabla\phi|\,\mathrm{d}x = 0.$$

The transport formula (7.14) gives

$$\frac{\mathrm{d}}{\mathrm{d}t}\int_\Omega u\eta|\nabla\phi|\,\mathrm{d}x = \int_\Omega (\partial^\bullet u + u\nabla_\phi\cdot v)\eta|\nabla\phi|\,\mathrm{d}x + \int_\Omega u\partial^\bullet\eta|\nabla\phi|\,\mathrm{d}x - \int_{\partial\Omega} u\eta v\cdot\nu_{\partial\Omega}|\nabla\phi|\,\mathrm{d}A,$$

https://doi.org/10.1017/S0962492913000056 Published online by Cambridge University Press

and because of $\mathcal{A}\nabla_\phi u \cdot \nu = 0$, integration by parts gives

$$\int_\Omega \mathcal{A}\nabla_\phi u \cdot \nabla_\phi \eta |\nabla\phi| \,\mathrm{d}x = \\ -\int_\Omega \eta \nabla_\phi \cdot (\mathcal{A}\nabla_\phi u)|\nabla\phi| \,\mathrm{d}x + \int_{\partial\Omega} \mathcal{A}\nabla_\phi u \cdot \nu_{\partial\Omega}\eta |\nabla\phi| \,\mathrm{d}A.$$

Finally we obtain the variational equation

$$\frac{\mathrm{d}}{\mathrm{d}t}\int_\Omega u\eta|\nabla\phi| \,\mathrm{d}x + \int_\Omega \mathcal{A}\nabla_\phi u \cdot \nabla_\phi \eta |\nabla\phi| \,\mathrm{d}x = \int_\Omega u\partial^\bullet \eta |\nabla\phi| \,\mathrm{d}x \tag{7.20}$$

for each sufficiently smooth test function.

The conservation equation

$$\frac{\mathrm{d}}{\mathrm{d}t}\int_\Omega u|\nabla\phi| \,\mathrm{d}x = 0$$

is obtained by taking $\eta = 1$.

*Weak solution and energy estimate*

The variational form (7.20) allows us to define a notion of weak solution of the degenerate Eulerian parabolic equation (7.16). To do this we introduce the normed linear spaces

$$L^2_\phi(\Omega_T) = \{\eta \mid \eta \text{ is measurable}, \|\eta\|_{L^2_\phi(\Omega_T)} < \infty\},$$
$$\|\eta\|^2_{L^2_\phi(\Omega_T)} = \int_0^T \int_\Omega \eta^2 |\nabla\phi| \,\mathrm{d}x \,\mathrm{d}t$$

and

$$H^1_\phi(\Omega_T) = \{\eta \in L^2_\phi(\Omega_T) \mid \partial^\bullet\eta, \nabla_\phi\eta \in L^2_\phi(\Omega_T)\},$$
$$\|\eta\|^2_{H^1_\phi(\Omega_T)} = \|\eta\|^2_{L^2_\phi(\Omega_T)} + \|\partial^\bullet\eta\|^2_{L^2_\phi(\Omega_T)} + \|\nabla_\phi\eta\|^2_{L^2_\phi(\Omega_T)}.$$

**Definition 7.7.** A function $u \in H^1_\phi(\Omega_T)$ is said to be a weak solution of (7.16) and (7.18) if, for almost every $t \in (0,T)$,

$$\frac{\mathrm{d}}{\mathrm{d}t}\int_\Omega u\eta|\nabla\phi| \,\mathrm{d}x + \int_\Omega \mathcal{A}\nabla_\phi u \cdot \nabla_\phi \eta |\nabla\phi| \,\mathrm{d}x = \int_\Omega u\partial^\bullet \eta |\nabla\phi| \,\mathrm{d}x \tag{7.21}$$

for every $\eta \in H^1_\phi(\Omega_T)$.

Weak solutions satisfy the following basic energy estimate, whose discrete counterpart implies stability for the numerical scheme. Throughout we will assume the initial condition $u(\cdot,0) = u_0$ on $\Omega$.

**Lemma 7.8.** Let $u$ satisfy (7.21). Then

$$\frac{1}{2}\frac{\mathrm{d}}{\mathrm{d}t}\int_\Omega u^2|\nabla\phi| \,\mathrm{d}x + \int_\Omega \mathcal{A}\nabla_\phi u \cdot \nabla_\phi u |\nabla\phi| \,\mathrm{d}x + \frac{1}{2}\int_\Omega u^2 \,\nabla_\phi \cdot v |\nabla\phi| \,\mathrm{d}x = 0.$$

https://doi.org/10.1017/S0962492913000056 Published online by Cambridge University Press

*Proof.* We choose $\eta = u$ in (7.21) and obtain

$$\begin{aligned}\frac{\mathrm{d}}{\mathrm{d}t}\int_\Omega u^2|\nabla\phi|\,\mathrm{d}x + \int_\Omega \mathcal{A}\nabla_\phi u\cdot\nabla_\phi u|\nabla\phi|\,\mathrm{d}x &= \int_\Omega u\partial^\bullet u|\nabla\phi|\,\mathrm{d}x\\ &= \frac{1}{2}\int_\Omega \partial^\bullet(u^2)\,|\nabla\phi|\,\mathrm{d}x\\ &= \frac{1}{2}\frac{\mathrm{d}}{\mathrm{d}t}\int_\Omega u^2|\nabla\phi|\,\mathrm{d}x - \frac{1}{2}\int_\Omega u^2\,\nabla_\phi\cdot v|\nabla\phi|\,\mathrm{d}x + \frac{1}{2}\int_{\partial\Omega} u^2 v\cdot\nu_{\partial\Omega}|\nabla\phi|\,\mathrm{d}A,\end{aligned}$$

where the last term vanishes because of (7.19), and this was the claim. □

## 8. Implicit surface finite element method

In this section we describe the numerical approximation of the implicit surface $\phi$-equations of Section 7. For computational purposes it is natural to seek to exploit these formulations by using a bulk triangulation and finite element space independent of the level set function. Of course, we may be interested only in the solution on just one level set of $\phi$ which, for convenience, we choose to be the zero level set and label it as $\Gamma$. Using this approach avoids the necessity of constructing a surface mesh, and has the potential advantage of using a bulk finite element mesh unaligned to the surface $\Gamma$. However, the resulting equation is then to be solved in a space one dimension higher. In this section we describe a naive approach in which the solution to a surface PDE is computed on all level surfaces of the prescribed level set function, $\phi$, in a bulk domain $\Omega$ using a finite element space defined on a triangulation of $\Omega$. In Section 9.1 we will localize to a narrow band.

### *8.1. Finite element scheme*

We suppose that the level set function satisfies $\nabla\phi \neq 0$ in $\Omega$. For simplicity we consider the variational model equations

$$\int_\Omega \nabla_\phi u\cdot\nabla_\phi\eta|\nabla\phi|\,\mathrm{d}x + \int_\Omega cu\eta|\nabla\phi|\,\mathrm{d}x = \int_\Omega f\eta|\nabla\phi|\,\mathrm{d}x, \tag{8.1}$$

for all $\eta \in H^{1,2}_\phi(\Omega)$, and

$$\int_\Omega u_t\eta|\nabla\phi|\,\mathrm{d}x + \int_\Omega \nabla_\phi u\cdot\nabla_\phi\eta|\nabla\phi|\,\mathrm{d}x = 0, \quad \text{for all } \eta \in H^{1,2}_\phi(\Omega),$$
$$u(\cdot,0) = u_0.$$

Here the data $c, f$ and $u_0$ are defined on a domain $\Omega \subset \mathbb{R}^{n+1}$ containing the zero level set $\Gamma$ of $\phi$. The data may be interpreted as suitable extensions of data given on $\Gamma$. Note that implicitly we have assumed the zero flux boundary condition

$$|\nabla\phi|\mathcal{A}\nabla_\phi u\cdot\nu_{\partial\Omega} = 0 \quad \text{on } \partial\Omega. \tag{8.2}$$

https://doi.org/10.1017/S0962492913000056 Published online by Cambridge University Press

If $\Omega$ satisfies (7.4) then this is automatic, and all level surfaces of $\phi$ are closed in $\Omega$. Otherwise it is possible that level surfaces of $\phi$ intersect $\partial\Omega$ and in that case a no-flux boundary condition has been imposed.

Let $\mathcal{T}_h$ be a triangulation of $\Omega$ and let $h = \max_{T\in\mathcal{T}_h} \operatorname{diam}(T)$ be the maximum mesh size. For ease of exposition we suppose that elements adjacent to the boundary $\partial\Omega$ have a curved edge so the triangulation of $\Omega$ is exact. Let $S_h$ be the space of continuous piecewise linear finite element functions on $\Omega$,

$$S_h = \{\eta_h \in C^0(\overline{\Omega}) \mid \eta_h|_T \text{ is a linear polynomial, } T \in \mathcal{T}_h\},$$

generated by the nodal basis functions, that is, $S_h = \operatorname{span}\{\chi_1, \dots, \chi_J\}$.

The natural finite element method for the elliptic equation (8.1) is to find $U_h \in S_h$ such that

$$\int_\Omega \nabla_\phi U_h \cdot \nabla_\phi \eta_h |\nabla\phi| \,\mathrm{d}x + \int_\Omega c\, U_h \eta_h |\nabla\phi| \,\mathrm{d}x = \int_\Omega f \eta_h |\nabla\phi| \,\mathrm{d}x,$$

for all $\eta_h \in S_h$. Setting $U_h = \sum_{j=1}^J \alpha_j \chi_j$, we find

$$(\mathcal{S} + \mathcal{C})\alpha = \mathcal{F},$$

where the weighted stiffness matrix $\mathcal{S}$ and the matrix $\mathcal{C}$ are given by

$$\mathcal{S}_{jk} = \int_\Omega \nabla_\phi \chi_j \cdot \nabla_\phi \chi_k |\nabla\phi| \,\mathrm{d}x, \quad \mathcal{C}_{jk} = \int_\Omega c \chi_j \chi_k |\nabla\phi| \,\mathrm{d}x$$

for $j, k = 1, \dots, J$, and $\mathcal{F}$ is given by $\mathcal{F} = (\mathcal{F}_1, \dots, \mathcal{F}_J)$,

$$\mathcal{F}_j = \int_\Omega f \chi_j |\nabla\phi| \,\mathrm{d}x \quad (j = 1, \dots, J).$$

Similarly, a semidiscrete Eulerian method for the parabolic equation is to find $U_h(\cdot, t) \in S_h$ such that

$$\int_\Omega U_{ht} \eta_h |\nabla\phi| \,\mathrm{d}x + \int_\Omega \nabla_\phi U_h \cdot \nabla_\phi \eta_h |\nabla\phi| \,\mathrm{d}x = 0, \quad \text{for all } \eta_h \in S_h.$$

Setting $U_h(\cdot, t) = \sum_{j=1}^J \alpha_j(t)\chi_j$ and $\alpha = (\alpha_1, \dots, \alpha_J)$ yields

$$\int_\Omega \sum_{j=1}^J \alpha_{j,t} \chi_j \eta_h |\nabla\phi| \,\mathrm{d}x + \int_\Omega \sum_{j=1}^J \alpha_j(t) \nabla_\phi \chi_j \cdot \nabla_\phi \eta_h |\nabla\phi| \,\mathrm{d}x = 0,$$

for all $\eta_h \in S_h$, and taking $\eta_h = \chi_k$ for $k = 1, \dots, J$, we obtain

$$\mathcal{M}\dot{\alpha} + \mathcal{S}\alpha = 0,$$

where $\mathcal{M}$ is the weighted mass matrix

$$\mathcal{M}_{jk} = \int_\Omega \chi_j \chi_k |\nabla\phi| \,\mathrm{d}x, \quad j, k = 1, \dots, J.$$

https://doi.org/10.1017/S0962492913000056 Published online by Cambridge University Press

A time discretization for this spatially discrete parabolic equation may be carried out by standard methods. As an example consider the implicit Euler method. Let $\tau > 0$ be a time step size, $m_T\tau = T$, and let us use upper indices for the time levels so that $U_h^m$ denotes $U_h(\cdot, m\tau)$. With this notation we propose the following method.

**Algorithm 8.1.** Given $U_h^0 \in S_h$, for $m = 0, \dots, m_T$, solve the linear system

$$\frac{1}{\tau}\int_\Omega U_h^{m+1}\eta_h|\nabla\phi|\,\mathrm{d}x + \int_\Omega \nabla_\phi U_h^{m+1}\cdot\nabla_\phi\eta_h|\nabla\phi|\,\mathrm{d}x = \frac{1}{\tau}\int_\Omega U_h^m\eta_h|\nabla\phi|\,\mathrm{d}x,$$

for all $\eta_h \in S_h$.

This leads to the linear algebraic system

$$(\mathcal{M} + \tau\mathcal{S})\alpha^{m+1} = \mathcal{M}\alpha^m. \tag{8.3}$$

Because of the assumption on $\phi$ the matrices $\mathcal{C}$ and $\mathcal{M}(t)$ are uniformly positive definite, so that, in each case, we get existence and uniqueness of the finite element solutions. A significant feature of our approach is the fact that the matrices $\mathcal{M}$, $\mathcal{C}$ and $\mathcal{S}$ depend only on the evaluation of the gradient of level set function $\phi$ and not on explicit numerical evaluation of surface quantities.

Numerical experiments concerning parabolic equations may be found in Dziuk and Elliott (2008). We refer to Bertalmío *et al.* (2001), Greer *et al.* (2006), Greer (2006) and Burger (2009) for further descriptions, applications and extensions of these methods.

### *8.2. Eulerian scheme for conservation and diffusion on moving surfaces*

Using implicit descriptions of evolving surfaces, we formulate an Eulerian ESFEM which is based on the weak form (7.20) of the $\phi$-diffusion equation and uses fixed-in-time finite element spaces as in Section 8.1. The test functions will now satisfy $\partial^\bullet\eta_h = v\cdot\nabla\eta_h$.

**Definition 8.2 (semidiscretization in space).** Find $U_h(\cdot,t) \in S_h$ such that

$$\begin{aligned}\frac{\mathrm{d}}{\mathrm{d}t}\int_\Omega U_h\eta_h|\nabla\phi|\,\mathrm{d}x + \int_\Omega \mathcal{A}\nabla_\phi U_h\cdot\nabla_\phi\eta_h|\nabla\phi|\,\mathrm{d}x \\ = \int_\Omega U_h v\cdot\nabla\eta_h|\nabla\phi|\,\mathrm{d}x, \quad \text{for all } \eta_h \in S_h.\end{aligned}$$

Using the Leibniz formula it is easily seen that an equivalent formulation is

$$\int_\Omega \partial^\bullet U_h\eta_h|\nabla\phi|\,\mathrm{d}x + \int_\Omega U_h\eta_h\nabla_\phi\cdot v|\nabla\phi|\,\mathrm{d}x + \int_\Omega \mathcal{A}\nabla_\phi U_h\cdot\nabla_\phi\eta_h|\nabla\phi|\,\mathrm{d}x = 0$$

https://doi.org/10.1017/S0962492913000056 Published online by Cambridge University Press

for all discrete test functions $\eta_h \in S_h$. Setting $U_h(\cdot,t) = \sum_{j=1}^J \alpha_j(t)\chi_j$, we find that

$$\frac{\mathrm{d}}{\mathrm{d}t}\left(\sum_{j=1}^J \alpha_j \int_\Omega \chi_j \eta_h |\nabla\phi|\,\mathrm{d}x\right) + \sum_{j=1}^J \alpha_j \int_\Omega \mathcal{A}\nabla_\phi\chi_j \cdot \nabla_\phi \eta_h |\nabla\phi|\,\mathrm{d}x$$
$$= \sum_{j=1}^J \alpha_j \int_\Omega \chi_j v \cdot \nabla\eta_h |\nabla\phi|\,\mathrm{d}x$$

for all $\eta_h \in S_h$, and taking $\eta_h = \chi_k$, $k = 1,\dots,J$, we obtain

$$\frac{\mathrm{d}}{\mathrm{d}t}(\mathcal{M}(t)\alpha) + \mathcal{S}(t)\alpha = \mathcal{C}(t)\alpha.$$

In the above $\mathcal{M}(t)$ is the evolving mass matrix,

$$\mathcal{M}(t)_{jk} = \int_\Omega \chi_j\chi_k |\nabla\phi|\,\mathrm{d}x,$$

$\mathcal{C}(t)$ is a transport matrix,

$$\mathcal{C}(t)_{jk} = \int_\Omega \chi_j v \cdot \nabla\chi_k |\nabla\phi|\,\mathrm{d}x,$$

and $\mathcal{S}(t)$ is the evolving stiffness matrix,

$$\mathcal{S}(t)_{jk} = \int_\Omega \mathcal{A}\nabla_\phi\chi_j \cdot \nabla_\phi\chi_k |\nabla\phi|\,\mathrm{d}x$$

$(j,k = 1,\dots,J)$. Existence and uniqueness of the semidiscrete finite element solution follows easily since the mass matrix $\mathcal{M}(t)$ is uniformly positive definite on $[0,T]$ and the other matrices are bounded.

Again a significant feature of our approach is the fact that the matrices $\mathcal{M}(t)$, $\mathcal{C}(t)$ and $\mathcal{S}(t)$ depend only on the evaluation of the gradient of the level set function $\phi$ and the velocity field $v$ (in the case of $\mathcal{C}$). The method does not require a numerical evaluation of the curvature: see (7.17).

*Stability*

The basic stability result for our spatially discrete scheme from Definition 8.2 is given in the following lemma, which follows analogously to the continuous case of Lemma 7.8 from the transport formula in Lemma 7.6 and a standard Gronwall argument.

**Lemma 8.3 (stability).** Let $U_h$ be a solution of the semidiscrete scheme as in Definition 8.2 with initial value $U_h(\cdot,0) = U_{h0}$. Assume that

$$\int_0^T \|\nabla_\phi \cdot v\|_{L^\infty(\Omega)}\,\mathrm{d}t < \infty,$$

https://doi.org/10.1017/S0962492913000056 Published online by Cambridge University Press

and that $\mathcal{A}$ satisfies the ellipticity condition (5.14). Then the following stability estimate holds:

$$\sup_{(0,T)} \|U_h\|^2_{L^2_\phi(\Omega)} + \int_0^T \|\nabla_\phi U_h\|^2_{L^2_\phi(\Omega)} \,\mathrm{d}t \le c\|U_{h0}\|^2_{L^2_\phi(\Omega)}. \tag{8.4}$$

Numerical examples illustrating the scheme may be found in Dziuk and Elliott (2010). Level set methods for approaching this problem which do not use this variational approach and which use finite difference methods on the equation (7.17) were formulated in Adalsteinsson and Sethian (2003) and Xu and Zhao (2003).

### *8.3. Examples of higher-order equations*

We formulate mixed finite element schemes based on the splitting into second-order elliptic operators: see Elliott *et al.* (1989) and Copetti and Elliott (1992).

*Cahn–Hilliard equation.* Find $(U_h(\cdot,t), W_h(\cdot,t)) \in (S_h)^2$ such that

$$\int_\Omega U_{ht}\eta_h|\nabla\phi| \,\mathrm{d}x + \int_\Omega \mathcal{A}\nabla_\phi W_h \cdot \nabla_\phi \eta_h |\nabla\phi| \,\mathrm{d}x = 0,$$

$$\varepsilon \int_\Omega \nabla_\phi U_h \cdot \nabla_\phi \eta_h |\nabla\phi| \,\mathrm{d}x + \int_\Omega \frac{1}{\varepsilon} I_h(\psi'(U_h))\eta_h |\nabla\phi| \,\mathrm{d}x - \int_\Omega W_h \eta_h |\nabla\phi| \,\mathrm{d}x = 0,$$

for every $\eta_h \in S_h$. Here we use $I_h$ to denote the interpolation operator for $S_h$. Setting

$$U_h(\cdot,t) = \sum_{j=1}^J \alpha_j(t)\chi_j(\cdot), \quad W_h(\cdot,t) = \sum_{j=1}^J \beta_j(t)\chi_j(\cdot), \tag{8.5}$$

we find that, for all $\eta \in S_h$,

$$\int_\Omega \sum_{j=1}^J \dot\alpha_j \chi_j \eta_h |\nabla\phi| \,\mathrm{d}x + \int_\Omega \mathcal{A} \sum_{j=1}^J \beta_j \nabla_\phi \chi_j \cdot \nabla_\phi \eta_h |\nabla\phi| \,\mathrm{d}x = 0,$$

$$\varepsilon \int_\Omega \sum_{j=1}^J \alpha_j \nabla_\phi \chi_j \cdot \nabla_\phi \eta_h |\nabla\phi| \,\mathrm{d}x + \frac{1}{\varepsilon} \int_\Omega \sum_{j=1}^J \psi'(\alpha_j)\chi_j \eta_h |\nabla\phi| \,\mathrm{d}x - \int_\Omega \sum_{j=1}^J \beta_j \chi_j \eta_h |\nabla\phi| \,\mathrm{d}x = 0,$$

and taking $\eta_h = \chi_k$ for $k = 1, \dots, J$ we obtain

$$\mathcal{M}\dot\alpha + \mathcal{S}\beta = 0, \quad \varepsilon \mathcal{S}^0 \alpha + \frac{1}{\varepsilon}\mathcal{M}\psi'(\alpha) - \mathcal{M}\beta = 0,$$

https://doi.org/10.1017/S0962492913000056 Published online by Cambridge University Press

where $\psi'(\alpha) = (\psi'(\alpha_1), \dots, \psi'(\alpha_J))$, which yields

$$\mathcal{M}\dot{\alpha} + \varepsilon \mathcal{S}\mathcal{M}^{-1}\mathcal{S}^0\alpha + \frac{1}{\varepsilon}\mathcal{S}\psi'(\alpha) = 0.$$

Of course, the method for fourth-order linear diffusion is recovered by taking $\psi$ to vanish.

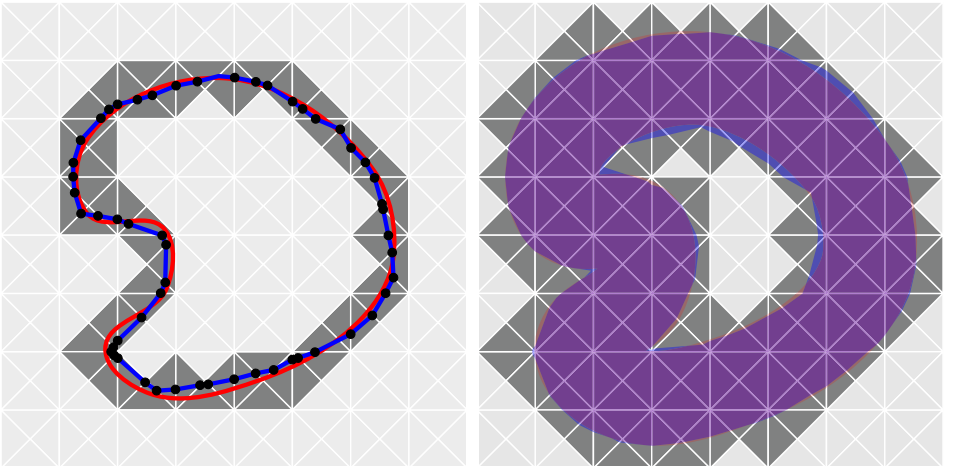
## 9. Unfitted bulk finite element method

In some applications it may be convenient to avoid triangulating a surface. This may be of particular value when the surface partial differential equation is coupled to a bulk system of equations and when the surface is described as a level set function or approximated by the zero level set of a phase field function and/or may be evolving. Further, it may be appropriate when one wishes to take advantage of existing bulk finite element codes. A common feature of a number of approaches is to use a bulk triangulation of a domain in the higher-dimensional ambient space on which bulk finite element spaces are used. The surface quantity is then approximated using the bulk finite element space and an appropriate discretization of the surface partial differential equation. Of course, the Eulerian approach described in Section 8 is of this form, but there the computational approach is to approximate the equation on all level sets of a prescribed level set function. From the practical perspective the solution to a surface PDE will often be required for just one surface. Thus it is desirable to localize the implicit surface approach.

There are a number of variants which we discuss below. In Section 9.1 we describe the method of Deckelnick *et al.* (2010) for a surface elliptic equation which uses a narrow computational band around the given surface in which the $\phi$-elliptic equation is approximated. It is natural to consider varying the width of the narrow band in the above approach, and it transpires that one obtains a new method by taking the width to zero: see Section 9.2. This leads to the interesting method proposed by Olshanskii, Reusken and Grande (2009); see also Olshanskii and Reusken (2010) and Demlow and Olshanskii (2012). In this approach bulk finite element spaces are used in a weak form of the surface equation based on tangential gradients and integration on an approximation of the surface. An extension of this method (Deckelnick, Elliott and Ranner 2013) uses the full gradient in the weak formulation. This is also described in Section 9.2.

In Figure 9.1(a) the surface is a smooth curve that is the zero level set of a function $\phi$. The triangulation is completely independent of this curve. Another piecewise linear curve approximating the desired surface is shown, which passes through black points. This is the computational surface: it is the zero level set of the bulk finite element piecewise linear interpolation of $\phi$. The dark triangles are those triangles which are intersected by the

https://doi.org/10.1017/S0962492913000056 Published online by Cambridge University Press



(a) (b)

Figure 9.1. Unfitted bulk finite element meshes.

approximate surface. It is on these triangles that a bulk finite element space is employed to find an approximation to the solution of the surface equation using a variational formulation which involves integration on the computational surface. In Figure 9.1(b) we see a set-up related to the narrow band method described in Section 9.1. Again the dark triangles are associated with the bulk finite element solution space, but now the domain of integration for the variational formulation is the narrow band defined by $\pm\delta$ level sets of the interpolation of the level set function describing the exact surface.

Meshes that form the computational domain but which are not fitted to the domain in which the PDE holds give rise to *unfitted finite element methods*, introduced in Barrett and Elliott (1982, 1984) for elliptic equations in curved domains. The motivation for using finite element spaces on meshes not fitting to the domain came from the desire to solve free or moving boundary problems; see also Barrett and Elliott (1985, 1987*a*, 1987*b*, 1988), Hansbo and Hansbo (2002), Bastian and Engwer (2009) and Engwer and Heimann (2012). In this setting we are concerned with bulk meshes independent of the surface.

Another approach involving bulk unfitted meshes arises from phase field methodology. Phase field models (see Caginalp 1989 and Deckelnick *et al.* 2005, for example) lead to an approximation of the interface by a *diffuse transition layer*, usually of width $\epsilon$, across which an order or phase field parameter ranges from $-1$ to 1. In this setting it is natural to consider formulating a method for solving surface equations in the diffuse layer

https://doi.org/10.1017/S0962492913000056 Published online by Cambridge University Press

(see Section 9.3). This *diffuse interface* approach (Elliott and Stinner 2009, Elliott *et al.* 2011, Rätz and Voigt 2006) approximates the surface equation by a bulk equation with coefficients which are zero or small outside a transition layer.

### *9.1. Narrow band bulk finite element scheme*

In this section we follow the work of Deckelnick *et al.* (2010). Let $\Omega$ be an open polyhedral domain for which there is a smooth function $\phi : \overline{\Omega} \to \mathbb{R}$ such that

$$\Gamma = \{x \in \Omega \mid \phi(x) = 0\}$$

with $\nabla\phi \neq 0$ on $\overline{\Omega}$, and assume that $U_\delta(\Gamma) \subset \Omega$ for some $\delta > 0$, where $U_\delta(\Gamma) = \{x \in \Omega \mid \operatorname{dist}(x, \Gamma) < \delta\}$.

*Variational form.* We consider the linear PDE

$$-\Delta_\Gamma u + u = f \tag{9.1}$$

on a smooth compact surface $\Gamma$, and seek to solve the weak form of (9.1): find $u \in H^1(\Gamma)$ such that

$$\int_\Gamma \nabla_\Gamma u \cdot \nabla_\Gamma \eta + u\eta \,\mathrm{d}A = \int_\Gamma f\eta \,\mathrm{d}A, \quad \text{for all } \eta \in H^1(\Gamma), \tag{9.2}$$

with $f \in L^2(\Gamma)$ given.

For a function $v : \Gamma \to \mathbb{R}$, we define the unique closest point extension of $v$ to $U_\delta$ by $v^e : U_\delta \to \mathbb{R}$ given by $v^e(x) = v(a(x))$, where $a(x) \in \Gamma$ is the closest point on $\Gamma$ to $x \in U_\delta$ and $\delta$ is chosen sufficiently small. For the notation see Lemma 2.8. Let $\mathcal{T}_h$ be a quasi-uniform triangulation of $\Omega$ with maximum mesh size $h = \max_{T\in\mathcal{T}_h} \operatorname{diam}(T)$. The nodes of the triangulation and corresponding linear basis functions are denoted by $X_1, \dots, X_N$ and by $\chi_1, \dots, \chi_N$, that is, $\chi_i \in C^0(\bar{\Omega}), \chi_i\big|_T \in \mathbb{P}_1(T)$ for all $T \in \mathcal{T}_h$ satisfying $\chi_i(X_j) = \delta_{ij}$ for all $i, j = 1, \dots, J$.

Let

$$\phi_h = I_h\phi = \sum_{i=1}^{N} \phi(X_i)\chi_i$$

be the usual Lagrange interpolation of a function $\phi$. In view of the smoothness of $\phi$ we have

$$\|\phi - \phi_h\|_{L^\infty(\Omega)} + h\|\nabla\phi - \nabla\phi_h\|_{L^\infty(\Omega)} \leq Ch^2,$$

from which we infer in particular that $|\nabla\phi_h| \geq c_0 > 0$ in $\bar{\Omega}$ for $0 < h \leq h_0$. Hence we can use, element by element, the piecewise constant projection $P_h = I - \nu_h \otimes \nu_h$, where

$$\nu_h = \frac{\nabla\phi_h}{|\nabla\phi_h|}$$

https://doi.org/10.1017/S0962492913000056 Published online by Cambridge University Press

is the element-by-element piecewise constant normal.

Given $\gamma > 0$, the computational domain is taken as a narrow band defined by the $\gamma h$ levels of the interpolant of $\phi$, that is,

$$D_h = \{x \in \Omega \,|\, |\phi_h(x)| < \gamma h\}.$$

Let $\mathcal{T}_h^C = \{T \in \mathcal{T}_h \mid T \cap D_h \neq \emptyset\}$ denote the computational elements, and consider the nodes of all simplices $T$ belonging to $\mathcal{T}_h^C$. After relabelling we may assume that these nodes are given by $X_1, \ldots, X_J$. Let $S_h = \operatorname{span}\{\chi_1, \ldots, \chi_J\}$. The discrete problem now reads: find $U_h \in S_h$ such that

$$\int_{D_h} P_h \nabla U_h \cdot \nabla \eta_h \, |\nabla \phi_h| \, \mathrm{d}x + \int_{D_h} U_h \, \eta_h \, |\nabla \phi_h| \, \mathrm{d}x = \int_{D_h} f^e \, \eta_h \, |\nabla \phi_h| \, \mathrm{d}x \quad (9.3)$$

for every discrete test function $\eta_h \in S_h$.

*Narrow band approximation assumption.* We require the narrow band approximation assumption

$$\Gamma \subset \bigcup_{\Gamma \cap T \neq \emptyset} T \subseteq \bar{D}_h, \quad 0 < h \leq h_1, \quad (9.4)$$

and

$$|D_h| \leq Ch, \quad (9.5)$$

where $|D_h|$ denotes the volume of $D_h$.

The condition (9.4) can be satisfied by choosing

$$\gamma \geq \max_{x \in \bar{\Omega}} |\nabla \phi(x)|.$$

This can be seen by noting that, if $x \in \Gamma \cap T, y \in T$, then, because $\phi_h$ is piecewise linear, we have

$$|\phi_h(y)| \leq |\phi_h(X)| = |\phi(X)| = |\phi(X) - \phi(x)| \leq h \max_{\bar{\Omega}} |\nabla \phi| = \gamma h,$$

for any vertex $X$ of $T$. When $\phi$ is a signed distance function to $\Gamma$, we can choose $\gamma = 1$.

The bound on the measure of $D_h$, (9.5), follows from the observation that for $h$ sufficiently small $|\phi| < 2\gamma h$ on $D_h$ and since $|\nabla \phi| \geq c_\phi > 0$ on $\Omega$, using the co-area formula we have

$$|D_h| \leq \int_{-2\gamma h}^{2\gamma h} \int_{\Gamma(r)} \frac{1}{|\nabla \phi|} \, \mathrm{d}A \, \mathrm{d}r \leq \frac{4\gamma |\Gamma_*|}{c_\phi} h,$$

where $|\Gamma_*|$ is a bound for the measure of the level sets of $\phi$ in $\Omega$.

*Error bound.* The main numerical analysis result of Deckelnick *et al.* (2010) is the following error bound.

https://doi.org/10.1017/S0962492913000056 Published online by Cambridge University Press

**Theorem 9.1.** Assume that the solution $u$ of (9.1) belongs to $H^{2,\infty}(\Omega)$ and that $f^e \in H^{1,\infty}(\Omega)$. Let $u_h$ be the trace of the solution $U_h$ on $\Gamma$ of the finite element scheme (9.3) satisfying the narrow band approximation assumption. Then

$$\|u - u_h\|_{H^1(\Gamma)} \leq ch.$$

*Another narrow band method.* We use $\phi = d$, $d$ being the signed distance function to $\Gamma$, as the level set function to create a polyhedral approximation $D_h$ of $\Gamma$. We interpolate $d$ on $\mathcal{T}_h$ and define

$$D_h = \{x \in \Omega \mid |I_h d(x)| < h\}.$$

The finite element problem is to find $u_h \in S_h$ such that

$$\int_{D_h} \nabla u_h \cdot \nabla \eta_h + u_h \eta_h \,\mathrm{d}x = \int_{D_h} f^e \eta_h \,\mathrm{d}x, \quad \text{for all } \eta_h \in S_h.$$

This is the same method as that of Deckelnick *et al.* (2010), except that it uses full instead of projected gradients. This allows simpler assembly of mass and stiffness matrices. See Deckelnick *et al.* (2013) for an error analysis and computational results.

Observe that in these unfitted finite element narrow band methods the computational domain $D_h$ has a polygonal boundary and that $\mathcal{T}_h|_{D_h}$, the restriction of $\mathcal{T}_h$ to $D_h$, is not shape-regular and can have arbitrary small elements: see Figure 9.1. Note that the region of integration involves parts of elements. Dealing with this is the price to pay for avoiding the triangulation of the surface. To implement the method one can divide the irregular regions into simplices and use appropriate quadrature rules. The term *cut cell* is used in this context (Engwer and Heimann 2012).

### *9.2. Sharp interface method using a bulk finite element space*

Another method for the model equation (9.1) is to use a bulk unfitted mesh independent of the surface and seek an approximate solution in a finite element space on that bulk mesh using a variational equation formulated on the zero level set of an approximate level set function. This is the method of Section 9.1 with $\gamma = 0$. This has been proposed and analysed in Olshanskii *et al.* (2009) and Olshanskii and Reusken (2010). An extension of this method has been proposed by Deckelnick *et al.* (2013).

The method calculates a sharp interface approximation to (9.2) using integrals over an approximation to $\Gamma$. We define $\widetilde{\mathcal{T}}_h$ to be an unfitted regular triangulation, consisting of closed simplices, of an arbitrary region containing $\Gamma$. We restrict this triangulation to $\mathcal{T}_h$ given by

$$\mathcal{T}_h = \{T \in \widetilde{\mathcal{T}}_h \mid \mathcal{H}^n(T \cap \Gamma) > 0\},$$

where $\mathcal{H}^n(\omega)$ denotes the $n$-dimensional measure of $\omega$. We impose further

https://doi.org/10.1017/S0962492913000056 Published online by Cambridge University Press

that $\Gamma \subseteq \bigcup_{T\in\mathcal{T}_h} T$ and

$$\mathcal{H}^n(\Gamma) = \sum_{T\in\mathcal{T}_h} \mathcal{H}^n(T\cap\Gamma).$$

This restriction means that in the case where $\Gamma$ is the face between two elements we must make an arbitrary, but fixed, choice of one of the two adjoining simplices. We define $h$ to be the diameter of the largest element in $\mathcal{T}_h$. We let $U_h$ denote the interior of the region covered by these elements:

$$\overline{U}_h = \bigcup_{T\in\mathcal{T}_h} T.$$

We assume $h$ is sufficiently small that $U_h \subseteq U_\delta$.

We now define a finite element space $S_h$ on the triangulation $\mathcal{T}_h$ given by

$$S_h = \{\eta_h \in C^0(U_h) \mid \eta_h|_T \text{ is linear affine, for each } T \in \mathcal{T}_h\}.$$

We use the distance function $d$ to construct a polyhedral approximation of $\Gamma_h$ of $\Gamma$ using the following procedure. We interpolate $d$ on $\mathcal{T}_h$ using the bulk piecewise linear finite element space $S_h$, and define

$$\Gamma_h = \{x \in U_h \mid I_h d(x) = 0\}.$$

This defines a polyhedral surface $\Gamma_h$ consisting of lines if $n = 1$ and triangles and quadrilaterals if $n = 2$. Notice that in general, $\mathcal{T}_h|_{\Gamma_h}$, the restriction of $U_h$ to $\Gamma_h$, is not shape-regular and can have arbitrary small elements.

This method could be implemented using a level set function instead of a distance function.

Both full gradients and tangential gradients may be used in the discrete weak formulation yielding two methods. The method of Deckelnick *et al.* (2013) is to find $u_h \in S_h$ such that

$$\int_{\Gamma_h} \nabla u_h \cdot \nabla \eta_h + u_h \eta_h \,\mathrm{d}A_h = \int_{\Gamma_h} f^e \eta_h \,\mathrm{d}A_h, \quad \text{for all } \eta_h \in S_h.$$

The method of Olshanskii *et al.* (2009) uses the tangential gradient to $\Gamma_h$ in the discrete variational form and a slightly different finite element space $S_{\Gamma_h}$ consisting of functions on $\Gamma_h$ which are the trace of functions in $S_h$. Both methods yields errors of order $h$ and $h^2$ in the $H^1$ and $L^2$ norms, respectively.

As an illustration of the motivation for unfitted finite element methods we consider the complicated two-dimensional surface $\Gamma = \{x \in \Omega \mid \phi(x) = 0\}$ given by

$$\begin{aligned}\phi(x) = (x_1^2 + x_2^2 - 4)^2 + (x_3^2 - 1)^2 + (x_2^2 + x_3^2 - 4)^2 + (x_1^2 - 1)^2 \\ + (x_3^2 + x_1^2 - 4)^2 + (x_2^2 - 1)^2 - 3.\end{aligned}$$

https://doi.org/10.1017/S0962492913000056 Published online by Cambridge University Press

The surface is shown in Figure 9.2 and is shaded to reflect the solution of the equation with right-hand side $f(x) = 100 \sum_{j=1}^{4} \mathrm{e}^{-|x-x_{(j)}|^2}$, with

$$x_{(1)} = (-1.0, 1.0, 2.04), \quad x_{(2)} = (1.0, 2.04, 1.0),$$
$$x_{(3)} = (2.04, 0.0, 1.0), \quad x_{(4)} = (-0.5, -1.0, -2.04).$$

The points $x_{(j)}$ are close to the surface $\Gamma$. In Figure 9.3 we see the intersection of the surface with a uniform bulk grid of tetrahedra. In this case the numerical method to obtain this solution is the one described in Section 9.2.

*9.3. Diffuse interface method*

Here we describe a diffuse interface method for the parabolic equation (5.13) modelling conservation on a moving hypersurface $\Gamma(t)$:

$$\partial^\bullet u + u \nabla_\Gamma \cdot v - \nabla_\Gamma \cdot (\mathcal{A} \nabla_\Gamma u) = 0. \tag{9.6}$$

For simplicity we take $\mathcal{A} = \mathcal{D}_c I$, $\mathcal{D}_c > 0$ and the velocity to be purely in the normal direction $v = V\nu$.

The approach is based on approximating $\Gamma(t)$ by an evolving thin interfacial layer $\Gamma(\varepsilon, t)$ of thickness $\varepsilon$ on which a bulk advection–diffusion equation is solved. The motivation for this diffuse interface approach arises from modelling evolving surface problems using phase field methods. A thin diffuse interfacial layer of width $O(\varepsilon)$ across which a phase field variable $\varphi_\varepsilon$ has a steep transition from the bulk values $\approx \pm 1$ on either side of the interface approximates the sharp interface: see Caginalp (1989) and Blowey and Elliott (1993). Diffuse interfaces with compact support occur naturally when the double-obstacle phase field models are employed (Blowey and Elliott 1991, 1993). In these models the bulk values are identically $\pm 1$ and the diffuse layer layer is sharp. This leads to the sharp diffuse interface front-tracking method formulated in Elliott and Styles (2003) and Deckelnick *et al.* (2005).

The bulk advection–diffusion equation is constructed using a family of non-negative, differentiable functions $\rho$ with compact spatial support which defines the evolving diffuse interface $\Gamma(\varepsilon, t)$. To be definite we set $\rho = 1 - \varphi_\varepsilon^2$, where $\varphi_\varepsilon$ is continuously differentiable double-obstacle phase field function such that the diffuse interface

$$\Gamma(\varepsilon, t) = \{x \mid |\varphi_\varepsilon(x, t)| < 1\}$$

is of finite small width approximately $\pi\varepsilon/2$. Phase field asymptotics indicate that the double-obstacle phase field approach yields the following approximation to the phase field variable (Blowey and Elliott 1993):

$$\varphi_\varepsilon(x, t) \approx \sin\left(\frac{d(x, t)}{\varepsilon}\right) \quad \text{for } |d(x, t)| \lessapprox \frac{\pi}{2}\varepsilon,$$
$$\varphi_\varepsilon(x, t) = \pm 1 \quad \text{for } |d(x, t)| \gtrapprox \frac{\pi}{2}\varepsilon,$$

https://doi.org/10.1017/S0962492913000056 Published online by Cambridge University Press

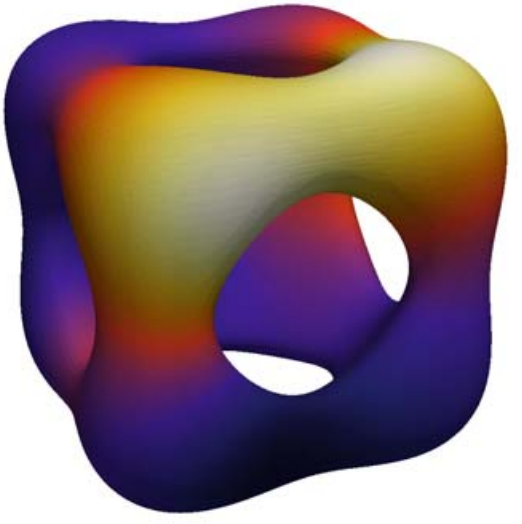


Figure 9.2. Example of the solution of an elliptic equation on a complicated surface.

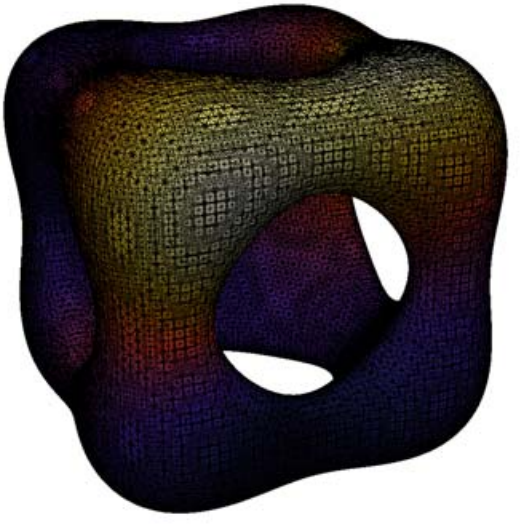


Figure 9.3. Example of the intersection of a bulk mesh with a complicated surface.

https://doi.org/10.1017/S0962492913000056 Published online by Cambridge University Press

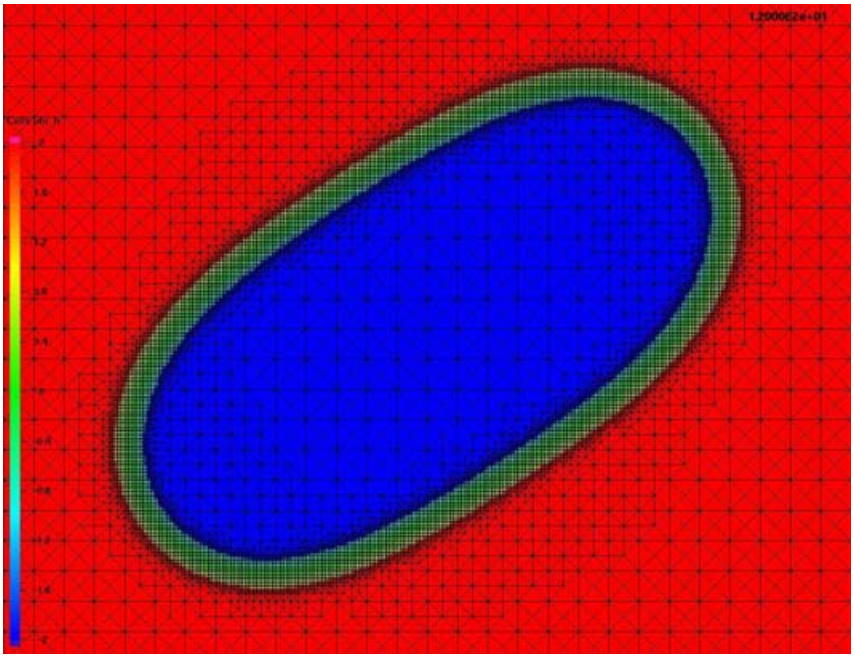


Figure 9.4. Example of a mesh arising in a diffuse interface computation.

where $d(\cdot,t)$ is the signed distance function to $\Gamma(t)$. If $\Gamma(t)$ is known through a level set function or distance function then the above formula for $\varphi_\varepsilon$ can be applied directly to define $\Gamma(\varepsilon,t)$. The normal velocity may be extended to all of $\Gamma(\varepsilon,t)$ by

$$v = d_t \nabla d \quad \text{or} \quad v = \frac{\varphi_{\epsilon t} \nabla \varphi_\epsilon}{|\nabla \varphi_\epsilon|^2}$$

In practical applications the surface $\Gamma(t)$ may be unknown and an approximation is determined by some phase field model. One calculates a phase field function $\varphi_\varepsilon$, and in that case the second of the above equation is appropriate to use.

Figure 9.4 displays a mesh used in a simulation of advection and diffusion of a surfactant on an interface separating a drop of one fluid in another (Elliott *et al.* 2011). The fluid equations were modelled using a double-obstacle Cahn–Hilliard variational inequality (Blowey and Elliott 1992, 1993), coupling with the Navier–Stokes equations. The double-obstacle approach generates a sharp diffuse interface which is used to solve the parabolic equation on the moving diffuse layer as described above. In the figure one can observe the diffuse interface transition layer, which has a finer triangulation than the two bulk triangulated regions it separates. In this simulation the diffuse layer evolves in time and mesh adaptivity is used.

https://doi.org/10.1017/S0962492913000056 Published online by Cambridge University Press

*Description of diffuse interface bulk equation.* Our goal is now to solve the parabolic equation

$$(\rho u)_t + \nabla \cdot (\rho u v) - \nabla \cdot \big(\mathcal{D}_c \rho \nabla u\big) = 0 \quad \text{on } \Gamma(\varepsilon, t), \tag{9.7}$$

which involves degenerating coefficients since $\rho$ vanishes on $\partial\Gamma$. The conserved bulk quantity $\rho u$ is transported with an appropriate extension of the velocity field $v$ away from the moving surface $\Gamma$. As analysed in Elliott and Stinner (2009) for curves, the equation (9.7) indeed approximates the surface equation (9.6) as $\varepsilon \to 0$. We remark that a degenerate equation of the form (9.7) appeared in a phase field model of diffusion-induced grain boundary motion (Fife, Cahn and Elliott 2001, Deckelnick, Elliott and Styles 2001).

Another diffuse interface approach in which the diffuse interface does not have compact support was proposed in Rätz and Voigt (2006), where the underlying phase field method is based on the classical double-well potential.

In the following description we assume that the function $\rho$ is given. The equation is to be solved in the time interval $I = [0, t_f)$ with $t_f > 0$ in a spatial domain $\Omega \subset \mathbb{R}^n$, $n = 2, 3$, which is an appropriate domain into which the evolving closed hypersurface $\Gamma(t)$ is embedded at all times and $\Gamma(\varepsilon, t) \subset \Omega$. The initial values for the sharp equation (9.6), denoted by $u_0$ and the velocity $v$, need to be extended to all of $\Gamma(\varepsilon, t)$. A choice is to extend $u_0$ constantly in the normal direction away from $\Gamma$ to obtain initial values for (9.7). On $\Omega \backslash \Gamma(\varepsilon, t)$ we set $u_0 = 0$.

*Weak solution.* A function $u : \Omega \times [0, t_f) \to \mathbb{R}$ with

$$u(x, t) = 0 \quad \text{if } x \notin \Gamma(\varepsilon, t)$$

is a weak solution to (9.7) if it satisfies

$$\int_\Omega ((\rho u)_t \chi - \rho u\, v \cdot \nabla \chi + \mathcal{D}_c \rho \nabla u \cdot \nabla \chi)\, \mathrm{d}x = 0 \tag{9.8}$$

for all test functions $\chi : \Omega \to \mathbb{R}$, and if

$$u(\cdot, 0) = u_0(\cdot) \quad \text{on } \Omega.$$

*Time and space discretization.* For simplicity let $\tau = \frac{t_f}{N_f}$, for an integer $N_f \in \mathbb{N}$, be a uniform time step, and define $t_n = n\tau$, $n = 0, \dots, N_f$. Function evaluations or approximations of functions at time $t_n$ will be denoted by an upper index $n$, and we define a discrete time derivative by

$$\partial_\tau f^n = \frac{f^{n+1} - f^n}{\tau}.$$

Again for simplicity we suppose that the bulk triangulation is fixed. Let $\mathcal{T}_h$ be a triangulation of the domain $\Omega \in \mathbb{R}^n, n = 2, 3$ consisting of simplices with maximum mesh size $h = \max_{e \in \mathcal{T}_h} \operatorname{diam}(e)$. Let $J$ be the number and $\mathcal{N}$ be the set of vertex indices. The vertex coordinates are denoted

https://doi.org/10.1017/S0962492913000056 Published online by Cambridge University Press

by $\{X_1, \dots, X_J\}$. For an index $i \in \mathcal{N}$ let $\omega_i$ denote the neighbouring vertices connected to vertex $i$ via an edge and let $\mathcal{T}_i = \{e \in \mathcal{T}_h \mid X_i \in e\}$ be the set of elements which have $i$ as a vertex. Further, let $\mathcal{N}_e = \{j \in \mathcal{N} \mid X_j \in e\}$ be the set of vertices belonging to an element $e \in \mathcal{T}_h$.

The numerical solution is to be found in the discrete finite element space defined by

$$\mathcal{S}^h = \{\eta \in C^0(\bar{\Omega}) \mid \eta \text{ is a linear affine on each } e \in \mathcal{T}_h\}.$$

We define an interpolation operator $\Pi^h : C^0(\bar{\Omega}) \to \mathcal{S}^h$ by

$$\Pi^h(\eta) = \sum_{i=1}^{J} \eta(X_i)\chi_i. \tag{9.9}$$

Here $\chi_1, \dots, \chi_J$ denote the standard basis functions of $\mathcal{S}^h$, that is, $\chi_i \in C^0(\bar{\Omega})$ and $\chi_i|_e \in P_1(e)$ for all $e \in \mathcal{T}_h$ satisfying $\chi_i(X_j) = \delta_{ij}$ for all $i, j = 1, \dots, J$.

*Evolving discrete diffuse interface.* The computational domain is defined using the interpolant of the given support function $\rho$. We set $\rho^n(X_k) := \rho(X_k, t^n)$. The *discrete interface* at time $t_n$ is defined by

$$\Gamma_h^n = \{e \in \mathcal{T}_h \mid \mathcal{N}_e \subset \mathcal{N}_h^n\}, \tag{9.10}$$

where

$$\mathcal{N}_h^n = \{i \in \mathcal{N} \mid \text{ there is } j \in \omega_i \text{ such that } \rho^n(X_j) > 0\}. \tag{9.11}$$

Note that this is a small subset of elements because of the underlying assumption of the small compact support of $\rho$.

The index set $\mathcal{N}_h^n$ is split up as follows:

$$\begin{aligned} \mathcal{N}_h^n &= \mathcal{N}_{I,h}^n \cup \mathcal{N}_{B,h}^n, \\ \mathcal{N}_{I,h}^n &= \{i \in \mathcal{N}_h^n \mid \rho^n(X_i) > 0\}, \\ \mathcal{N}_{B,h}^n &= \{i \in \mathcal{N}_h^n \mid \rho^n(X_i) = 0\}. \end{aligned} \tag{9.12}$$

In order for the numerical scheme to be well defined the following assumption is required.

*Discrete interface assumption.* It holds for all $n = 0, \dots, N_f - 1$ that if an index $i \in \mathcal{N}_h^n$ does not belong to $\mathcal{N}_h^{n+1}$, then $\rho^n(X_i) = 0$ (*i.e.*, $i \in \mathcal{N}_{B,h}^n$). This is a restriction on the time step depending on the magnitude of the interface velocity, which may be guaranteed by applying an adaptive time-stepping strategy or a condition of the form $\tau \le Ch/(\|v\|_\infty)$.

https://doi.org/10.1017/S0962492913000056 Published online by Cambridge University Press

*Numerical scheme.* In order to formulate a numerical method for (9.8) we introduce the following forms for functions $\xi, \eta \in \mathcal{S}^h$:

$$\mathcal{M}(\xi,\eta)_h^n = \int_\Omega \Pi^h(\rho^n \xi\eta)\,\mathrm{d}x, \tag{9.13}$$

$$\mathcal{C}(\xi,\eta)_h^n = \int_\Omega \Pi^h(\rho^n \xi)\Pi^h(v^n)\cdot\nabla\eta\,\mathrm{d}x, \tag{9.14}$$

$$\mathcal{A}(\xi,\eta)_h^n = \int_\Omega \mathcal{D}_c\Pi^h(\rho^n)\,\nabla\xi\cdot\nabla\eta\,\mathrm{d}x. \tag{9.15}$$

We denote by $U_h^n$ the finite element approximation to $u(\cdot,t_n)$. Let $u_0^e$ be an extension to $\Omega$ of the initial data $u_0$ on $\Gamma(0)$. We define $U_h^0$ by

$$U_h^0(X_k) = u_0^e(X_k) \quad \text{if} \quad k \in \mathcal{N}_h^0, \tag{9.16}$$

$$U_h^0(X_k) = 0 \qquad\quad \text{if} \quad k \notin \mathcal{N}_h^0. \tag{9.17}$$

For example, we may extend constantly in the normal direction and cut off to zero outside the narrow band corresponding to the initial diffuse layer defined by the compact support of $\rho(\cdot,0)$.

**Algorithm 9.2.** For each $n = 0,\dots,N_f-1$ we seek a function $U_h^{n+1} \in \mathcal{S}^h$ such that

$$U_h^{n+1}(X_k) = 0, \quad \text{if} \quad k \notin \mathcal{N}_h^{n+1}, \tag{9.18}$$

and satisfying

$$\partial_\tau \mathcal{M}(U_h^n,\eta)_h^n - \mathcal{C}(U_h^{n+1},\eta)_h^{n+1} + \mathcal{A}(U_h^{n+1},\eta)_h^{n+1} = 0, \quad \text{for all } \eta \in \mathcal{S}^h. \tag{9.19}$$

The discrete interface assumption together with the *boundary condition* (9.18) implies that the variational scheme (9.19) may be localized so that the nodal variables at the new time level $U_h^{n+1}(X_i)$ for $i \in \mathcal{N}_h^{n+1}$ are determined from

$$\begin{aligned}\frac{1}{\tau}\Big(\int_\Omega \{(\Pi^h\big(\rho^{n+1}U_h^{n+1}\chi_j\big) - \Pi^h\big(\rho^n U_h^n\chi_j\big)\}\,\mathrm{d}x\Big) \\ + \int_\Omega \{(-\Pi^h\big(\rho^{n+1}U_h^{n+1}\big)\Pi^h(v^{n+1}) + \mathcal{D}_c\Pi^h(\rho^{n+1})\,\nabla U_h^{n+1})\cdot\nabla\chi_j\}\,\mathrm{d}x = 0,\end{aligned} \tag{9.20}$$

for all $j \in \mathcal{N}_h^{n+1}$.

*Unique solvability and mass conservation.* The following estimate is useful for showing that the above system (9.20) is solvable.

**Lemma 9.3.** For $n = 1,\dots,N_f$, $\delta > 0$, and $\xi,\eta \in S_h$ we have that

$$|\mathcal{C}(\xi,\eta)_h^n| \le \delta\mathcal{A}(\eta,\eta)_h^n + \frac{\|v^n\|_{\infty,\Omega_I}^2}{4\delta\mathcal{D}_c}\mathcal{M}(\xi,\xi)_h^n. \tag{9.21}$$

https://doi.org/10.1017/S0962492913000056 Published online by Cambridge University Press

*Proof.* The desired estimate follows from

$$\begin{aligned}
|\mathcal{C}(\xi,\eta)_h^n| &= \left|\int_\Omega \Pi^h(\rho^n\xi)\Pi^h(v^n)\cdot\nabla\eta\,\mathrm{d}x\right| \\
&\le \int_\Omega \|v^n\|_{\infty,\Omega}\left|\sum_{i=1}^N \rho_i^n\xi_i\chi_i\right||\nabla\eta|\,\mathrm{d}x \\
&\le \sum_{i=1}^N \int_\Omega (\rho_i^n\chi_i)^{1/2}|\nabla\eta|\,\|v^n\|_\infty(\rho_i^n\chi_i)^{1/2}|\xi_i|\,\mathrm{d}x \\
&\le \sum_{i=1}^N \int_\Omega \left(\mathcal{D}_c\delta\rho_i^n\chi_i|\nabla\eta|^2 + \frac{\|v^n\|_{\infty,\Omega}^2}{4\delta\mathcal{D}_c}\rho_i^n\chi_i\xi_i^2\right)\mathrm{d}x \\
&= \delta\mathcal{D}(\eta,\eta)_h^n + \frac{\|v^n\|_{\infty,\Omega}^2}{4\delta\mathcal{D}_c}\mathcal{M}(\xi,\xi)_h^n,
\end{aligned}$$

where we use the abbreviation $\rho_i^n = \rho(X_i,t_n)$. □

**Proposition 9.4.** If $\tau < 4\mathcal{D}_c/\|v\|_{\infty,\Omega_I}^2$ then the scheme (9.19) has a unique solution.

It holds that for every $n$

$$\mathcal{M}(U_h^n,1)_h^n = \mathcal{M}(U_h^0,1)_h^0.$$

*Proof.* Proceeding by induction, given the assumption on the initial datum $U_h^0$, we may suppose that $U_h^n(X_k) = 0$ if $k \notin \mathcal{N}_h^n$. Taking $W_h^{n+1}$ to be the difference of two possible solutions, it is sufficient to show that $W_h^{n+1} = 0$ is the only solution of

$$\mathcal{M}(W_h^{n+1},\eta)_h^{n+1} - \tau\mathcal{C}(W_h^{n+1},\eta)_h^{n+1} + \tau\mathcal{A}(W_h^{n+1},\eta)_h^{n+1} = 0, \quad \text{for all } \eta\in\mathcal{S}^h.$$

Taking $\eta = W_h^{n+1}$ and using (9.21) gives

$$\left(1 - \tau\frac{\|v^{n+1}\|_{\infty,\Omega}^2}{4\delta\mathcal{D}_c}\right)\mathcal{M}(W_h^{n+1},W_h^{n+1})_h^{n+1} + (1-\delta)\mathcal{D}(W_h^{n+1},W_h^{n+1})_h^{n+1} \le 0,$$

which, upon taking $\delta$ arbitrarily close to 1, yields for $\tau < 4\mathcal{D}_c/\|v^{n+1}\|_{\infty,\Omega}^2$,

$$\mathcal{M}(W_h^{n+1},W_h^{n+1})_h^{n+1} = 0, \tag{9.22}$$

$$\mathcal{D}(W_h^{n+1},W_h^{n+1})_h^{n+1} = 0. \tag{9.23}$$

It follows from (9.22) that $W_h^{n+1}(X_i) = 0$ for all $i \in \mathcal{N}_{I,h}^{n+1}$. By (9.23) we

https://doi.org/10.1017/S0962492913000056 Published online by Cambridge University Press

have that $\nabla W_h^{n+1} = 0$ in every finite element $e \in \Gamma_h^{n+1}$, whence we conclude that also $W_h^{n+1}(X_i) = 0$ for $i \in \mathcal{N}_{B,h}^{n+1}$. The mass conservation is immediate. □

*Discrete equations.* Let $J_n$ be the number of nodes in $\mathcal{N}_h^n$. We can decompose $U_h^n$ as

$$U_h^n = \sum_{j \in \mathcal{N}_h^n} \alpha_j^n \chi_j = \sum_{j \in \mathcal{N}_h^{n+1}} \widetilde{\alpha}_j^n \chi_j + \sum_{j \in \mathcal{N}_h^n \setminus \mathcal{N}_h^{n+1}} \alpha_j^n \chi_j,$$

where we note that

$$\widetilde{\alpha}_j^n = \alpha_j^n \quad \text{for } j \in \mathcal{N}_h^{n+1} \cap \mathcal{N}_h^n \quad \text{and} \quad \widetilde{\alpha}_j^n = 0 \quad \text{for } j \in \mathcal{N}_h^{n+1} \setminus \mathcal{N}_h^n.$$

We now define the matrices $M^{n+1}, S^{n+1}, C^{n+1}, \widetilde{M}^{n+1} \in \mathbb{R}^{J_{n+1} \times J_{n+1}}$ with the entries

$$\begin{aligned}
M_{i,j}^{n+1} &= \int_\Omega \Pi^h(\rho_h^{n+1} \chi_i \chi_j)\, \mathrm{d}x, \\
S_{i,j}^{n+1} &= \int_\Omega \mathcal{D}_c \Pi^h(\rho_h^{n+1}) \nabla \chi_i \cdot \nabla \chi_j \, \mathrm{d}x, \\
C_{i,j}^{n+1} &= \int_\Omega \Pi^h(\rho_h^{n+1} \chi_i) \Pi^h(v^{n+1}) \cdot \nabla \chi_j \, \mathrm{d}x, \\
\widetilde{M}_{i,j}^{n} &= \int_\Omega \Pi^h(\rho_h^{n} \chi_i \chi_j)\, \mathrm{d}x,
\end{aligned}$$

where the indices $i, j$ belong to the set $\mathcal{N}_h^{n+1}$. To evaluate these forms it is useful to employ quadrature.

At each time step $n+1$ the solution $U_h^{n+1}$ is obtained by solving the system

$$\left(\tfrac{1}{\tau} M^{n+1} + S^{n+1} - C^{n+1}\right) \underline{\alpha}^{n+1} = \tfrac{1}{\tau} \widetilde{M}^n \underline{\widetilde{\alpha}}^n$$

of $J_{n+1}$ linear equations which have a unique solution (Proposition 9.4). Because $\rho^{n+1}$ is zero at boundary points of $\mathcal{N}_h^{n+1}$ there may be some equations with small diagonal elements, which leads to ill-conditioning. This may be remedied by preconditioning using the inverse diagonal of $\frac{1}{\tau} M^{n+1} + S^{n+1} - C^{n+1}$.

Numerical tests in Elliott *et al.* (2011) indicate that reducing the width of the interface together with the mesh size $h$ in a constant ratio can lead to errors in the $L^2$ norm on the surface of order $h^2$. The concentration profile becomes flat as the approximation parameters tend to zero. This is in accordance with the rigorous $\varepsilon$ asymptotic analysis of Elliott and Stinner (2009).

https://doi.org/10.1017/S0962492913000056 Published online by Cambridge University Press

*9.4. Other methods*

*Thick interface method.* Let $\Gamma_\varepsilon = \{x \in U \mid |d(x)| < \varepsilon\}$. Consider the following problem: find $u^\varepsilon : \Gamma_\varepsilon \to \mathbb{R}$ such that

$$\begin{aligned} -\Delta u^\varepsilon + u^\varepsilon &= f^e \quad \text{in } \Gamma_\varepsilon, \\ \frac{\partial u^\varepsilon}{\partial \nu} &= 0 \quad \text{on } \partial\Gamma_\varepsilon. \end{aligned}$$

It can be shown that the solution of this bulk equation converges to the solution of the surface equation as $\varepsilon \to 0$. This is the basis of a method proposed in Schwartz *et al.* (2005). It is a narrow band approximation analogous to the phase field method in Section 9.3, but only for stationary interfaces, based on choosing $\rho$ to be the characteristic function of $\Gamma$ in the equation (9.7).

*Closest point approach.* The closest point method for partial differential equations on stationary surfaces (Ruuth and Merriman 2008, Macdonald and Ruuth 2008, 2009, Macdonald, Brandman and Ruuth 2011, Marz and Macdonald 2013) is based on considering $u(a(x))$, where $a(x) \in \Gamma$ is the point closest to $x$. The surface partial differential equation is then embedded and discretized in a neighbourhood of $\Gamma$ using $u(a(x))$. Implementation requires the knowledge or calculation of the closest point $a(x)$. In the cited references this approach has been used to solve a wide variety of equations on stationary surfaces.

## 10. Applications

*10.1. Coupling geometric evolution to diffusion on a surface*

A generic example of geometric coupling to surface physics is diffusion on a surface coupled to a geometric equation for the evolution of the surface. A general system might take the following form: find a scalar field $u$ and an evolving hypersurface $\Gamma(t) \subset \mathbb{R}^3$ such that $u$ solves the conservation law

$$\partial^\bullet u - \nabla_\Gamma \cdot q + u \nabla_\Gamma \cdot v = f(V, u) \quad \text{on } \Gamma(t) \tag{10.1a}$$

and $\Gamma(t)$ evolves with the velocity law

$$V = g(\nu, H, u), \tag{10.1b}$$

with $q$ being a flux for $u$, $v = V\nu + v_\tau$, where $V$ is the normal velocity of $\Gamma(t)$, $v_\tau$ is a material tangential velocity, $\partial^\bullet$ is the associated material derivative and $H$ and $\nu$ are the mean curvature and normal to $\Gamma(t)$. This system (10.1) is strongly coupled as the evolution of $\Gamma(t)$ is determined by the solution of the PDE that holds on $\Gamma(t)$. We look at a couple of examples in Sections 10.4 and 10.5.

https://doi.org/10.1017/S0962492913000056 Published online by Cambridge University Press

*10.2. Surfactants*

Surface partial differential equations often arise as subproblems in complex systems of partial differential equations in which surface processes couple geometry and physics. A strongly motivating example is that of the advection and diffusion of a surface active agent on a fluid interface. A particular situation concerns two immiscible viscous fluids with a drop of one fluid inside the other separated by an energetic interface. We suppose that there is a surfactant which is insoluble in the fluids and is confined to the fluid interface, and that the surface energy depends on the concentration of the surfactant and thus leads to a concentration-dependent surface tension and the Marangoni effect. The mathematical model then comprises a moving interface problem for the Navier–Stokes equations coupled to an advection–diffusion equation on the interface. The problem is to find two fluid domains $\Omega^+(t)$, $\Omega^-(t)$ separated by a surface $\Gamma(t)$, a fluid velocity $v$ and a surfactant concentration $u$. Within the bulk fluid domains we have the Navier–Stokes system

$$\nabla \cdot v = 0, \quad \partial_t v + (v \cdot \nabla) v = -\nabla p + \frac{1}{Re} \Delta v.$$

On the unknown moving hypersurface $\Gamma(t)$ we require the mass and momentum balances

$$[v]_-^+ = 0, \quad v \cdot \nu = V,$$

$$\left[ -pI + \frac{2}{Re} D(v) \right]_-^+ \nu = -\frac{1}{Re\, Ca} \big( \sigma(u) H + \nabla_\Gamma \sigma(u) \big)$$

to be satisfied, where $\nu$ is the unit normal pointing into $\Omega^+$, $p$ is the pressure within the fluids, $H$ is the mean curvature of $\Gamma(t)$, $\sigma(u)$ is the concentration-dependent surface tension, $Re$ and $Ca$ are dimensionless numbers derived from physical parameters, $V$ is the normal velocity of $\Gamma$ in this direction, and

$$D(v) = \tfrac{1}{2} (\nabla v + (\nabla v)^T).$$

The concentration $U$ satisfies the advection–diffusion equation

$$\partial^\bullet u - \nabla_\Gamma \cdot q + u \nabla_\Gamma \cdot v = 0 \quad \text{on } \Gamma(t),$$

where $v$ is the material fluid velocity.

We refer to James and Lowengrub (2004), Xu, Li, Lowengrub and Zhao (2006), Lowengrub, Xu and Voigt (2007), Lai, Tseng and Huang (2008), Ganesan and Tobiska (2009), Elliott *et al.* (2011), Ganesan, Hahn, Held and Tobiska (2012) and Xu, Yang and Lowengrub (2012) for a variety of numerical methods for solving this problem. These include level set, phase field and surface finite element approaches.

https://doi.org/10.1017/S0962492913000056 Published online by Cambridge University Press

*10.3. Phase separation on a surface*

As an example of an advection–diffusion equation with a fourth-order elliptic operator we may consider a Cahn–Hilliard equation on a moving surface. The equation for conservation of mass is

$$\partial^\circ u + HVu + \nabla_\Gamma \cdot q = 0,$$

which is of the form (10.1a) with $f = 0$.

Taking a constitutive law for the flux to be of Cahn–Hilliard type which allows up-hill diffusion and leads to phase separation yields

$$\begin{aligned} q &= -b(u)\nabla_\Gamma w, \\ w &= -\gamma \Delta_\Gamma u + \psi'(u), \end{aligned}$$

where $w$ is the chemical potential, $b(\cdot)$ is a concentration-dependent mobility, and $\psi(\cdot)$ is a double-well free energy. Associated with this model is the surface Cahn–Hilliard surface free energy functional

$$E(c) = \int_{\Gamma(t)} \left( \frac{\gamma}{2} |\nabla_\Gamma u|^2 + \psi(u) \right),$$

where $\gamma$ is a gradient energy coefficient. The classical quartic double-well potential is

$$\psi(u) = \frac{1}{4}(u^2 - 1)^2.$$

Placing ourselves in the context of the evolving surface finite element method described in Section 5, we formulate a semidiscretization of the Cahn–Hilliard equation in the case $b(u) = 1$. Given $U_{h0} \in S_h(0)$, find

$$U_h \in S_h^T = \left\{ \phi_h \text{ and } \partial_h^\bullet \phi_h \in C^0(\mathcal{G}_T^h) \mid \phi_h(\cdot, t) \in S_h(t)\ t \in [0,T] \right\}$$

and

$$W_h \in \widetilde{S}_h^T = \left\{ \phi_h\ \in C^0(\mathcal{G}_T^h) \mid \phi_h(\cdot, t) \in S_h(t)\ t \in [0,T] \right\}$$

such that, for all $\phi_h \in S_h^T$ and $t \in (0,T]$,

$$\frac{\mathrm{d}}{\mathrm{d}t} m_h(U_h, \phi_h) + a_h(W_h, \phi_h) = m_h(U_h, \partial_h^\bullet \phi_h), \quad U_h(\cdot, 0) = U_{h0},$$

and

$$m_h(W_h, \phi_h) = \gamma a_h(U_h, \phi_h) + m_h(\Pi_h \psi'(U_h), \phi_h),$$

which is the natural analogue of the splitting into second-order equations of Elliott *et al.* (1989). For a stationary surface an analysis of the error is given in Du, Ju and Tian (2011). See also Schonborn and Desai (1997) and Marenduzzo and Orlandini (2013) for models and computations on stationary surfaces. Mercker *et al.* (2012) consider a more complicated version of the Cahn–Hilliard equation, which involves an energy depending on mean

https://doi.org/10.1017/S0962492913000056 Published online by Cambridge University Press

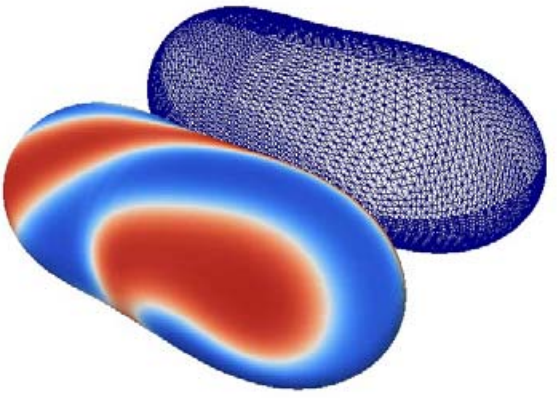


Figure 10.1. Phase separation on a growing surface.

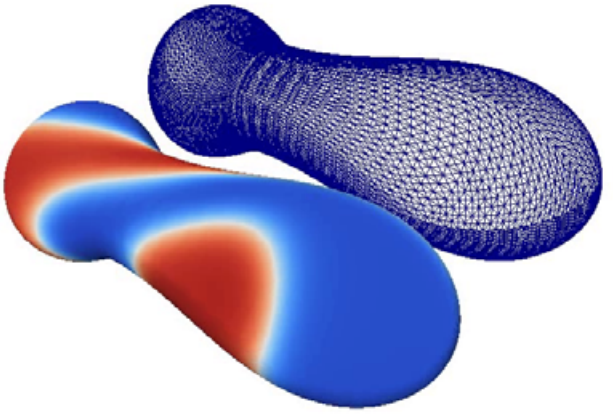


Figure 10.2. Phase separation at a later time than Figure 10.4.

curvature of the surface, in the context of modelling curvature modulated sorting in biomembranes.

Examples of a numerical experiment for an implementation of this scheme is shown in Figures 10.1 and 10.2. In each figure the evolving surface is shaded with respect to the values of $U_h$ and the associated triangulation is shown by the side.

### *10.4. Surface dissolution*

An example of coupling a surface evolution with a surface process which leads to a highly nonlinear system with complex surface morphology is a model for the etching of silver in an Ag–Au alloy whose surface is immersed in an electrolyte. The dissolution of silver atoms occurs at the surface,

https://doi.org/10.1017/S0962492913000056 Published online by Cambridge University Press

leaving a monolayer of gold adatoms on the surface which are mobile within the electrolyte. The gold adatoms agglomerate in clusters exposing the next layer of silver atoms for dissolution. This may lead to the growth of porosity into the bulk and formation of nanoporosity: see Erlebacher *et al.* (2001) and Erlebacher and McCue (2012). The model developed in Erlebacher *et al.* (2001) and also Eilks and Elliott (2008) comprises an evolution equation for the time-dependent dissolving surface $\Gamma(t)$ and an equation for conservation of mass. It leads to a system of the form (10.1).

The geometric surface evolution equation is of forced mean curvature type,

$$V = -J_{\text{diss}} = v_0(c)(1 - \delta H) \tag{10.2}$$

where $V\nu$ is the normal velocity of the surface and the rate of dissolution is denoted by $J_{\text{diss}}$ which depends on a surface-concentration-dependent etching rate $v_0(c) \geq 0$ and the mean curvature of the surface, $H$. Physically, in portions where the surface is completely covered by gold, etching cannot take place because the electrolyte is no longer in contact with silver atoms and the etching rate satisfies $v_0(1) = 0$. We use $c$ to denote the surface concentration of gold atoms in the binary mixture of gold and electrolyte adatoms in the surface monolayer, $C_0$ to be the bulk gold concentration and $q$ to denote the diffusive surface flux of adatoms.

Then the equation for conservation of mass is

$$\partial^\circ c + HVc = VC_0 - \nabla_\Gamma \cdot q, \tag{10.3}$$

which is of the form (10.1a) with $f = VC_0$. This latter term is due to the picking up on the surface of gold adatoms from the bulk where diffusion is neglected.

The constitutive law for the flux is of Cahn–Hilliard type, which allows up-hill diffusion and leads to phase separation so that

$$\begin{aligned} q &= -b(c)\nabla_\Gamma w, \\ w &= -\gamma \Delta_\Gamma c + \psi'(c), \end{aligned}$$

where $\mu$ is the chemical potential, $b(\cdot)$ is a concentration-dependent mobility, and $\psi(\cdot)$ is the double-well free energy occurring in Cahn–Hilliard theory. Assuming a regular solution model for homogeneous free energy of the binary mixture of gold and electrolyte adatoms in the monolayer leads to the logarithmic function

$$\psi(c) = \frac{\theta_{cr}}{2} c(1-c) + \frac{\theta}{4}(c \log(c) + (1-c)\log(1-c)).$$

This precludes values of $c$ outside the interval $[-1, 1]$ and a typical form for

https://doi.org/10.1017/S0962492913000056 Published online by Cambridge University Press

the mobility is the degenerate mobility

$$b(c) = B(1 - c^2).$$

Thus we are led to the study of the highly nonlinear coupled system of forced mean curvature flow for an evolving surface with the forcing depending on the solution of a degenerate Cahn–Hilliard equation. On the surface we expect surface phase separation to take place, yielding gold-rich and gold-depleted regions on the surface monolayer $\Gamma(t)$. Numerical simulations are shown in Figure 10.3. See Eilks and Elliott (2008) for a description of the computational methods and further simulations. These computations are based on the evolving surface finite element method for the solution of the Cahn–Hilliard equations and a variant of the scheme of Dziuk (1991) for forced mean curvature flow. The surfaces shown in Figure 10.3 are triangulated surfaces. Adaptivity is used to refine and coarsen depending on the solution of the Cahn–Hilliard equation, and from time to time a new triangulation is required in order to avoid degenerate shapes for the triangles.

### *10.5. Pattern formation on biological surfaces*

Following the classical paper of Turing (1952), pattern formation on a growing biological surface may be modelled by reaction–diffusion equations which exhibit diffusion-driven instability of spatially uniform structures and thus lead to spatial patterns. In biological applications it is natural to consider this mechanism for pattern formation to hold on evolving curved surfaces which form the boundaries of growing three-dimensional domains. The numerical solution of a number of models using the evolving surface finite element method was proposed in Barreira *et al.* (2011). A Lagrangian particle method using level set ideas for reaction–diffusion equations on moving surfaces was presented in Bergdorf, Sbalzarini and Koumoutsakos (2010).

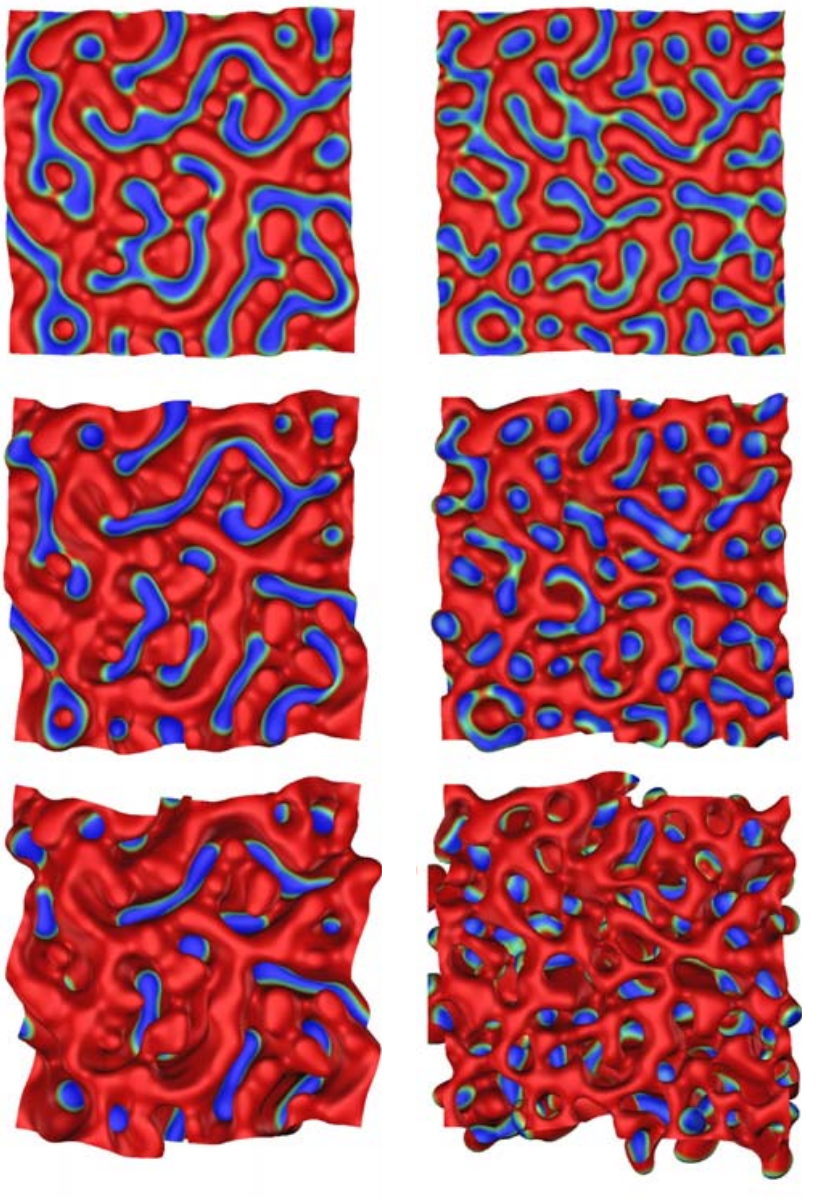
An example of an application is presented by Chaplain, Ganesh and Graham (2001), who propose a model for the growth of solid tumours. In the model the evolution of the solid bulk tumour is determined by a concentration of a growth-promoting factor causing growth on the surface. The resulting mathematical problem is that of determining $\Gamma(t) \subset \mathbb{R}^3$ modelling the tumour surface and scalar functions $u(x,t)$ and $w(x,t)$ that diffuse and react on the surface, which satisfy

$$\partial^\bullet u + u\nabla_\Gamma \cdot V\nu = \Delta_\Gamma u + f_1(u,w) \quad \text{on } \Gamma(t),$$
$$\partial^\bullet w + w\nabla_\Gamma \cdot V\nu = D_w\Delta_\Gamma w + f_2(u,w) \quad \text{on } \Gamma(t),$$

with normal velocity $V\nu$ and

$$V = -\varepsilon H + \delta u. \tag{10.4}$$

https://doi.org/10.1017/S0962492913000056 Published online by Cambridge University Press



(a) (b)

Figure 10.3. The early stages of spinodal decomposition on a dissolving surface. (a) The surface with constant mobility and (b) a surface with degenerate mobility, $t = 0.1$, $t = 0.2$ and $t = 0.3$.

https://doi.org/10.1017/S0962492913000056 Published online by Cambridge University Press

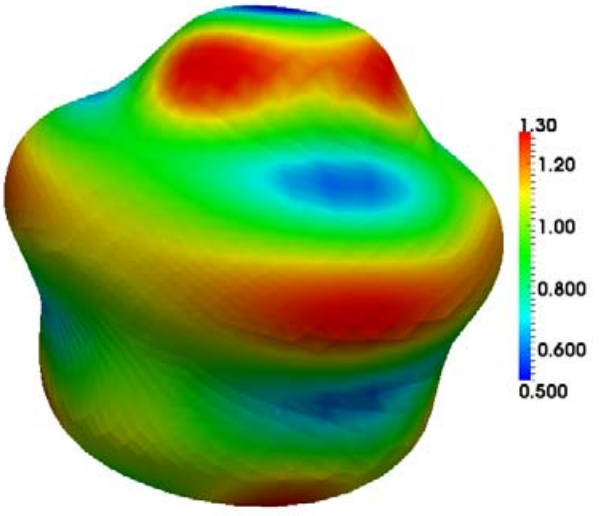



Figure 10.4. Pattern formation on growing surface.

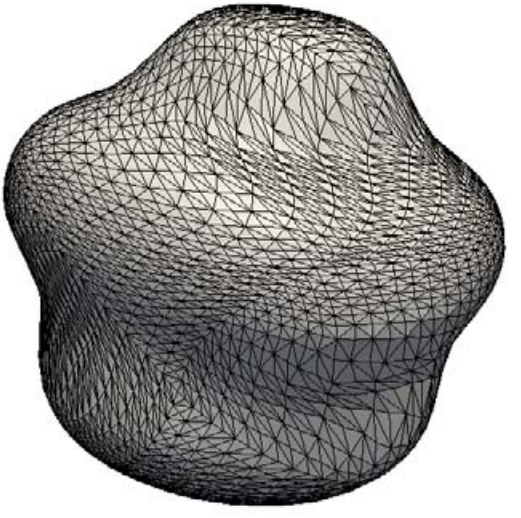


Figure 10.5. Associated triangulation for Figure 10.4.

https://doi.org/10.1017/S0962492913000056 Published online by Cambridge University Press

In the velocity law (10.4) the second term on the right comes from the suggestion in Crampin, Gaffney and Maini (1999) that growth should be faster in regions of higher concentration of the growth-promoting factor $u$, and the first term on the right is a surface tension term which has the effect of yielding smooth surfaces in the short term. Finally $D_w$, $\delta$ and $\varepsilon$ are positive parameters. The reaction functions $f_1$ and $f_2$ model the interactions between the two surface concentrations. An example is the activator-depleted substrate model (Schnakenberg 1979), known as the Brusselator model, in which

$$f_1(u,w) = \gamma(a - u + u^2 w) \quad \text{and} \quad f_2(u,w) = \gamma(b - u^2 w),$$

where $\gamma, a$ and $b$ are positive constants.

An example of a simulation together with the associated triangulation is given in Figures 10.4 and 10.5. The shading corresponds to the computed values of $u$. The simulation was carried out with the ALE evolving-surface finite element method (Elliott and Styles 2012), coupled with the method of Barrett, Garcke and Nürnberg (2008*a*).

For examples of studies of reaction–diffusion pattern formation on surfaces we refer to Aragón, Barrio and Varea (1999), Barrio *et al.* (2004), Barreira (2009) and Rätz and Röger (2012). Other examples in computational biology which involve the coupling of surface evolution to diffusion and phase separation on the surface are models for cell motility (Elliott *et al.* 2012) and phase separation on biomembranes (Elliott and Stinner 2010).

## Acknowledgements

The authors wish to thank Carsten Eilks, Thomas Ranner, Björn Stinner and Vanessa Styles for providing computational results. This article was completed whilst one of the authors was visiting the Freie Universität Berlin in association with the award of a Humboldt Forschungspreis by the Alexander von Humboldt Foundation. The work was supported by the Deutsche Forschungsgemeinschaft via SFB/TR 71 'Geometric partial differential equations'. Some of the computational results were obtained by using the finite element toolbox ALBERTA (Schmidt and Siebert 2005) and the DUNE software package (Bastian *et al.* 2008*a*, 2008*b*) and visualized using the visualization applications ParaView (Henderson 2007) and GRAPE (Rumpf, Schmidt, *et al.* 1990).

https://doi.org/10.1017/S0962492913000056 Published online by Cambridge University Press

## REFERENCES[1]


D. Adalsteinsson and J. A. Sethian (2003), 'Transport and diffusion of material quantities on propagating interfaces via level set methods', *J. Comput. Phys.* **185**, 271–288.

J. Aragón, R. A. Barrio and C. Varea (1999), 'Turing patterns on a sphere', *Phys. Rev. E* **60**, 4588–4592.

R. Barreira (2009), Numerical solution of nonlinear partial differential equations on triangulated surfaces. DPhil thesis, University of Sussex.

R. Barreira, C. M. Elliott and A. Madzvamuse (2011), 'The surface finite element method for pattern formation on evolving biological surfaces', *J. Math. Biology* **63**, 1095–1119.

J. W. Barrett and C. M. Elliott (1982), A finite element method on a fixed mesh for the Stefan problem with convection in a saturated porous medium. In *Numerical Methods for Fluid Dynamics, Conference proceedings: University of Reading, 29-31 March, 1982* (K. W. Morton and M. J. Baines, eds), Conference Series (Institute of Mathematics and its Applications), Academic Press, pp. 389–409.

J. W. Barrett and C. M. Elliott (1984), 'A finite-element method for solving elliptic equations with Neumann data on a curved boundary using unfitted meshes', *IMA J. Numer. Anal.* **4**, 309–325.

J. W. Barrett and C. M. Elliott (1985), 'Fixed mesh finite element approximations to a free boundary problem for an elliptic equation with an oblique derivative boundary condition', *Comput. Math. Appl.* **11**, 335–345.

J. W. Barrett and C. M. Elliott (1987*a*), 'Fitted and unfitted finite-element methods for elliptic equations with smooth interfaces', *IMA J. Numer. Anal.* **7**, 283–300.

J. W. Barrett and C. M. Elliott (1987*b*), 'A practical finite element approximation of a semi-definite Neumann problem on a curved domain', *Numer. Math.* **51**, 23–36.

J. W. Barrett and C. M. Elliott (1988), 'Finite-element approximation of elliptic equations with a Neumann or Robin condition on a curved boundary', *IMA J. Numer. Anal.* **8**, 321–342.

J. W. Barrett, H. Garcke and R. Nürnberg (2007), 'A parametric finite element method for fourth order geometric evolution equations', *J. Comput. Phys.* **222**, 441–467.

J. W. Barrett, H. Garcke and R. Nürnberg (2008*a*), 'On the parametric finite element approximation of evolving hypersurfaces in $R^3$', *J. Comput. Phys.* **227**, 4281–4307.

J. W. Barrett, H. Garcke and R. Nürnberg (2008*b*), 'Parametric approximation of Willmore flow and related geometric evolution equations', *SIAM J. Sci. Comput.* **31**, 225–253.


[1] The URLs cited in this work were correct at the time of going to press, but the publisher and the authors make no undertaking that the citations remain live or are accurate or appropriate.

https://doi.org/10.1017/S0962492913000056 Published online by Cambridge University Press

R. A. Barrio, P. K. Maini, P. Padilla, R. G. Plaza and Sánchez-Garduno (2004), 'The effect of growth and curvature on pattern formation', *J. Dynam. Diff. Equations* **16**, 1093–1121.

P. Bastian and C. Engwer (2009), 'An unfitted finite element method using discontinuous Galerkin', *Internat. J. Numer. Methods Engng* **79**, 1557–1576.

P. Bastian, M. Blatt, A. Dedner, C. Engwer, R. Klofkorn, M. Oldberger and O. Sander (2008*a*), 'A generic grid interface for parallel and adaptive scientific computing I: Abstract framework', *Computing* **82**, 103–119.

P. Bastian, M. Blatt, A. Dedner, C. Engwer, R. Klofkorn, M. Oldberger and O. Sander (2008*b*), 'A generic grid interface for parallel and adaptive scientific computing II: Implementation and tests in DUNE', *Computing* **82**, 121–138.

M. Bergdorf, I. Sbalzarini and P. Koumoutsakos (2010), 'A Lagrangian particle method for reaction–diffusion systems on deforming surfaces', *J. Math. Biology* **61**, 649–663.

M. J. Berger, D. A. Calhoun, C. Helzel and R. J. Leveque (2009), 'Logically rectangular finite volume methods with adaptive refinement on the sphere', *Phil. Trans. Royal Soc. London A* **367**, 4483–4496.

M. Bertalmío, L.-T. Cheng, S. J. Osher and G. Sapiro (2001), 'Variational problems and partial differential equations on implicit surfaces', *J. Comput. Phys.* **174**, 759–780.

J. F. Blowey and C. M. Elliott (1991), 'The Cahn–Hilliard gradient theory for phase separation with non-smooth free energy I: Mathematical analysis', *European J. Appl. Math.* **2**, 233–280.

J. F. Blowey and C. M. Elliott (1992), 'The Cahn–Hilliard gradient theory for phase separation with non-smooth free energy II: Numerical analysis', *European J. Appl. Math.* **3**, 147–179.

J. F. Blowey and C. M. Elliott (1993), Curvature dependent phase boundary motion and parabolic obstacle problems. In *Degenerate Diffusion* (W.-M. Ni, L. A. Peletier and J. L. Vasquez, eds), Vol. 47 of *IMA Volumes in Mathematics and its Applications*, Springer, pp. 19–60.

M. Burger (2009), 'Finite element approximation of elliptic partial differential equations on implicit surfaces', *Comput. Vis. Sci.* **12**, 87–100.

G. Caginalp (1989), 'Stefan and Hele-Shaw type models as asymptotic limits of the phase field equations', *Phys. Rev. A* **39**, 5887–5896.

D. A. Calhoun and C. Helzel (2009), 'A finite volume method for solving parabolic equations on logically Cartesian curved surface meshes', *SIAM J. Sci. Comput.* **31**, 4066–4099.

P. Cermelli, E. Fried and M. E. Gurtin (2005), 'Transport relations for surface integrals arising in the formulation of balance laws for evolving fluid interfaces', *J. Fluid Mech.* **544**, 339–351.

M. A. J. Chaplain, M. Ganesh and I. G. Graham (2001), 'Spatio-temporal pattern formation on spherical surfaces: Numerical simulation and application to solid tumour growth', *J. Math. Biology* **42**, 387–423.

P. G. Ciarlet (1978), *The Finite Element Method for Elliptic Problems*, North-Holland.

M. I. M. Copetti and C. M. Elliott (1992), 'Numerical analysis of the Cahn–Hilliard equation with a logarithmic free energy', *Numer. Math.* **63**, 39–65.

https://doi.org/10.1017/S0962492913000056 Published online by Cambridge University Press

E. J. Crampin, E. A. Gaffney and P. K. Maini (1999), 'Reaction and diffusion on growing domains: Scenarios for robust pattern formation', *Bull. Math. Biology* **61**, 1093–1120.

K. Deckelnick, G. Dziuk and C. M. Elliott (2005), Computation of geometric partial differential equations and mean curvature flow. In *Acta Numerica*, Vol. 14, Cambridge University Press, pp. 139–232.

K. Deckelnick, G. Dziuk, C. M. Elliott and C.-J. Heine (2010), 'An $h$-narrow band finite element method for implicit surfaces', *IMA J. Numer. Anal.* **30**, 351–376.

K. Deckelnick, C. M. Elliott and T. Ranner (2013), Unfitted finite element methods using bulk meshes for surface partial differential equations. In preparation.

K. Deckelnick, C. M. Elliott and V. Styles (2001), 'Numerical diffusion-induced grain boundary motion', *Interfaces Free Bound.* **6**, 329–349.

A. Dedner, P. Madhavan and B. Stinner (2013), 'Analysis of the discontinuous Galerkin method for elliptic problems on surfaces', *IMA J. Numer. Anal.*, to appear.

A. Demlow (2009), 'Higher-order finite element methods and pointwise error estimates for elliptic problems on surfaces', *SIAM J. Numer. Anal.* **47**, 805–827.

A. Demlow and G. Dziuk (2007), 'An adaptive finite element method for the Laplace–Beltrami operator on surfaces', *SIAM J. Numer. Anal.* **45**, 421–442.

A. Demlow and M. Olshanskii (2012), 'An adaptive surface finite element method based on volume meshes', *SIAM J. Numer. Anal.* **50**, 1624–1647.

Q. Du, L. Ju and L. Tian (2011), 'Finite element approximation of the Cahn–Hilliard equation on surfaces', *Comput. Methods Appl. Mech. Engng* **200**, 2458–2470.

G. Dziuk (1988), Finite elements for the Beltrami operator on arbitrary surfaces. In *Partial Differential Equations and Calculus of Variations* (S. Hildebrandt and R. Leis, eds), Vol. 1357 of *Lecture Notes in Mathematics*, Springer, pp. 142–155.

G. Dziuk (1991), 'An algorithm for evolutionary surfaces', *Numer. Math.* **58**, 603–611.

G. Dziuk and C. M. Elliott (2007*a*), 'Finite elements on evolving surfaces', *IMA J. Numer. Anal.* **25**, 385–407.

G. Dziuk and C. M. Elliott (2007*b*), 'Surface finite elements for parabolic equations', *J. Comput. Math.* **25**, 385–407.

G. Dziuk and C. M. Elliott (2008), 'Eulerian finite element method for parabolic PDEs on implicit surfaces', *Interfaces Free Bound.* **10**, 119–138.

G. Dziuk and C. M. Elliott (2010), 'An Eulerian approach to transport and diffusion on evolving implicit surfaces', *Comput. Vis. Sci.* **13**, 17–28.

G. Dziuk and C. M. Elliott (2012), 'Fully discrete evolving surface finite element method', *SIAM J. Numer. Anal.* **50**, 2677–2694.

G. Dziuk and C. M. Elliott (2013), '$L^2$ estimates for the evolving surface finite element method', *Math. Comp.* **82**, 1–24.

G. Dziuk, D. Kröner and T. Müller (2012), Scalar conservation laws on moving hypersurfaces. Technical report, Freiburg.

https://doi.org/10.1017/S0962492913000056 Published online by Cambridge University Press

G. Dziuk, C. Lubich and D. Mansour (2012), 'Runge–Kutta time discretization of parabolic differential equations on evolving surfaces', *IMA J. Numer. Anal.* **32**, 394–416.

C. Eilks and C. M. Elliott (2008), 'Numerical simulation of dealloying by surface dissolution via the evolving surface finite element method', *J. Comput. Phys.* **227**, 9727–9741.

C. M. Elliott and T. Ranner (2013), 'Finite element analysis for a coupled bulk–surface partial differential equation', *IMA J. Numer. Anal.*, to appear.

C. M. Elliott and B. Stinner (2009), 'Analysis of a diffuse interface approach to an advection diffusion equation on a moving surface', *Math. Mod. Methods Appl. Sci.* **5**, 787–802.

C. M. Elliott and B. Stinner (2010), 'Modeling and computation of two phase geometric biomembranes using surface finite elements', *J. Comput. Phys.* **229**, 6585–6612.

C. M. Elliott and B. Stinner (2012), 'Computation of two-phase biomembranes with phase dependent material parameters using surface finite elements', *Commun. Comput. Phys.* **13**, 325–360.

C. M. Elliott and V. Styles (2003), 'Computations of bidirectional grain boundary dynamics in thin metallic films', *J. Comput. Phys.* **187**, 524–543.

C. M. Elliott and V. M. Styles (2012), 'An ALE ESFEM method for solving PDEs on evolving surfaces', *Milan J. Math.* **80**, 469–501.

C. M. Elliott, D. A. French and F. A. Milner (1989), 'A second order splitting method for the Cahn–Hilliard equation', *Numer. Math.* **54**, 575–590.

C. M. Elliott, B. Stinner and C. Venkataraman (2012), 'Modelling cell motility and chemotaxis with evolving surface finite elements', *J. Royal Society Interface* **9**, 3027–3044.

C. M. Elliott, B. Stinner, V. Styles and R. Welford (2011), 'Numerical computation of advection and diffusion on evolving diffuse interfaces', *IMA J. Numer. Anal.* **31**, 786–812.

C. Engwer and F. Heimann (2012), DUNE-UDG: A cut-cell framework for unfitted discontinuous Galerkin methods. In *Advances in DUNE*, Springer, pp. 89–100.

J. Erlebacher and I. McCue (2012), 'Geometric characterization of nanoporous metals', *Acta Materialia* **60**, 6164–6174.

J. Erlebacher, M. Aziz, A. Karma, N. Dimitrov and K. Sieradzki (2001), 'Evolution of nanoporosity in dealloying', *Nature* **410**, 450–453.

L. C. Evans (1998), *Partial Differential Equations*, first edition, Graduate Studies in Mathematics, AMS.

P. C. Fife, J. W. Cahn and C. M. Elliott (2001), 'A free-boundary model for diffusion-induced grain boundary motion', *Interfaces Free Bound.* **3**, 291–336.

S. Ganesan and L. Tobiska (2009), 'A coupled arbitrary Lagrangian–Eulerian and Lagrangian method for computation of free-surface flows with insoluble surfactants', *J. Comput. Phys.* **228**, 2859–2873.

S. Ganesan, A. Hahn, K. Held and L. Tobiska (2012), An accurate numerical method for computation of two-phase flows with surfactants. In *European Congress on Computational Methods in Applied Sciences and Engineering* (J. Eberhardsteiner *et al.*, eds), Vol. CD-ROM, TU Vienna. office@eccomas2012.tuwien.ac.at

https://doi.org/10.1017/S0962492913000056 Published online by Cambridge University Press

D. Gilbarg and N. S. Trudinger (1998), *Elliptic Partial Differential Equations of Second Order*, Grundlehren der Mathematischen Wissenschaften, Springer.
J. B. Greer (2006), 'An improvement of a recent Eulerian method for solving PDEs on general geometries', *J. Sci. Comput.* **29**, 321–352.
J. B. Greer, A. L. Bertozzi and G. Sapiro (2006), 'Fourth order partial differential equations on general geometries', *J. Comput. Phys.* **216**, 216–246.
A. Hansbo and P. Hansbo (2002), 'An unfitted finite element method, based on Nitsche's method, for elliptic interface problems', *Comput. Methods Appl. Mech. Engng* **191**, 5537–5552.
A. Henderson (2007), *ParaView Guide: A Parallel Visualization Application*, Kitware.
A. J. James and J. Lowengrub (2004), 'A surfactant-conserving volume-of-fluid method for interfacial flows with insoluble surfactant', *J. Comput. Phys.* **201**, 685–722.
L. Ju and Q. Du (2009), 'A finite volume method on general surfaces and its error estimates', *J. Math. Anal. Appl.* **352**, 645–668.
L. Ju, L. Tian and D. Wang (2009), '*A posteriori* error estimates for finite volume approximations of elliptic equations on general surfaces', *Comput. Methods Appl. Mech. Engng* **198**, 716–726.
M.-C. Lai, Y.-H. Tseng and H. Huang (2008), 'An immersed boundary method for interfacial flows with insoluble surfactant', *J. Comput. Phys.* **227**, 7279–7293.
J. Lowengrub, J.-J. Xu and A. Voigt (2007), 'Surface phase separation and flow in a simple model of multicomponent drops and vesicles', *Fluid Dynamics and Material Processing* **3**, 1–20.
C. Lubich and D. Mansour (2012), Variational discretisation of linear wave equation on evolving surfaces. Technical report, Tübingen.
C. B. Macdonald and S. J. Ruuth (2008), 'Level set equations on surfaces via the closest point method', *J. Sci. Comput.* **35**, 219–240.
C. B. Macdonald and S. J. Ruuth (2009), 'The implicit closest point method for the numerical solution of partial differential equations on surfaces.', *SIAM J. Sci. Comput.* **31**, 4330–4350.
C. B. Macdonald, J. Brandman and S. J. Ruuth (2011), 'Solving eigenvalue problems on curved surfaces using the closest point method.', *J. Comput. Phys.* **230**, 7944–7956.
D. Marenduzzo and E. Orlandini (2013), 'Phase separation dynamics on curved surfaces', *Soft Matter* **9**, 1178–1187.
T. Marz and C. B. Macdonald (2013), 'Calculus on surfaces with general closest point functions', *SIAM J. Numer. Anal.* **50**, 3303–3328.
M. Mercker, M. Ptashnyk, J. Kühnle, D. Hartmann, M. Weiss and W. Jäger (2012), 'A multiscale approach to curvature modulated sorting in biological membranes', *J. Theoret. Biology* **301**, 67–82.
J. Nedelec (1976), 'Curved finite element methods for the solution of singular integral equations on surfaces in $R^3$', *Comput. Methods Appl. Mech. Engng* **8**, 61–80.
I. L. Novak, F. Gao, Y.-S. Choi, D. Resasco, J. C. Schaff and B. M. Slepchenko (2007), 'Diffusion on a curved surface coupled to diffusion in the volume: Application to cell biology', *J. Comput. Phys.* **226**, 1271–1290.

https://doi.org/10.1017/S0962492913000056 Published online by Cambridge University Press

M. A. Olshanskii and A. Reusken (2010), 'A finite element method for surface PDEs: Matrix properties', *Numer. Math.* **114**, 491–520.

M. A. Olshanskii, A. Reusken and J. Grande (2009), 'A finite element method for elliptic equations on surfaces', *SIAM J. Numer. Anal.* **47**, 3339–3358.

S. Osher and R. Fedkiw (2003), *Level Set Methods and Dynamic Implicit Surfaces*, Vol. 153 of *Applied Mathematical Sciences*, Springer.

A. Rätz and M. Röger (2012), 'Turing instabilities in a mathematical model for signaling networks', *J. Math. Biology* **65**, 1215–1244.

A. Rätz and A. Voigt (2006), 'PDEs on surfaces: A diffuse interface approach', *Commun. Math. Sci.* **4**, 575–590.

M. Rumpf, A. Schmidt *et al.* (1990), GRAPE: Graphics programming environment. SFB 256 Report 8, Universität Bonn.

S. J. Ruuth and B. Merriman (2008), 'A simple embedding method for solving partial differential equations on surfaces', *J. Comput. Phys.* **227**, 1943–1961.

A. Schmidt and K. G. Siebert (2005), *Design of Adaptive Finite Element Software: The Finite Element Toolbox ALBERTA*, Vol. 42 of *Lecture Notes in Computational Science and Engineering*, Springer.

J. Schnakenberg (1979), 'Simple chemical reaction systems with limit cycle behaviour', *J. Theoret. Biology* **81**, 389–400.

O. Schonborn and R. C. Desai (1997), 'Phase-ordering kinetics on curved surfaces', *Physica A* **239**, 412–419.

P. Schwartz, D. Adalsteinsson, P. Colella, A. P. Arkin and M. Onsum (2005), 'Numerical computation of diffusion on a surface', *Proc. Nat. Acad. Sci.* **102**, 11151–11156.

J. A. Sethian (1999), *Level Set Methods and Fast Marching Methods*, Cambridge Monographs on Applied and Computational Mathematics, Cambridge University Press.

H. A. Stone (1990), 'A simple derivation of the time dependent convective diffusion equation for surfactant transport along a deforming interface', *Phys. Fluids A* **2**, 111–112.

A. M. Turing (1952), 'The chemical basis of morphogenesis', *Phil. Trans. Royal Soc. London B* **237**, 37–72.

J.-J. Xu and H.-K. Zhao (2003), 'An Eulerian formulation for solving partial differential equations along a moving interface', *J. Sci. Comput.* **19**, 573–594.

J.-J. Xu, Z. Li, J. Lowengrub and H. Zhao (2006), 'A level-set method for interfacial flows with surfactant', *J. Comput. Phys.* **212**, 590–616.

J.-J. Xu, Y. Yang and J. Lowengrub (2012), 'A level-set continuum method for two-phase flows with insoluble surfactant', *J. Comput. Phys.* **231**, 5897–5909.

https://doi.org/10.1017/S0962492913000056 Published online by Cambridge University Press